SPECTROSCOPIC STUDIES ON THE NATURE OF THE METAL-AXIAL LIGAND BOND IN HEMOPROTEINS AND THEIR MODEL COMPOUNDS

A Thesis Submitted to

the Faculty of Science, Osaka University

Yukihiro OZAKI

Institute for Protein Research

Osaka University

1978

CONTENTS

INTRODUCTION

During the last decade, physical chemistry have provided a number of novel and powerful methods for our understanding and knowledge of the molecular structures and dynamic properties of hemoproteins (1-4). Success in X-ray analysis of the tertiary structures of myoglobin and hemoglobin have opened a new stage in this field. Untill now the molecular structures of several kinds of hemoproteins including hemoglobin (Hb), myoglobin (Mb), cytochromes c, c_2, and b_5 were described in detail by X-ray crystallography. These results have strongly stimulated the structural studies of hemoproteins. In spite of its usefulness, however, X-ray crystallography can not always come up to our expectations in the study of the correlation between molecular structures and physiological functions. Highly resolved X-ray data have only been obtained in single crystals, therefore it is still desirable to get structural informations on the molecules in solution at on near physiological conditions. In addition to the molecular structures, it is quite necessary to examine the dynamic properties of active sites and the kinetic functions of enzymes. Especially in the study of hemoproteins it is quite important to survey structural changes of heme and heme moiety or dynamic behaviors of the higher order structure which are of functionally significant.

A number of spectroscopic and other physicochemical methods have been so far introduced for the above purpose (1-4). Ultraviolet and infrared spectroscopy, high-resolution nuclear magnetic resonance (NMR), Mössbauer effect, resonance Raman spectroscopy, circular and magnetic circular-dichroism,electron spin resonance (ESR), magnetic susceptibility, field-and temperature jump relaxation, flash photolysis, and equilibrium methods have been applied to the studies of hemoproteins to examine the electronic structures of heme, the conformational changes of the heme moiety and the mechanisms of kinetics. Each of these physicochemical methods has advantages and characteristics. The effective use of various probes with hemoproteins has permitted an approach to our goal. A recent progress of

hemoprotein research owes much to experimental development of these techniques. In parallel to the physicochemical studies, synthetic chemists have been driving the studies of model compounds. Porphyrins and metallo-porphyrins are simple models systems which have analogous structures of hemes and/or similar functions as hemoproteins. Almost all of them were imposed to the spectroscopic measurements and the studies on these model compounds have made large contributions to interprete the results of the spectroscopic measurements of hemoproteins. Today cooperation among the fields of physical chemistry, synthetic chemistry, and biochemistry have been gone on and a number of fruites have been obtained. However there still remain many unresolved problems about the relationship between the structural features and the functional behaivor of hemoproteins. In this thesis the studies were focused in correlating spectroscopic behaviors in the resonance Raman and ^{15}N nuclear magnetic resonance spectra to the nature of the axial ligand-metal bonding. Many of the functions of hemoproteins are regulated by the kinds of ligands. Thus if any correlation between the both spectroscopic evidences and the nature of the bonding could be established it would be quite useful for surveying the mechanism of functioning of hemoproteins.

1. General Properties of Hemoproteins

Hemoproteins can exhibit distinctly different functions which include reversible oxygen binding for transport (hemoglobin) of storage of oxygens (myoglobin), oxygen reduction (cytochrome c oxidase), mixed-function oxidation with oxygen (e.g. cytochrome P-450) electron-transfer (cytochromes b and c) and hydrogen peroxide utilization (catalases and peroxidases) (5-8). Iron porphyrins serve as prosthetic groups for hemoproteins, so that hemoproteins differ in both polypeptide and heme components. Protein structures vary markedly as function and species change whereas only a few differences in porphyrin structure are known. Allmost all of them are shown in Fig. 1. They differ from each other in the peripheral substituents. There are six coordination sites about the heme iron atom, four of which are occupied by the pyrrole nitrogen atoms of the

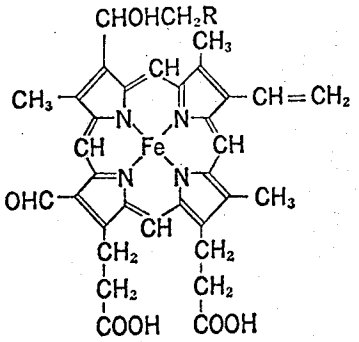

heme a

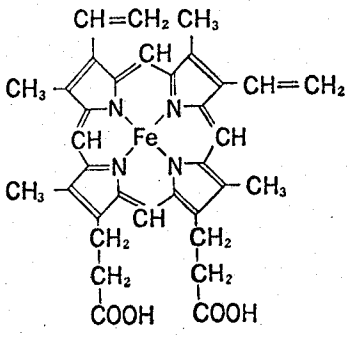

heme b
(protoheme IX)

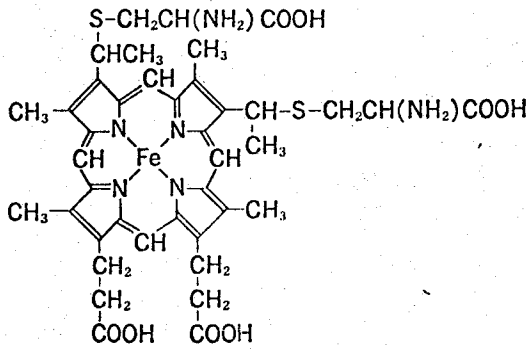

heme c

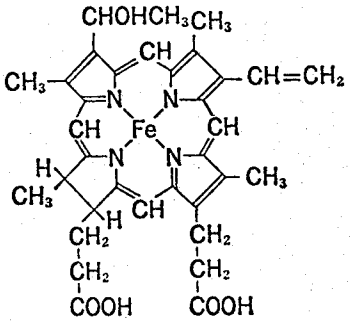

heme d

Fig. 1 Chemical structures of hemes.

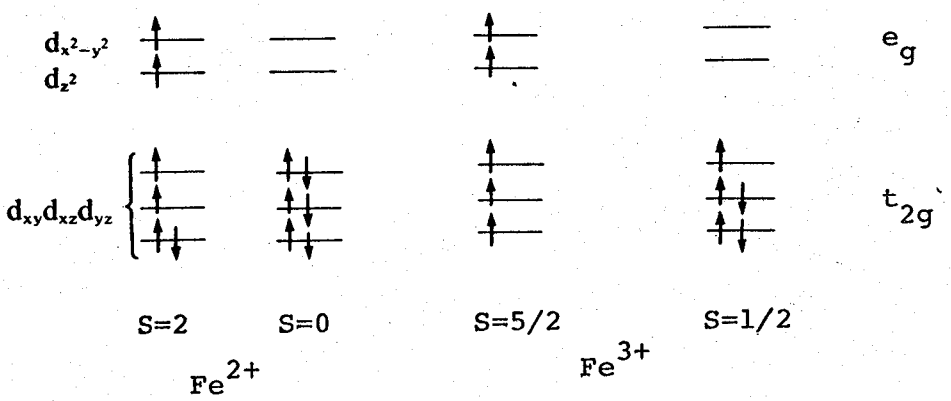

Fig. 2 Four different electronic configurations of hemes.

porphyrin ring. The fifth and sixth ligand sites are available to bind with axial ligands. In an octahedral molecular environment the metal valence d orbitals split into two sublevels. The more energetic sublevel is called e_g and includes the two d orbitals ($d_{x^2-y^2}$ and d_{z^2}) whereas the less energetic sublevel is called t_{2g} and includes the three d orbitals (d_{xz}, d_{yz}, d_{xy}). Heme iron exists in ferrous or ferric state. Fe^{3+} has five d-electrons while Fe^{2+} has six d-electrons. The ground state configurations of octahedral metal complexes are constructed by placing the appropriate number of d electrons in the t_{2g} and e_g orbitals, in accordance with Hund's rule or Pauli's exclusion principle. There are usually four different electronic configurations of the heme iron as shown in Fig. 2. They are the ferric high spin (Fe^{3+}, S=5/2), ferric low spin (Fe^{3+}, S=1/2). ferrous high spin (Fe^{2+}, S=2), and ferrous low spin (Fe^{2+}, S=0) forms. Only a low spin ferrous iron is diamagnetic. Many biochemical reactions of hemoproteins are accompanied by changes of the valence and spin states of the heme iron, e. g. the oxygenation of myoglobin and hemoglobin.

deoxy Hb (Fe^{2+}, S=2) + O_2 $\rightleftharpoons$ HbO_2 (Fe^{2+}, S=0)

and the electoron transfer in cytochromes e. g.

cyt c (Fe^{3+}, S=1/2) + e^- $\rightleftharpoons$ cyt c (Fe^{2+}, S=0)

In addition to high and low spin states recently the existence of intermediate spin state (S=3/2) is discussed. Maltempo (9), and Strekas and Spiro (10) suggested the intermidiate spin state for oxidized cytochrome c' at neutral pH.

As mentioned above in order to reveal the structure-function relationship of hemoproteins, it is the most significant to inguire the state of heme iron and the structure of heme moiety, especially the nature of the heme iron-axial ligand bonding. The importance of the interaction between the axial ligand and the heme iron has been emphasized in many points of view. For example, the formation of binding between oxygen and the heme iron at one subunit of hemoglobin increases the affinity of the other subunit for subsequent oxygen addition. Further it is pointed out that the iron-ligand bond of HbO_2 or HbCO differs from that of reduced cytochrome b_5 or cytochrome c, although the oxidation and spin states are same for these hemoproteins. The

reduced CO complex of cytochrome P-450 exhibits the Soret absorption band at about 450 nm, a wavelength which is approximately 30 nm longer than that observable for usual ferrous protoheme-CO complexes (11). It is suggested this and other spectral anomalies of P-450 can be ascribed to the coordination of a thiolate anion (RS^-) as a axial ligand. The spectral anomalies disappear when it is converted into the catalytically inactive form called cytochrome P-420. Probably, a significant difference exists in the feature of the axial ligand between P-450 and P-420.

2. Raman Spectroscopy

Raman spectroscopy is a new 're-vitalized' technique. The appearance of the laser and its application to Raman spectroscopy has effected a renaissance during the last ten years or so. Raman scattering was first predicted from theoretical consideration by A. Smekal in 1923 and C. V. Raman discovered the effect later in 1928. At first Raman spectroscopy was well established as the most important and practical method for obtaining information on rotational and vibrational transitions. However, the measurement of Raman spectra was not always feasible due to incredibly low intensity. With the development of infrared absorption spectroscopy, the Raman spectroscopy dwindled rapidly in importance between 1940-1960. The advent of lasers as high power monochromatic sources, coupled with technical advances in spectrometer and detectors, modernized the Raman spectroscopy. Today Raman spectroscopy serves as a unique tool for investigating the molecular structures of inorganic-, organic-, and biological-molecules in solutions and solids (12-14).

The Raman process is an inelastic light scattering phenomenon. In the Raman effect the original photon energy $h\nu_0$ may be either reduced or augmented. If the frequency of the incident light is ν_0 and that of a component of the scattered light is ν_r, then the frequency shift $\Delta\nu$ $\nu_r - \nu_0 = \Delta\nu$ is referred to as a Raman frequency. A frequency shift is equivalent to an energy change $\frac{\Delta E}{h}$. Although the activity of a paticular vibrational mode in the infrared region is dependent upon

whether or not there is a change in the dipole moment during the vibration, for a mode to be Raman active there must be a change in the polarizability of the molecule during the vibration. The vibrations observed in the Raman spectra have the following characteristics.

1. The stretching vibrational bands of homopolar covalent bonds are strong in the Raman. (C=C, C≡C, S-S, N-N)
2. The C-S and S-H stretching vibrations are relatively strong in the Raman.
3. The O-H vibrations are weak in the Raman compared to C-H and N-H vibrations.
4. The vibrational modes due to the aromatic ring are particularly strong in the Raman.

The Raman and infrared spectra are not alternatives but complemental, both being necessary if the maximum amount of information is to be obtained about molecular vibrations. Both methods have each advantages, respectively, but there are several clear merits which favor the use for Raman as listed below.

1. Water gives rise to very weak Raman scattering, so the Raman spectra of aqueous solution can be readily obtainable, while there are strong absorption in the infrared region.
2. The laser-excitation permits the use of small quantities of sample. Further, the sample can be any conventional shape and need not be transparent to the laser radiation.
3. Glass is almost completely transparent in the visible region, and so a very good material for sample tubes and capillaries.
4. Resonance Raman scattering makes possible to observe the spectra of solutions at high dilution (10^{-3}-10^{-5} M).

Raman spectra observed when the exciting frequency approaches or enters the region of electronic (vibronic) absorption of the molecule are called resonance Raman spectra. The general theory of the effect is rather well developed, but it is only recently that experimental data have been obtained on the rigorous resonance Raman effect in liquids. This resonance enhancement effect has extended markedly the usefulness of the Raman spectroscopy. As a consequence of resonance enhancement

of Raman scattering intensities the vibrational frequencies of biological chromophores and their model compounds, organometallic and coordination compounds., etc. may be easily detectable even at highly dilute concentrations.

Resonance Raman enhancement could be predicted from the Kramers -Heisenberg-Dirac dispersion equation used by van Vleck. This equation is described below

$$(\alpha_{ij})_{mn} = \sum_e \left[\frac{(M_j)_{me}(M_i)_{en}}{\nu_e - \nu_o + i\Gamma_e} + \frac{(M_i)_{me}(M_j)_{en}}{\nu_e + \nu_r + i\Gamma_e}\right] \text{----------(i)}$$

Here i,j are suffices defining the tensor components in the molecular coordinate system, and m,n are the initial and final states of the molecule while e is an excited state. The summation is over all the intermediate levels e. M's are the components of the transition moments along the directions j and i, from m to e, while ν_e is the frequency of the transition from m to e, and ν_o and ν_r are the frequencies of the incident and scattered photons. If ν_o approaches a vibronic transition frequency, ν_e, the corresponding term in Eq. (i) becomes dominant and this situation is reflected in the resonance Raman scattering. The magnitude of resonance enhancement is predicted to vary directly with the oscillator strength of the resonant electronic transition and inversely with its breadth. Then maximal resonance effects could be expected for strong sharp absorption bands. The frequency dependence of scattered intensity and the depolarization measurements have been usufully applied to elucidate the electronic structures of some molecules, solvent and substituent effects, and to interprete the Raman spectra of colored substances. In fact, the resonance Raman effect is a sensitive method of studing the structural changes in molecules and excited electronic states can successfully supplement absorption and fluorescence studies.

Raman spectroscopy has been employed widely to study proteins nucleic acids, lipids and more complex biological materials, such as membranes, and viruses (15-19). Since water gives rise to very weak Raman scattering, it is easy to measure the Raman spectra of biological materials in aqueous solution. In addition, Raman scattering can be measured both in crystal state and solution, so that Raman spectral

data is combined with X-ray data. The resonance Raman effect is now being applied profitably as a useful probe to investigate biological chromophores at physiological condition.

3. Resonance Raman Scattering of Hemoproteins

Among the many active works concerned with biological applications of Raman scattering, resonance Raman studies of hemoproteins have been invaluablely successful (15-20). Resonance Raman spectra of hemoproteins were first presented by Spiro et al.(21,22) and Brunner et al.(23) in 1972. Since then, resonance Raman studies of hemoproteins and porphyrins have been extensively pursued in several laboratories. Today, resonance Raman scattering has become a powerful tool of investigating a number of hemoproteins. It was just favorable that the heme group has strong absorption bands in the visible and near-ultraviolet region where there are many exciting lines (457.9-514.5 nm) of argon laser, the currently most common Raman light source. The vibrational modes of the heme can be observed in aqueous solution at high dilution (10^{-3}-10^{-5} M) without interference from the protein. Resonance Raman studies of hemoproteins have two main aspects, the mechanism of resonance Raman scattering and structural monitor of the heme group. In the former view a great deal of interest has been created by the first observation of the phenomenon of inverse polarization scattering (24). Peticolas and coworkers (25) and Spiro and coworkers (26) have demonstrated the measurement of the reversal coefficient that would permit the determination of the three invariants of the anisotropy of the general scattering tensor using circularly polarized excitation as well as the depolarization ratio. They concluded that several resonance Raman bands of cytochrome c are of mixed symmetry and the effective symmetry of the heme chromophore is significantly lower than D_{4h} or C_{4v}. Excitation profiles for HbO_2 (27) and reduced cytochrome c (24) showed that the resonance enhanced bands reach intensity maxima at the center of the α band. They reach second intensity maxima within the β band envelope, but at different positions. This latter phenomenon reflects resonance scattering from individual 0-1 vibronic levels ($\nu_e + \Delta\nu_{excited} = \nu_0$)

of the β band, since little frequency change is expected for the porphyrin skeletal vibrations in the excited state. The most intense Raman bands from high-frequency (1100-1650 cm^{-1}) porphyrin ring modes, involve contributions from the stretching of C-C and C-N bonds and the bending of C-H bonds at the methine bridges. The assignments of the Raman lines to the individual vibrational modes has been performed by measuring the Raman spectra of highly symmetric metallo-porphyrins including meso-deuterated (28) and ^{15}N-substituted (29) derivatives of metallo-octaethylporphyrins. In addition a normal coordinate analysis have been carried out for nickel-octaethylporphyrin (29). These assignments are essential in order to discuss the detailed relationships between the Raman spectra of hemoproteins and the structures of their heme groups.

Some of the Raman lines display characteristic frequency shifts when the heme oxidation or spin state is changed (30-32). Some empirical rules have already been established regarding the Raman lines sensitive to the oxidation and/or spin states of the heme iron. Four kinds of typical Raman spectra of hemoproteins were shown in Fig. 3. Deoxy Mb is in a ferrous high spin state (S=2), cytochrome b_5 in a ferrous low spin state (S=0), MbF in a ferric high spin state (S=5/2) and MbCN in a ferric low spin state (S=1/2). It is fairly feasible to decide the oxidation and spin state of hemoprotein by measuring the resonance Raman spectrum. The oxidation state marker Raman line which is due to the ring vibration of pyrrole accompanied with in-phase displacement of the four nitrogens toward the heme iron is markedly valuable to examine the feature of iron-igand bond (29). This Raman line is usually located between 1355 and 1364 cm^{-1} for ferrous hemoproteins and between 1370 and 1375 cm^{-1} for ferric compounds. However, it must be kept in mind that several kinds of hemoproteins in ferrous low spin state such as HbO_2, HbCO, and $HbNCC_2H_5$ also give the Raman spectra of the ferric low spin type. Kitagawa, et al. suggested that there are two kinds of ferrous low spin states (32). They are specified by the binding nature of the sixth ligand to heme iron. The iron-ligand bond in HbO_2, HbCO, and $HbNCC_2H_5$ is of π type while that in ferrous cytochromes b_5 and c is of σ type.

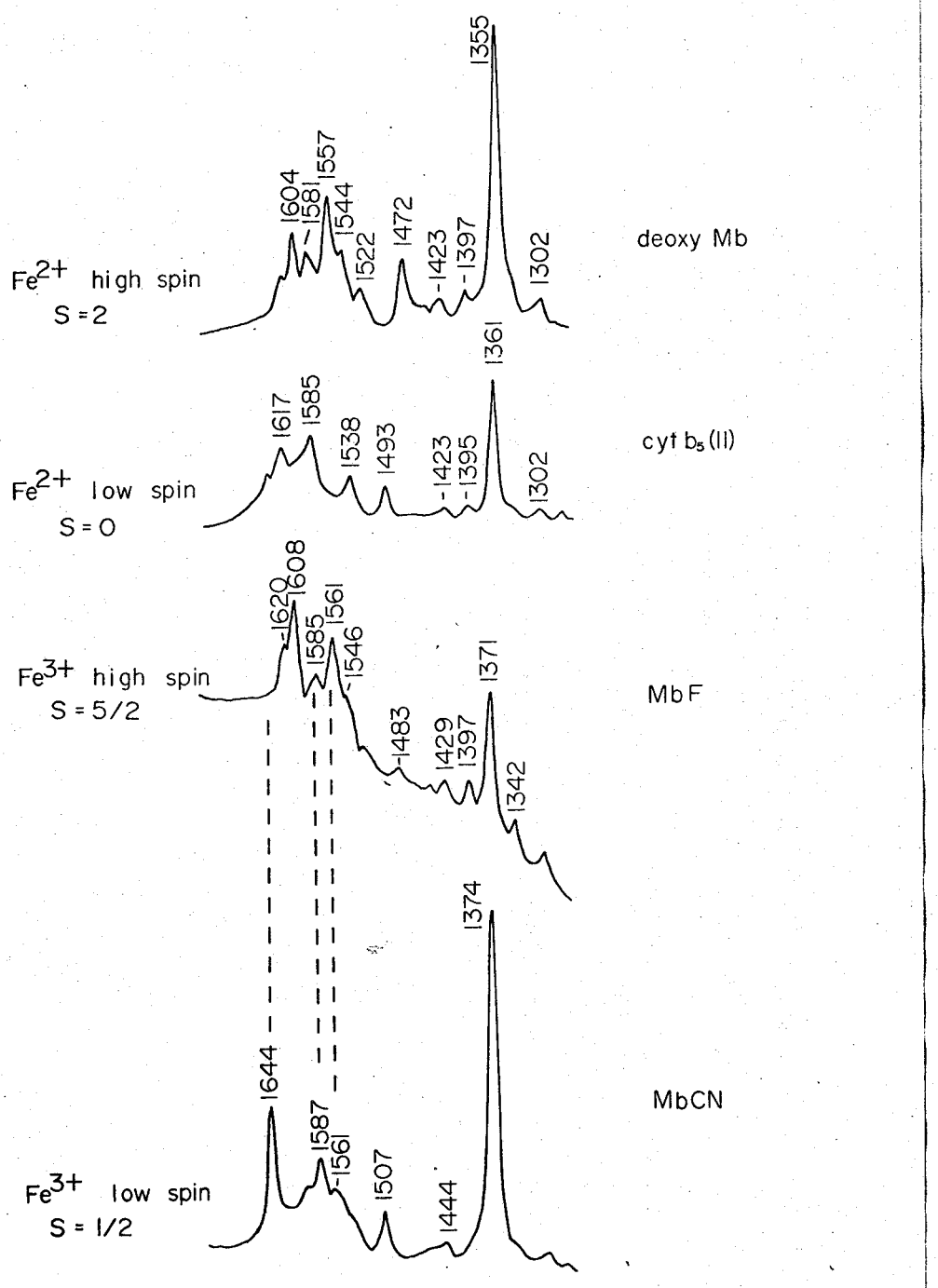

Fig. 3 Four kinds of typical Raman spectra of hemoproteins.

The frequency of Band IV of horseradish peroxidase (HRP) compound II was higher than that of any Fe^{3+} hemoproteins studied so far, suggesting an Fe^{4+} state (33,34). The anomaly of this Raman line was found for cytochrome P-450 (35,36) and chloroperoxidase (37). It is one of the main purposes of this thesis to elucidate this anomaly. The Raman lines near 1565 cm^{-1} (ferric) and 1540 cm^{-1} (ferrous) are sensitive to the replacement of the sixth ligand (38). The Raman line around 1540 cm^{-1} of ferrous carboxymethyl-methionyl cytochrome c (alkyl-c) was shifted sensitively with pH despite the negligible change of the oxidation state marker or other bands (39). The change in the spectrum was associated with the status change of lysine. The spin state marker Raman line near 1620 cm^{-1} associated primarily with methine-bridge CC-stretching vibrations are also quite useful to discuss the structural difference among the various ferric high spin type hemoproteins (40,41). The Raman line is located around 1640 cm^{-1} for ferric low spin hemes whereas this line is widely spread among ferric high spin hemes. Ferric high spin complexes of Mb yielded the Raman line around 1610 cm^{-1} however, oxidized P-450, native horse radish peroxidase, and Type II of cytochrome c' give rise to between 1625 and 1631 cm^{-1} (41). Further this line of Type I of cytochrome c' was observed unusually at high frequency (1637 cm^{-1}). This wide spread of the frequencies can be explained by the fact that the heme irons are generally located out of the porphyrin plane in the high spin state and the exact distance between the heme iron and the fifth ligand might be inherent in individual hemoproteins. It would be desirable to monitor features of the axial ligation of the heme group through measurement of axial-ligand vibrational frequencies, but such modes are at best very weak in the resonance Raman spectra. The one confirmed axial ligand mode so far observed was the Fe-O stretching mode of HbO_2 at 567 cm^{-1} (42). Its relatively high frequency suggests an unusually strong bond, consistent with the short Fe-O distance found for the O_2 adduct of Collman's "picket fence" porphyrin. Champion et al. insisted that the Raman line at 691 cm^{-1} of oxidized $P\text{-}450_{cam}$ was due to the C-S stretching vibration of a cystein axial ligand. The out of-plane iron-axial ligand mode is rather easely observed for model compounds. The iron-ligand

stretching bands were clearly detected for iron-porphyrins and chlorins in high and low spin states. A more careful measurement, using a variety of laser wavelength, will reveal other iron-ligand modes which would provide more direct information on structural features of the heme moiety.

4. Nitrogen-15 Nuclear Magnetic Resonance Spectroscopy

Another powerful method of studing the nature of metal-axial ligand bonding is nuclear magnetic resonance spectroscopy (43-45). In the last twenty years or so NMR has become one of the principal techniques for investigations of the molecular structures and dynamic properties of inorganic-, organic-, and biological molecules. The rapid development of NMR has had a strong influence on almost all field of chemistry and biochemistry. In recent years NMR has undergone a revolutionary change intechnique from swept to pulsed excitation coupled with Fourier transform system (46,47). Majar advantages of the Fourier transform NMR are enhanced sensitivity and tremendous saving in the time required to obtain the NMR signal. As a result of the time saving the Fourier transform technique has distinct advantages for studing such phenomena as unstable species, chemical exchange rates, molecular dynamics, and T_1 and T_2 relaxation times of each of the resonance lines in a spectrum.

The introduction of the superconducting proton NMR spectrometers highly improved the sensitivity for detection of the NMR signals of a given nucleus. Since the chemical shifts increase with H_0 (Magnetic field) and the spin-spin coupling constants J are independent of the field, by the use of spectrometers operating at 220 MHz and higher frequencies it became possible to resolve and identify the resonances of individual protons in biological macromolecules (48,49).

In addition to ^{1}H-NMR the studies with a considerable variety of another nuclei including ^{13}C, ^{15}N, ^{31}P, etc. have been pursued extensively. ^{13}C-NMR permits direct observation of the skeletons of organic compounds and certain carbon-containing functional group with no protons attached (50). ^{31}P is well suited for NMR experiments because the chemical shift range for ^{31}P extends over more than 700 p.p.m. and the

natural line width are smaller than for protons, ^{31}P-NMR promises to be of particular value in the study of organo-phosphorus compounds, nucleic acids, and phospholipids (51). NMR experiments with other nuclei can be also of much interest for certain chemical and biological investigations. In this thesis the discussion is focused on ^{15}N-NMR (52). Nitrogen has a variety of valence states with various types of bonding and stereochemistry. There can be no doubt that nitrogen is one of the most dominant atoms in organic-, inorganic-, and bio-molecules. It is special emphasis that nitrogen is generally located at the sites of hydrogen bond of coordination bond. Thus ^{15}N-NMR, very young field of spectroscopy, has the extensive possibility of giving the direct and specific informations about the interactions of biological importance. In spite of its significance, the development of ^{15}N-NMR was rather slow, mainly because of the experimental difficulties arising from the low NMR sensitivity and natural abundance of ^{15}N. The sensitivity of the ^{15}N nucleus is 0.00104 relative to that of ^{1}H for equal numbers of nuclei at the same magnetic field. In natural abundance nitrogen exists in two isotopic forms, the most common is ^{14}N which has an abundance of 99.635% while the abundance of ^{15}N is 0.365%. Both of these isotopes may be studied by means of NMR, however, the line broadening due to the nuclear quadrupole moment of ^{14}N may obscure small chemical shift differences and disturb the appearances of spin-spin coupling between nitrogen and other nuclei. Thus this application of ^{14}N-NMR to biological systems is severely limited. The isotopic enrichment of ^{15}N is usually desirable to detect the high signal-to-noise ratio spectrum easely, although it is rather expensive. The range of nitrogen chemical shifts is 900 p.p.m. and may be even larger for paramagnetic complexes. NO_3^- is one of the commonly used standards. Structural correlations of nitrogen chemical shifts in representative groups of organic molecules have been considerably discussed, however, theoretical interpretation of nitrogen chemical shifts are fairly difficult. No satisfactory theoretical explanations have so far been offered for nitrogen chemical shifts. Saika and Slichter (53) have considered σ (nitrogen chemical shift) to consist of three components.

$$\sigma = \sigma_D + \sigma_P + \sigma_A$$

where σ_D and σ_P represent the diamagnetic and paramagnetic contributions from the electrons associated with the atom containing the nucleus and σ_A refers to the contribution from the other electrons in the molecule. Spin-spin couplings with ^{15}N such as ^{15}N-^{1}H and ^{15}N-^{13}C have been observed in a number of nitrogen-containing molecules. The vicinal coupling constant ^{3}J (^{15}N-H) is useful for the determination of the angle of the peptide bonds. The relaxation times for ^{15}N are generally long, so that ^{15}N-NMR gives sharp linewidths. The long relaxation times sometimes need the long pulse interval.

Currently ^{15}N-NMR has been applied to many biological substances from small amino acids to proteins (48). The pH titrations of chemical shifts and confomational dependence of the coupling constants of amino acids were studied at first. Small peptides were also suited materials for ^{15}N-NMR. Most of the amino acid and a selection of model peptide ^{15}N-NMR spectral data are quite well established by now. ^{15}N-NMR has already made useful contribution to the conformational studies of peptides. The recent progress of NMR instrumentation makes it possible to measure the ^{15}N-NMR of proteins and transfer RNA at natural abundance, although the method requires large sample volumes and high solute concentrations.

^{15}N-NMR of organic and inorganic molecules has been also studied by many authors (52). As for porphyrins and their related compounds, Katz et al. were successful in measuring the ^{15}N-NMR of chlorophyll-a indirectly by heteronuclear double resonance (54). Since then ^{15}N-NMR studies of porphyrins have been actively pursued by several groups (55-59). ^{15}N-NMR seems to be very unique and important because nitrogen atoms of the pyrrole rings in porphyrins are located at the sites coordinated to the central metal or interacted to the inner hydrogens. The nature of the metal-axial ligand bond may have strong influence on the chemical shift and line width of the ^{15}N resonance. ^{15}N-NMR also plays an important role in the study of tautomerism of porphyrins.

4. Purposes and Scope of This Thesis

This thesis is concerned with the spectroscopic studies on the nature of the metal-axial ligand of hemoproteins and their model compounds. The author took up resonance Raman spectroscopy and ^{15}N -nuclear magnetic resonance spectroscopy as powerful tools of investigating the studies. This thesis is divided into two parts.

PART I deals with the resonance Raman studies of various hemoproteins. The usefulness and uniqueness of resonance Raman scattering in studing hemoproteins are emphasized.

An anomaly in the resonance Raman spectra of cytochrome P-450 are analyzed and a Raman evidence for the strong π basicity of the fifth ligand in their reduced state is presented in Chapter 1. of PART I. The P-450 gave the so called "oxidation state marker" (Band IV) at unusually low frequencies in the reduced state and its CO-complex. This anomaly is explained by assuming the large delocalization of electrons from the fifth ligand to the porphyrin $\pi^*(e_g)$ orbital. The significance of the $d_\pi(Fe^{2+})$ orbital-$Py(S^-)$ orbital- $\pi^*(e_g$, porphyrin) orbital interaction is discussed in detail for reduced form. The two types of reduced P-450 are also discussed in connection with the iron (Fe^{2+})-ligand (S^-)distance. The iron-ligand interaction and the distortion of the heme controled by the apoprotein are examined for oxidized P-450.

Chapter 2. demonstrates the sensitivity of the method to the status change of the ligand and to spin states of the heme iron; resonance Raman spectoroscopy is applied to analyze the spin-state equilibrium in the acid-base transition of ferric Mb. Direct evidence of the existence of two molecular species at alkaline pH is presented for the first time. It is shown that the prominant species is the high spin state and both the high and low spin forms of MbOH are structurally different from MbH_2O. It is also pointed out that the intensity ratio of the Raman lines in the lower frequency region is dependent upon the planarity of the heme group.

Chapter 3. studies the characteristics of Raman spectra of various C-type cytochromes and their classification. The assignment of several

Raman lines which are used as structural monitors are established on the basis of the previous works of Kitagawa et al. (28). It is elucidated from the frequency of the oxidation state marker that the sixth ligand binds to the heme iron mainly through the σ type interaction in the reduced C-type cytochromes. By the relative intensity of Raman lines the Raman spectra of reduced C-type cytochromes are apparently classified into two group. The excitation profile of the representatives of two groups are examined to clarify the apparent classification.

The pH dependence of resonance Raman spectra are studied for ferric and ferrous various C-type cytochromes in Chapter 4. It is the purpose of this Chapter to establish an empirical rule which relate the pH induced changes of the resonance Raman spectra of various C-type cytochromes with structure changes around their heme moieties. The detail model compound studies are performed carefully to investigate the effect of the replacement of the axial ligand and hydrophobicity in the heme pocket upon the resonance Raman spectra. It is elucidated that the frequencies of the 1565 cm^{-1}(ferric) and 1539 cm^{-1}(ferrous) are sensitive to the replacement of the sixth ligand while the intensity ratio 1587 cm^{-1}/1561 cm^{-1} are sensitive to hydrophobicity of the heme moieties.

The structural characterization of the spectral alterations of cytochrome c' has currently been a matter of physicochemical concerns. There are two and three, at least, spectroscopically distinguishable forms in the reduced and oxidized states, respectively (60). In Chapter 5. the resonance Raman spectra of cytochrome c' and the structure changes of its heme moiety upon the pH change and additions of detergent or alcohols are investigated. The reason why the frequencies of the methine-bridge CC-stretching modes are widely spread among the high spin hemes including those of Type I and Type II of cytochrome c' is discussed in connection with the change of electron distribution among the heme iron, porphyrin ring, and the fifth ligand and structural difference around the heme iron-ligand bonding.

Octaethylchlorin (OEC) is a profitable model compound of chlorophyll and heme d. Chapter 6. investigates the resonance Raman spectra of

metal complexes of OEC. The effects of the saturation of one of the conjugated bond on the vibrational spectra are examined carefully and the assignment of the Raman lines of metallo-octaethylchlorin is performed on the basis of the observed frequency shifts upon the γ,δ -meso-deuteration and ^{15}N substitution of the four pyrrole nitrogens. The similarity and difference between the resonance Raman spectra of M(OEC) and M(OEP) is also discussed in this chapter. In addition the axial-ligand band is clearly detected for Fe^{3+}(OEC) in high and low spin states. These studies on chlorins provides a basic knowledge for the analysis of the resonance Raman spectra of chlorophyll and heme d.

PART II takes up the ^{15}N-NMR studies of metallo-octaethylporphyrins M(OEP). ^{15}N-NMR presents novel informations on the structural investigations of metallo-porphyrins.

Chapter 1. of PART II deals with the ^{15}N-NMR spectra of various metal complexes of ^{15}N-enriched octaethylporphyrin. The anomaly of ^{15}N resonance position of Ni(OEP) is discussed in connection with the results of the absorption and infrared spectra. $^{15}N_4$-Fe^{2+}(OEP) and $^{15}N_4$-Co^{3+}(OEP) with axial ligands are taken up as model compounds of hemoproteins and vitamin B_{12}, respectively. It can be expected that the ligand substitution at the fifth and sixth coordination positions would induce the chemical shift change of ^{15}N nuclei. Thus it was shown that the feature of axial ligand-metal bond could be examined by the use of ^{15}N-NMR for Fe^{2+}(OEP) and Co^{3+}(OEP).

Nitrogen-15 nuclear magnetic resonance spectroscopy is applied to the investigation of paramagnetic species of porphyrin in Chapter 2. The NMR studies succeeded in detecting a trace amounts of molecular species of Ni(OEP) which was not found by electronic absorption and resonance Raman spectra. In pyridine - chloroform mixed solution $^{15}N_4$-Ni(OEP) showed marked shifts of the resonance signalof the pyrrole nitrogens to lower field as well as greater broadening of resonance. These shift and broadening can be explained by assuming the presence of paramagnetic species which is formed as a consequence of the addition of two axial ligands.

REFERENCES

1. Chance, B., Estabrook, R. W., and Yonetani, T. eds. (1966) "Hemes and hemoproteins" Academic Press, New York.
2. Okunuki, K., Kamen, M. D., and Sekuzu, I., eds. (1968) "Structure and Function of Cytochromes" Univ. Tokyo Press, Tokyo.
3. Chance, B., Yonetani, T., and Mildvan, A. S., eds. (1971) "Probes of Structure and Function of Macromolecules and Membranes" Vol. II, Academic Press, New York.
4. Kotani, M., ed. (1978) "Advances in Biophysics" Vol.11, Univ. Tokyo Press, Tokyo.
5. Antonini, E. and Brunori, M., eds. (1971) "Hemoglobin and Myoglobin in Their Reactions" North-Holland, Amsterdam.
6. Lemberg, R. and Barrett, J., (1972) "The Cytochromes" Academic Press, New York.
7. Eichhorn, G. I., ed. (1973) "Inorganic Biochemistry" Vol. 2, Elsevier Scientific Publishing Company, Amsterdam.
8. Hayaishi, O., ed. (1974) "Molecular Mechanisms of Oxygen Activation" Academic Press, New York.
9. Maltempo, M. M. (1976) Biochim. Biophys. Acta, 434, 513.
10. Strekas, T. C. and Spiro, T. G. (1974) Biochim. Biophys. Acta, 351, 237.
11. Sato, R., Satake, H., and Imai, Y. (1973) Drug Metab. Dispos. 1, 6.
12. Szymanski, H. A., ed. (1967) "Raman Spectroscopy" Plenum Press, New York.
13. Gilson, T. R. and Hendra, P. J., (1970) "Laser Raman Spectroscopy" Wiley-Interscience, London.
14. Anderson, A. ed. (1971) "The Raman Effect" Marcel Dekker, New York.
15. Thomas, Jr. G. J. (1975) "Raman Spectroscopy of Biopolymers" in Vibrational Spectra and Structure, (Durig, J. R. ed.) Vol. 3, 239, Mercel Dekker, New York.
16. Spiro, T. G. (1974) "Chemical and Biological Applications of Lasers" (Moore, B. ed.) Academic Press, New York.
17. Spiro, T. G. and Gaber, B. P. (1977) "Laser Raman Scattering as a Probe of Protein Structure" in Ann. Rev. Biochem. 46, 553.

18. Thomas, Jr. G. J. and Kyogoku, Y. (1977) "Biological Sciences" in Vibrational Spectroscopy (Practical Spectroscopy Series, Vol.1, Brame, Jr. E. G. and Grasse-li, J. G. eds.) Mercel Dekker, New York.
19. Spiro, T. G. (1976)"Biochemical Applications of Resonance Raman Spectroscopy" in Vibrational Spectra and Structure, (Durig, J. R. ed.) Vol. 5, 101, Marcel Dekker, New York.
20. Spiro, T. G. (1975) Biochim. Biophys. Acta, 416, 169.
21. Strekas, T. C. and Spiro, T. G. (1972) Biochim. Biophys. Acta, 263, 830.
22. Strekas, T. C. and Spiro, T. G. (1972) Biochim. Biophys. Acta, 278, 188.
23. Brunner, H., Mayer, A., and Sussner, H. (1972) J. Mol. Biol. 70, 153.
24. Spiro, T. G. and Strekas, T. C. (1972) Proc. Natl. Acad. Sci. U. S. 69, 2622.
25. Pezolet, M., Nafie, L. A., and Peticolas, W. L. (1973) J. Raman Spectrosc., 1, 455.
26. Nestor, J. and Spiro, T. G. (1973) J. Raman Spectrosc., 1, 539.
27. Strekas, T. C. and Spiro, T. G. (1973) J. Raman Spectrosc., 1, 197.
28. Kitagawa, T., Ogoshi, H., Watanabe, E., and Yoshida, Z. (1975) J. Phys. Chem. 79, 2629.
29. Kitagawa, T., Abe, M., Kyogoku, Y., Ogoshi, H., Sugimoto, H., and Yoshida, Z. (1977) Chem. Phys. Lett., 249.
30. Yamamoto, T., Palmer, G., Gill, D., Salmeen, I., and Rimai, L. (1973) J. Biol. Chem. 248, 5211.
31. Spiro, T. G. and Strekas, T. C. (1974) J. Am. Chem. Soc. 96, 338.
32. Kitagawa, T., Kyogoku, Y., Iizuka, T., and Saito, M. (1976) J. Am. Chem. Soc. 98, 5169.
33. Felton, R. H., Romans, A. Y., Yu, N. T., and Schonbaum, G. R. (1976) Biochim. Biophys. Acta, 434, 82.
34. Rakhit, G., Spiro, T. G., and Uyeda, M. (1976) Biochem. Biophys. Res. Commun., 71, 803.
35. Ozaki, Y., Kitagawa, T., Kyogoku, Y., Shimada, H., Iizuka, T., and Ishimura, Y. (1976) J. Biochem. 80, 1447.

36. Ozaki, Y., Kitagawa, T., Kyogoku, Y., Imai, Y., Hashimoto-Yutsudo, C., and Sato, R., submitted to J. Am. Chem. Soc.
37. Champion, P. M., Remba, R., Chiang, R., Fitchen, D. B., and Hager, L. P. (1976) Biochim. Biophys. Acta, 446, 486.
38. Kitagawa, T., Ozaki, Y., Teraoka, J., Kyogoku, Y., and Yamanaka, T. (1977) Biochim. Biophys. Acta, 494, 100.
39. Ikeda-Saito, M., Kitagawa, T., Iizuka, T., and Kyogoku, Y. (1975) FEBS Lett. 50, 233.
40. Spiro, T. G. and Burke, J. M. (1976) J. Am. Chem. Soc. 98, 5482.
41. Kitagawa, T., Ozaki, Y., Kyogoku, Y., and Horio, T. (1977) Biochim. Biophys. Acta, 495, 1.
42. Brunner, H. (1974) Naturwissenschaften 61, 129.
43. Pople, J. A., Schneider, W. G., and Bernstein, H. J., (1959). "High Resolution NMR" McGraw-Hill, New York.
44. Carrington, A. and McLachlan, A. D. (1967) "Introduction to Manetic Resonance with Applications to Chemistry and Chemical Physics" Harper and Row, New York.
45. Bovey, F. A. (1969) "Nuclear Magnetic Resonance Spectroscopy" Academic Press, New York.
46. Farrar, T. C. and Becker, E. D. (1971) "Pulse and Fourier Transform NMR" Academic Press, New York.
47. Shaw, D. (1976) "Fourier Transform N.M.R. Spectroscopy" Elsevier Scientific Publishing Company, Amsterdam.
48. Wüthrich, K. (1976) "NMR in Biological research" North-Holland, Amsterdam.
49. James, T. L. (1975) "Nuclear Magnetic Resonance in Biochemistry" Academic Press, New York.
50. Stothers, J. B., (1972) "Carbon-13 NMR Spectroscopy" Academic Press, New York.
51. Crutchfield, M. M., Dungun, C. H., Letcher, J. H., Mark, V., and Van Wazer, J. R., (1967) "^{31}P Nuclear Magnetic Resonance" J. Wiley New York.
52. Witanowski, M., and Webb, G. A. (1972) "Nitrogen NMR" Plenum Press, London.
53. Saika, A. and Slichter, C. P. (1954) J. Chem. Phys. 22, 26.

54. Boxer, S. G., Closs, G. L., and Katz, J. J. (1974) J. Am. Chem. Soc., 96, 7058.
55. Irving, C. S. and Lapidot, A., (1977) J. Chem. Soc. Chem. Comm., 184.
56. Kawano, K., Ozaki, Y., Kyogoku, Y., Ogoshi, H., Sugimoto, H., and Yoshida, Z., (1977) J. Chem. Soc. Chem. Comm. 226.
57. Gust, D. and Roberts, J. D., (1977) J. Am. Chem. Soc., 99, 3637.
58. Yeh, H. J. C., and Sato, M., and Morishima, I., (1977) J. Magn. Resonance, 26, 365.
59. Kawano, K., Ozaki, Y., Kyogoku, Y., Ogoshi, H., Sugimoto, H., and Yoshida, Z. J. Chem. Soc. Perkin II in press.
60. Imai, Y., Imai, K., Sato, R., and Horio, T. (1969) J. Biochem. 65, 225.

PART I Resonance Raman Studies on the Nature of the Metal-axial Ligand Bond in Hemoproteins and Their Model Compounds.

Chapter 1.

Resonance Raman Spectra of Cytochrome P-450. A Raman Evidence for the Strong π Basicity of the Fifth Ligand in Their Reduced State.

ABSTRACT

The resonance Raman spectra were observed for the cytochrome P-450 (P-450), their catalitically inactive form (P-420) and their heme-CO complex (P-450·CO and P-420·CO). The proteins obtained from Pseudomonas putida ($P\text{-}450_{cam}$), and from the phenobarbital-treated rabbit liver microsomes (PB P-450 and PB P-448) and the 3-methylcholanthlene-treated one (MC P-448), gave the so called oxidation state marker (Band IV) at unusually low frequencies in the reduced state. This demonstrated large delocalization of electrons to the porphyrin $\pi^*(e_g)$ orbital and accordingly the strong π basicity of the fifth ligand. The ferquency of Band IV of P-450·CO was also markedly lower than those of HbCO and MbCO. The characteristic features observed for reduced P-450 and P-450·CO disappeared upon the conversion to P-420 and P-420·CO, respectively, suggesting the $d_\pi(Fe^{2+})$-$p_y(S^-)$-$\pi^*(e_g$, porphyrin) interactions would disappear. Oxidized PB P-450 exhibited the Raman spectrum of typical ferric low spin type while those of oxidized $P\text{-}450_{cam}$, PB P-448, and MC P-448 were of ferric high spin type. The two types of P-450 were also distinguished definitely in the reduced state. Reduced PB P-420 converted by the laser illumination, provided two sets of Raman lines and consequently was inferred to be a mixture of high spin and low spin species. The Raman spectra of reduced $P\text{-}450_{cam}$·metyrapone and $P\text{-}450_{cam}$·pyridine complexes were closely similar to that of ferrous cytochrome b_5.

INTRODUCTION

Cytochrome P-450 (P-450) is a class of protoheme-containing monoxygenase which catalyze the hydroxylation reaction involved in detoxification, drug metabolism, carcinogenesis, and steroid biosynthesis

(1). The heme-CO complex of its catalitically active form (P-450·CO) gives rise to the Soret band near 450 nm, at the wavelength ca. 30 nm longer than the usual heme-CO complexes. Elucidation of the spectral anomaly in terms of structural characteristics of the heme moiety has currently been a matter of physicochemical as well as organochemical concerns.

The EPR spectrum of P-450 in the ferric low spin state was nearly reproduced by the synthetic iron-porphyrins having a thiolate anion (RS^-) and an arbitrary N base as two axial ligands of the heme iron (3-6). For the oxidized P-450 in the presence of substrate, on the other hand, the synthetic analogues suggested the penta-coordinated high spin state with RS^- as the fifth ligand (3,5). The conclusion was supported by Mössbauer (4) and MCD studies (7). As to the ferrous state, the NMR (8) and Mössbauer spectra (9) of camphor P-450 ($P\text{-}450_{cam}$) with substrate indicated the presence of the high spin ferrous iron (8). The characteristic Soret band of P-450·CO was provided by the synthetic analogues with RS^- but not N-base as the trans ligand of CO (10-13). The MCD studies (14-16) reached almost the same conclusion.

The resonance Raman spectra of hemoproteins have revealed the vibrational spectra of the iron-porphyrin in situ interacting with the immediate environment (17). The frequency of so called "oxidation state marker" (referred to as Band IV hereafter as in Ref. 18) distinguished two types (σ or π) of iron-ligand interactions, that is, d_{z^2} (Fe)-lone pair (ligand) and d_π(Fe)-π^*(ligand) interactions for ferrous low spin hemoproteins (18). The study of the ^{15}N enriched iron-porphyrin has clarified the assignment of Band IV and elucidated qualitatively the reason why the frequency of Band IV reflects the amount of electrons delocalized to the porphyrin $\pi^*(e_g)$ orbital (19). Thus one may expected that the resonance Raman spectra of P-450 are characterized by the strong π basicity of the thiolate anion of its fifth ligand as deduced by other methods.

Recent advances in the purification techniques of P-450, on the other hand, enabled us to specify the molecular species of the P-450 (20-26). Accordingly, in the present study, the resonance Raman spectra of P. putida $P\text{-}450_{cam}$, phenobarbital-induced microsomal P-450

(PB P-450 and PB P-448), 3-methylcholanthrene-induced microsomal P-450 (MC P-448), their catalitically inactive form and their heme-CO complexes (P-450·CO and P-420·CO) were observed. The intact oxidized PB P-450 contains the ferric low spin heme whereas intact $P\text{-}450_{cam}$, PB P-448, and MC P-448 do the ferric high spin one.

EXPERIMANTAL

Pseudomonas putida P-450 ($P\text{-}450_{cam}$)

The $P\text{-}450_{cam}$ was purified from camphor-grown Pseudomonas putida by a similar method to that described by Peterson (20). The details will be described elsewhere (21). The purity of the $P\text{-}450_{cam}$, estimated by the ratio of absorbances at 392 nm/ 280 nm (27), was 1.1. The concentration of $P\text{-}450_{cam}$ was determined spectrophotometrically using ε_{mM}^{392}=87.0 of the high spin ferric form (28). $P\text{-}420_{cam}$ was prepared by the treatment of ca. 0.1 mM $P\text{-}450_{cam}$ solution with 23% V/V acetone at room temperature in the absence of D-camphor according to the method of Yu and Gunsalus (29). For the measurement of Raman spectra, 0.1 mM $P\text{-}450_{cam}$ in potassium phosphate buffer (50 mM, pH 7.4) with D-camphor was used.

Rabbit liver microsomal P-450 (PB P-450, PB P-448, and MC P-448)

The PB P-450 and PB P-448 were isolated from liver microsomes of the phenobarbital-treated rabbits and were purified by the method of Imai and Sato (22,23). The MC P-448 was obtained from the 3-methylcholanthrene-treated rabbit by the method of Hashimoto and Imai (26). The proteins were dissolved in 100 mM potassium phosphate buffer (pH 7.25) containing 20% (V/V) glycerol. In the case of PB P-450, buffer contained also 0.2% (W/V) Emalgen 913. Equine muscle Mb (Sigma Type I) was purified on CM cellulose column. $MbSCH_3$ was formed by adding excess $NaSCH_3$ to 0.7 mM Mb solution in 0.01 M phosphate buffer. Iron-protoporphyrin chloride $Fe^{3+}(PP)Cl$ was obtained as 0.5 mM bovine hemin (Sigma Type I) in 0.1% SDS aqueous solution.

Procedures

Upon the measurement of Raman spectra, 100 µl of the 0.02-0.2 mM P-450 solution was put in the cylindrical cell. The laser light was

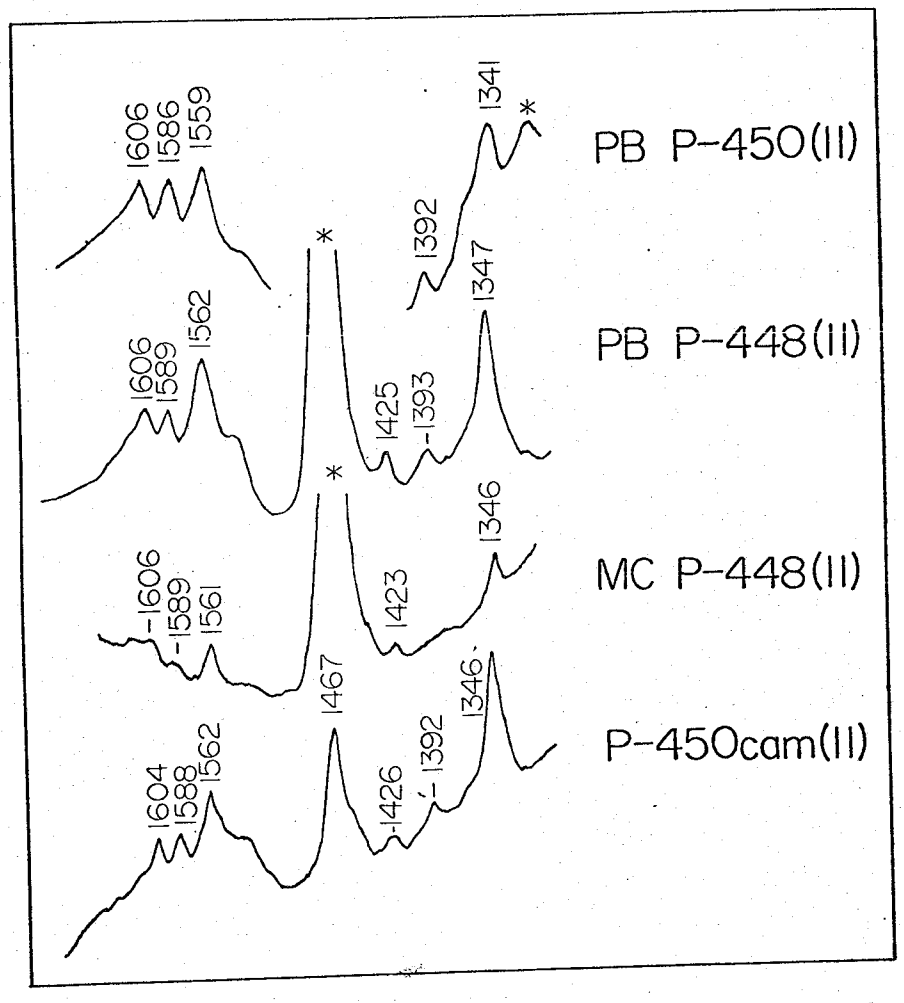

Fig. 1 The resonance Raman spectra of reduced PB P-450 (100 μM), PB P-448 (100 μM), MC P-448 (50 μM), and P-450$_{cam}$ (100 μM). Instrumental conditions: excitation, 488.0 nm; laser power at sample point, 60 mW for PB P-450, 180 mW for the others; slit width, 3 cm^{-1}; time constant, 8 sec; scan speed 10 cm^{-1}/min.

illuminated from the bottom of the cell and the scattered light collected at right angle form the incident light. Temperature of the sample was maintained below 10°C by flushing cold nitrogen gas to the front edge of the cell, where the laser light entered. After each measurement, the absorption spectrum of the heme-CO complex obtained by bubbling CO gas into the reduced P-450 in the Raman cell, was measured with a micro cell (1x3x30 mm^3) and a Hitachi-124 spectrophotometer. Raman spectra were excited by the 488.0 nm line of an argon ion laser (Spectra Physics Model 164-02) and were recorded on a JEOL-400D Raman spectrometer equipped with HTV-R649 photomultiplier. The frequency calibration of the spectrometer was performed with indene (30) within the accuracy of ± 1 cm^{-1}.

RESULTS

The resonance Raman spectra of reduced PB P-450, PB P-448, MC P-448, and $P\text{-}450_{cam}$ were shown in Fig. 1. The intence Raman line near 1465 cm^{-1} was due to glycerol. Since reduced PB P-450 was unstable, one solution was used for recording of the spectrum between 1300 and 1400 cm^{-1} and another fresh solution from the same batch was used to record the rest of it. All of reduced PB P-450, PB P-448, MC P-448, and $P\text{-}450_{cam}$ exhibited the Raman spectra of ferrous high spin type (18).

Band IV of reduced PB P-450, PB P-448, MC P-448, and $P\text{-}450_{cam}$ were found at 1341, 1347, 1346, and 1346 cm^{-1} respectively. The lines were confirmed to be polarized. Band IV of the reduced MC P-448 moved to 1342 cm^{-1} when n-pentanol was added to the oxidized MC P-448 and then reduced (final concentration of n-pentanol was 1% against 107 μM MC P-448). This change in the reduced state corresponded with the change of the spin state in the oxidized state from high spin to low spin upon the addition of n-pentanol (31). Thus Band IV of reduced P-450 appears at 1341-1342 cm^{-1} or 1346-1348 cm^{-1} in accordance with whether its oxidized form takes low spin or high spin state. Either frequency of them is markedly lower than the standard frequencies of Band IV for ferrous high spin hemoproteins [1356 cm^{-1} for deoxy Hb, 1355 cm^{-1} for deoxy Mb (18) and 1355 cm^{-1} for Type a of cytochrome c'

(32)].

When metyrapone was bound to the sixth coordination position of reduced P-450$_{cam}$, the Band IV moved to 1358 cm^{-1} and the resulting resonance Raman spectrum appeared closely similar to that of reduced cytochrome b_5, as shown in Fig. 2, where two histidyl imidazoles are coordinated to the heme iron (33). The resonance Raman spectrum of reduced pyridine complex of P-450$_{cam}$ was also similar to that of reduced cytochrome b_5. It is notable that the resonance Raman spectra of P-450$_{cam}$·Mp (Mp; metyrapone) and P-450$_{cam}$·Py (Py; pyridine) were of typical ferrous low spin type, in which two axial ligands are bound to the heme iron through the σ type interaction (18).

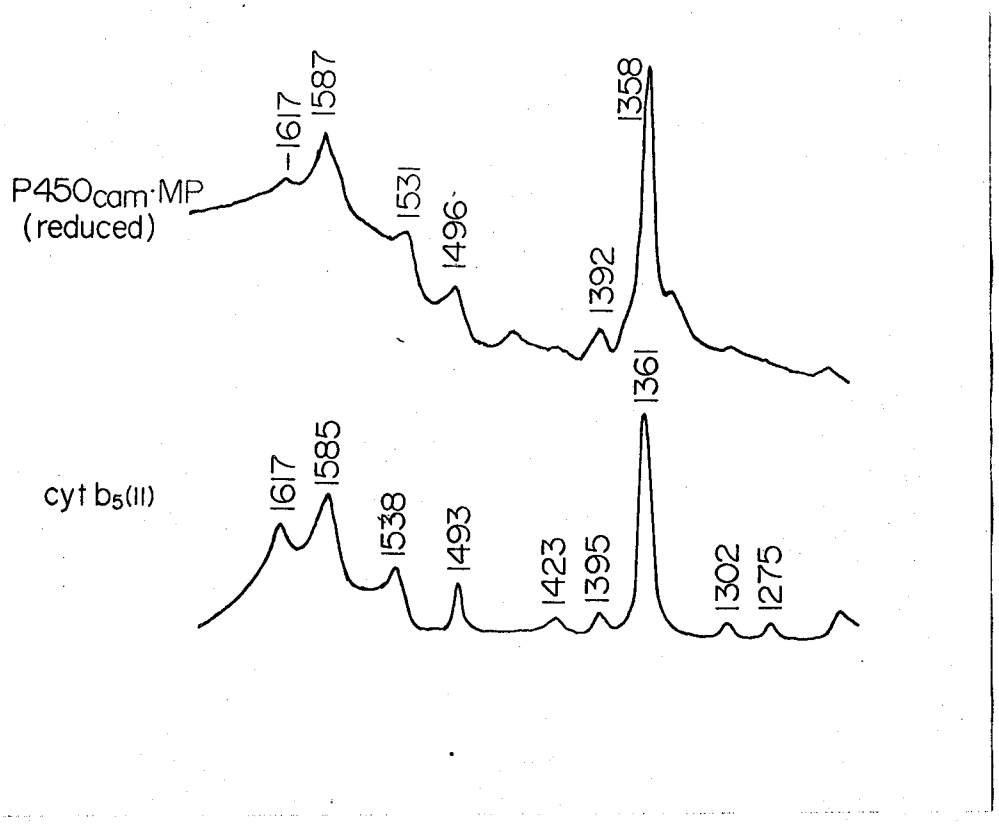

Fig. 2 The resonance Raman spectrum of reduced P-450$_{cam}$·metyrapone complex and that of ferrous cytochrome b_5. Instrumental conditions; excitation; 488.0 nm, laser power; 200 mW, slit width; 3 cm^{-1}, time constant; 3.2 sec, scan speed; 25 cm^{-1}/min.

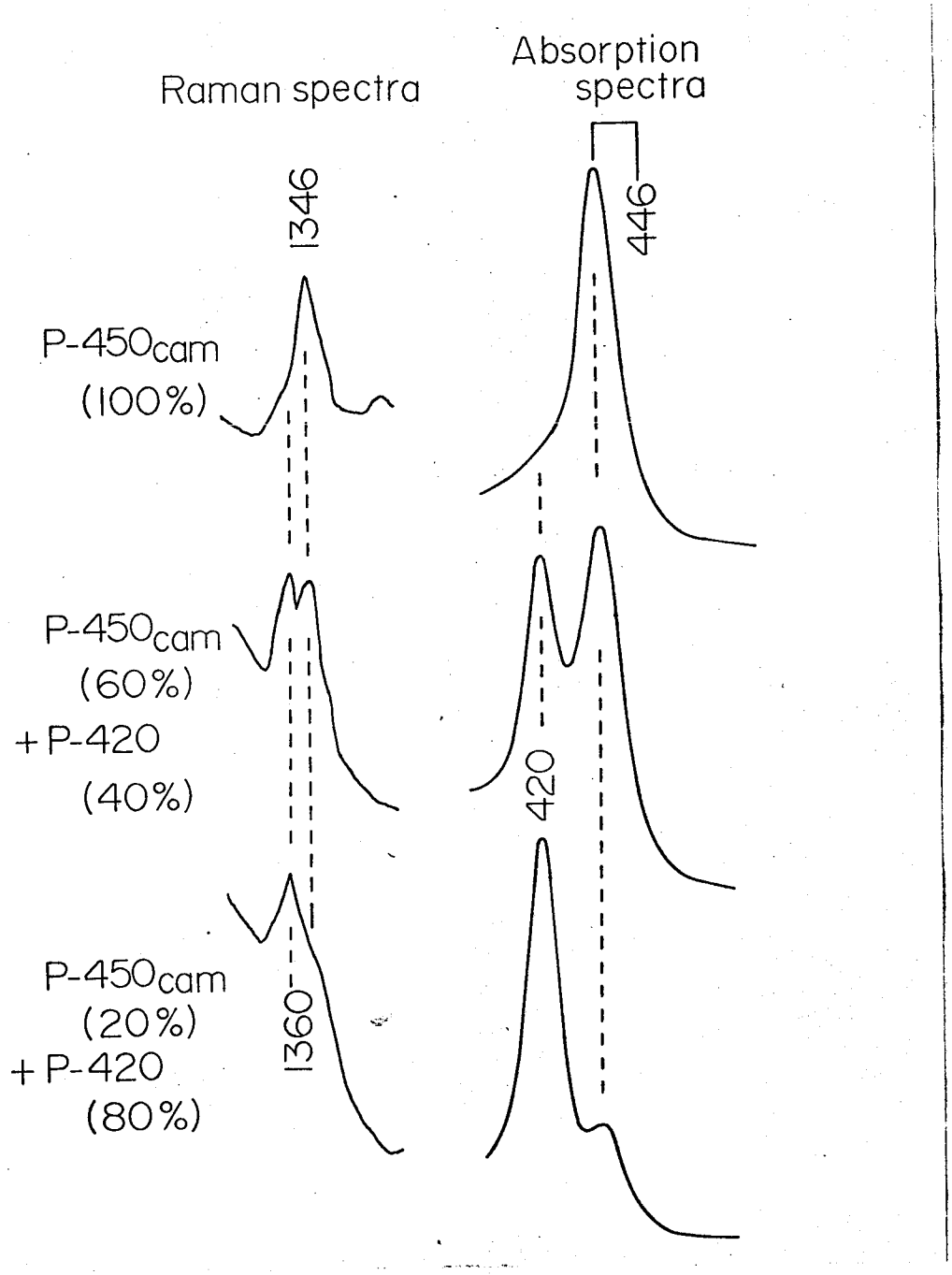

Fig. 3 The resonance Raman spectra in the frequency region of Band IV of P-450$_{cam}$ and P-420$_{cam}$ (left) and the absorption spectra in the Soret region of the CO adduct of the sample used for the Raman spectroscopy (right).

Fig. 3 illustrated the visible and Raman spectral changes upon the conversion from P-450$_{cam}$ to P-420$_{cam}$ in the reduced state. The relative concentration of P-450 to P-420 was monitored by the absorption spectra of thier CO adduct before and after the Raman experiment. When the sample solution contained both P-450$_{cam}$ and P-420$_{cam}$, two Raman lines (Band IV) appeared at 1346 and 1360 cm^{-1}. Thus, it became confident that the reduced P-450$_{cam}$ and P-420$_{cam}$ gave rise to Band IV exclusively at 1346 and 1360 cm^{-1}, respectively. This frequency change from anomalous 1346 cm^{-1} to normal 1360 cm^{-1} may suggest a status change or a replacement of the fifth ligand of the heme iron upon conversion from P-450$_{cam}$ to P-420$_{cam}$ as discussed below.

When reduced PB P-450 was subjected to the laser illumination (~180 mW) for 2 hr at 10°C, its CO complex gave the Soret band near 420 nm, and therefore the conversion from PB P-450 to PB P-420 occurred during the laser illumination. Fig. 4 exhibited the Raman spectral change in the Band IV region of reduced PB P-450 with time. Here the scan-starting time measured from the beginning of the laser illumination is represented beside each spectrum. It was apparent that the Raman line at 1359 cm^{-1} grew with time. The 1341 cm^{-1} line disappeared completely 150 min after the laser illumination. Consequently the 1341 and 1359 cm^{-1} lines are assigned to Band IV of PB P-450 and PB P-420, respectively.

The intensity decrease of the 1341 cm^{-1} line should parallel the intensity increase of the 1359 cm^{-1} line but the estimation of their precise intensities relative to the standard line (1317 cm^{-1} line of solvent) was impossible because of a serious variation of the base line with time. A rough estimate of the peak height from a reasonable base line indicated that ca. 50% conversion to PB P-420 took 20 min at 180 mW of the laser power and 40 min at 60 mW. The experiments of the laser illumination to reduced PB P-448 and MC P-448 under the same experimental condition did not show the evidence of the P-420 conversion.

The Raman spectra in the Band IV region of the P-450·CO complexes were shown in Fig. 5. Band IV of PB P-448·CO and PB P-450·CO appeared both at 1365 cm^{-1} despite distinct difference in Band IV of their ferrous high spin states. It was noted for this measurement that the

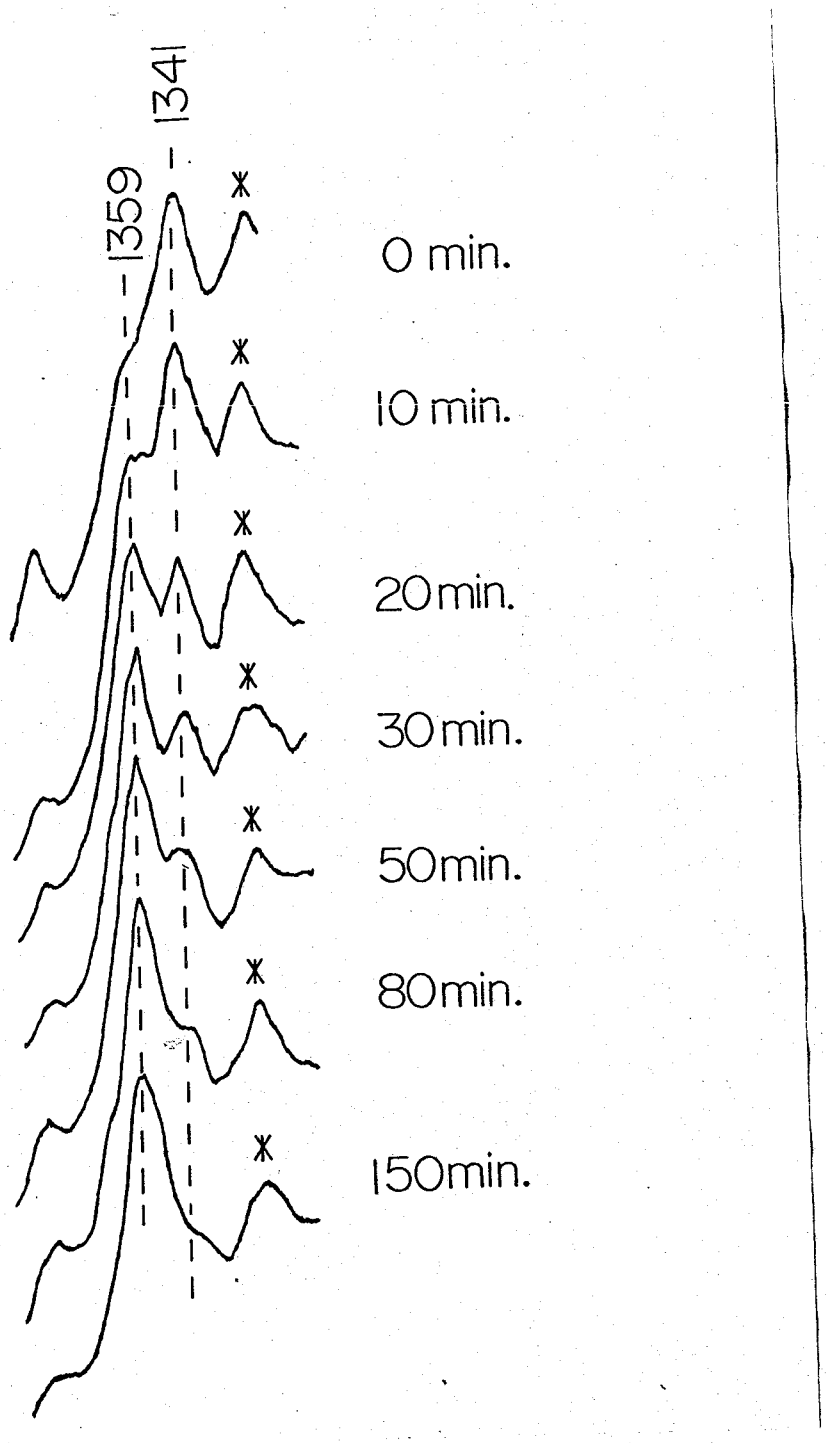

Fig. 4 The Raman spectral change of reduced PB P-450 with time during the laser illumination. Time represented beside each spectrum denotes the scan-starting time measured from the beginning of the laser illumination. Laser power was 180 mW and other conditions were same with those in Fig. 1.

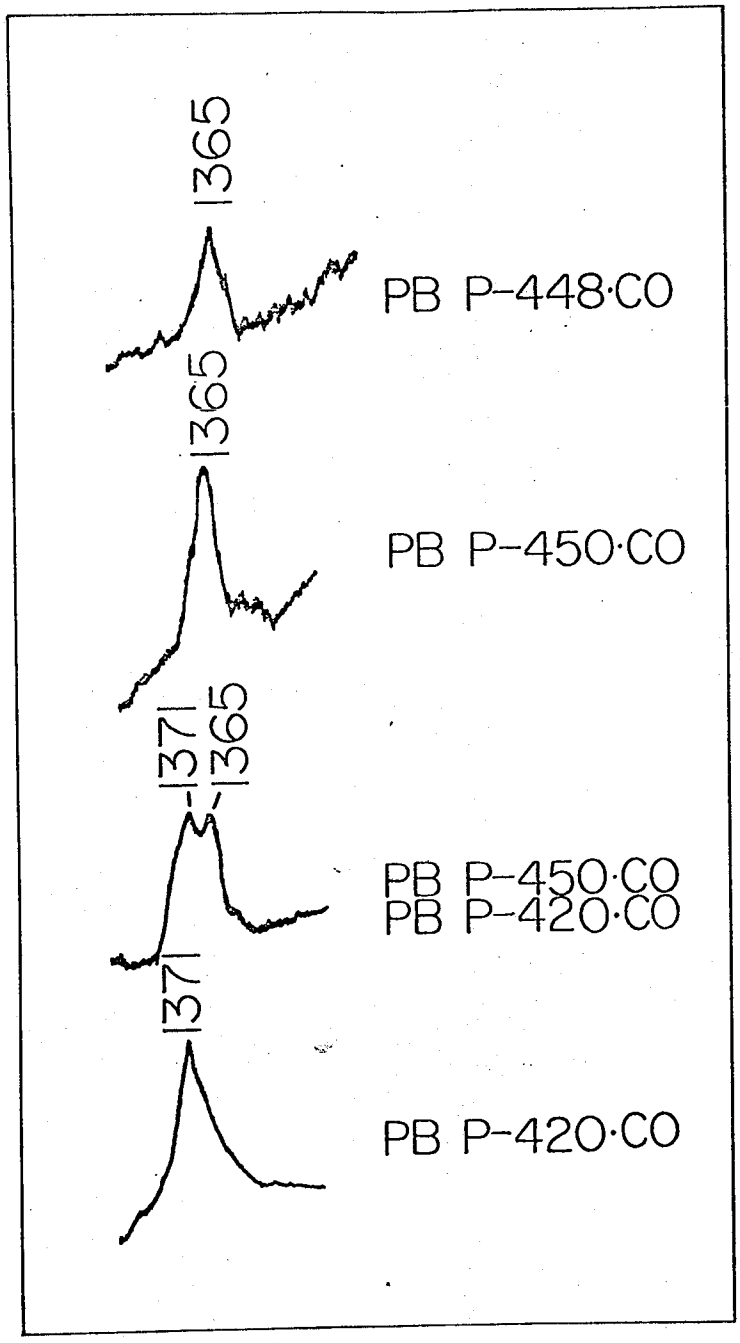

Fig. 5 Band IV of PB P-448·CO (100 μM), PB P-450·CO (100 μM) and P-420·CO. The spectrum designated by PB P-450·CO +P-420·CO was measured 14 min after the beginning of the laser illumination (50 mW). The P-420·CO was converted from PB P-450·CO by the laser illumination for 30 min.

laser power was set as low as 50 mW since P-450·CO is photodissociable. Despite the low laser power used, PB P-450·CO was converted to PB P-420·CO during the laser illumination. As shown in the third spectrum, two Raman lines appeared at 1365 and 1371 cm^{-1} 14 min after and finally, in 30 min, the 1365 cm^{-1} line disappeared completely while the 1371 cm^{-1} line was intensified. Thus the frequency of Band IV of P-420·CO lies at 1371 cm^{-1}. The implications of the frequencies of Band IV will be discussed in detail later.

Fig. 6 represented the Raman spectra of oxidized PB P-450 and $MbSCH_3$. $MbSC_2H_5$ gave the similar Raman spectrum (not shown). The frequencies of the Raman lines of PB P-450 coincided with those of $MbSCH_3$ though the relative intensities differed a little. This coincidence, however, served as a less conclusive evidence for the coordination of the thiolate anion to the heme iron, because MbN_3 also provided almost the same frequencies with $MbSCH_3$. It rather implied that intact oxidized PB P-450 contains the normal ferric low spin hemes with no strain from the protein moiety. The resonance Raman spectra of oxidized $P\text{-}450_{cam}$·Mp and $P\text{-}450_{cam}$·Py were similar to oxidized PB P-450 (not shown).

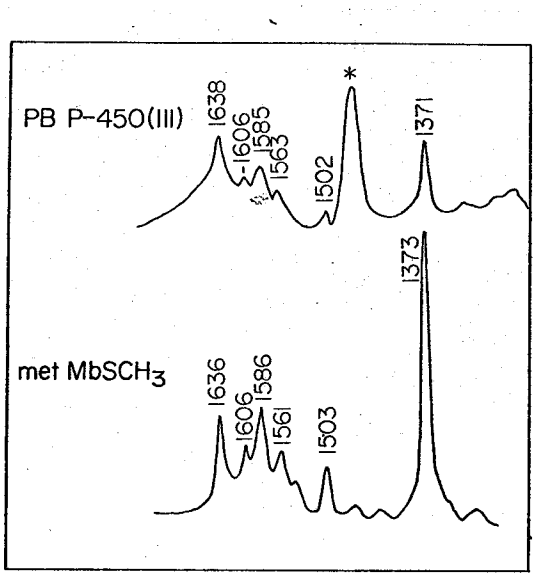

Fig. 6 The resonance Raman spectra of oxidized PB P-450 (100 μM) and $MbSCH_3$ (500μM). laser power; 60 mW for PB P-450 and 180 mW for $MbSCH_3$. Other conditions were same with those in Fig. 1.

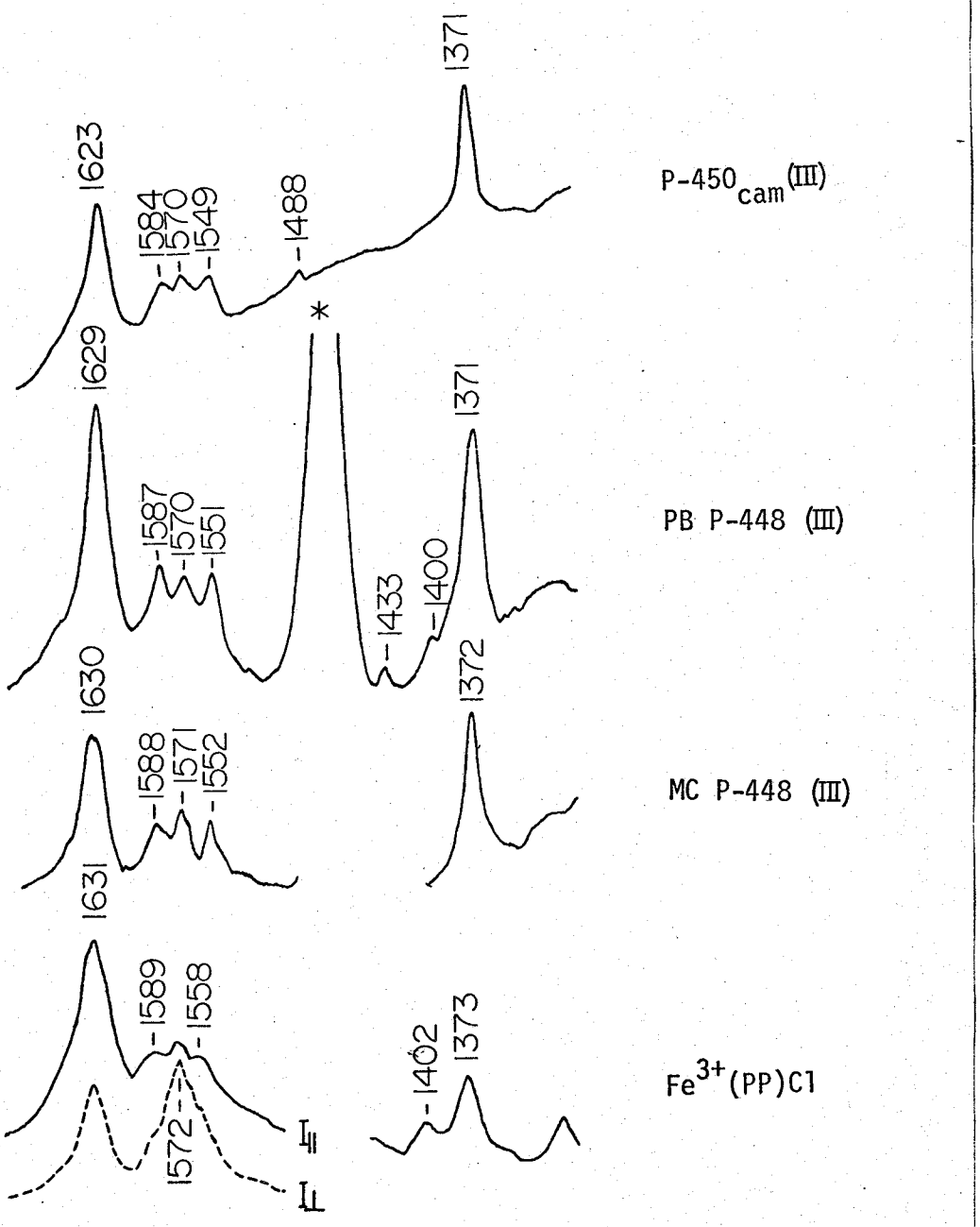

Fig. 7 The resonance Raman spectra of oxidized P-450$_{cam}$ (100 μM), PB P-448 (100 μM), MC P-448 (30 μM) and hemin in 1% SDS aqueous solution [Fe^{2+}(PP)Cl]. Polarized spectra were shown for hemin in the 1500-1650 cm^{-1} region. $I_{\parallel}$ and $I_{\perp}$ denote the electric vector of the scatterd radiation parallel and perpendicular to that of the incident radiation, respectively. Instrumental conditions were same with those in Fig. 1.

The resonance Raman spectra of oxidized P-450$_{cam}$, PB P-448, and MC P-448 were compared with that of Fe^{3+}(PP)Cl in Fig. 7. Spiro and Burke (34) pointed out that the protein effect upon the heme structure appeared most sensitively in the ferric high spin state. However, the resemblance of those Raman spectra in Fig. 7 implies that P-450$_{cam}$, PB P-448, and MC P-448 contain the normal ferric high spin heme with no particular distortion. It was emphasized that, in Figs. 6 and 7, the frequencies of Band IV of oxidized P-450 exhibited no more such an anomaly as was pointed out for its reduced state.

In the frequency region below 800 cm^{-1}, oxidized PB P-448 gave two prominent Raman lines at 349 and 755 cm^{-1} (not shown). The two lines corresponded to those of oxidized P-450$_{cam}$ at 351 and 754 cm^{-1} reported by Champion and Gunsalus (35), who found an additional line at 691 cm^{-1} suggesting the appearance of C-S stretching mode of the fifth ligand. Since the intense Raman line of glycerol screened that frequency region, the Raman experiment with 5% glycerol solution was tried. Nevertheless, because of unstability of the solution, It was failed to affirm the presence of the 691 cm^{-1} line.

The Raman spectra of reduced and oxidized PB P-420 were shown in Fig. 8. Since there are several ways to convert P-450 to P-420, the individual P-420 would probably have their inherent structural characteristics. Reduced PB P-420 converted from reduced PB P-450 by the laser illumination for 150 min, gave five prominent Raman lines (1622, 1609, 1589, 1559 and 1524 cm^{-1}) in the frequency region above 1500 cm^{-1}, where only three Raman lines were usually observed for typical ferrous low spin heme such as cytochrome b_5 (1617, 1585, and 1538 cm^{-1}) (18). Therefore the line at 1622, 1589, and 1524 cm^{-1} of PB P-420 belong undoubtedly to the ferrous low spin heme. The Raman lines at 1609 and 1559 cm^{-1} were usually intense in the ferrous high spin hemoprotein such as deoxy Mb (18) and accordingly were assigned to the ferrous high spin heme. The presence of the two sets of Raman lines strongly suggested coexistence of two molecular species in the reduced PB P-420. To prove the spin equilibrium between the high spin and low spin species, temperature dependence of the intensities of the Raman lines should be measured in wide range of temperature, although

the measurement of the Raman spectrum at lower temperature was unsuccesful in the present study.

Oxidized PB P-420 was obtained by adding KSCN to oxidized PB P-450. Two more preparations of oxidized PB P-420 were tried; one by the illumination of the laser light (240 mW) for 4 hr, and the other by adding NaOH until pH 7.8. Both gave almost the same Raman spectra with that shown in Fig. 8. It was remarked that the Raman spectra of PB P-450 and PB P-420 were closely alike. This indicated that the Fe^{3+}-S^- interaction in intact PB P-450 did not characterize the resonance Raman spectrum and therefore it was unaltered by the protonation or replacement of the axial ligand (RS^-) upon the P-420 conversion.

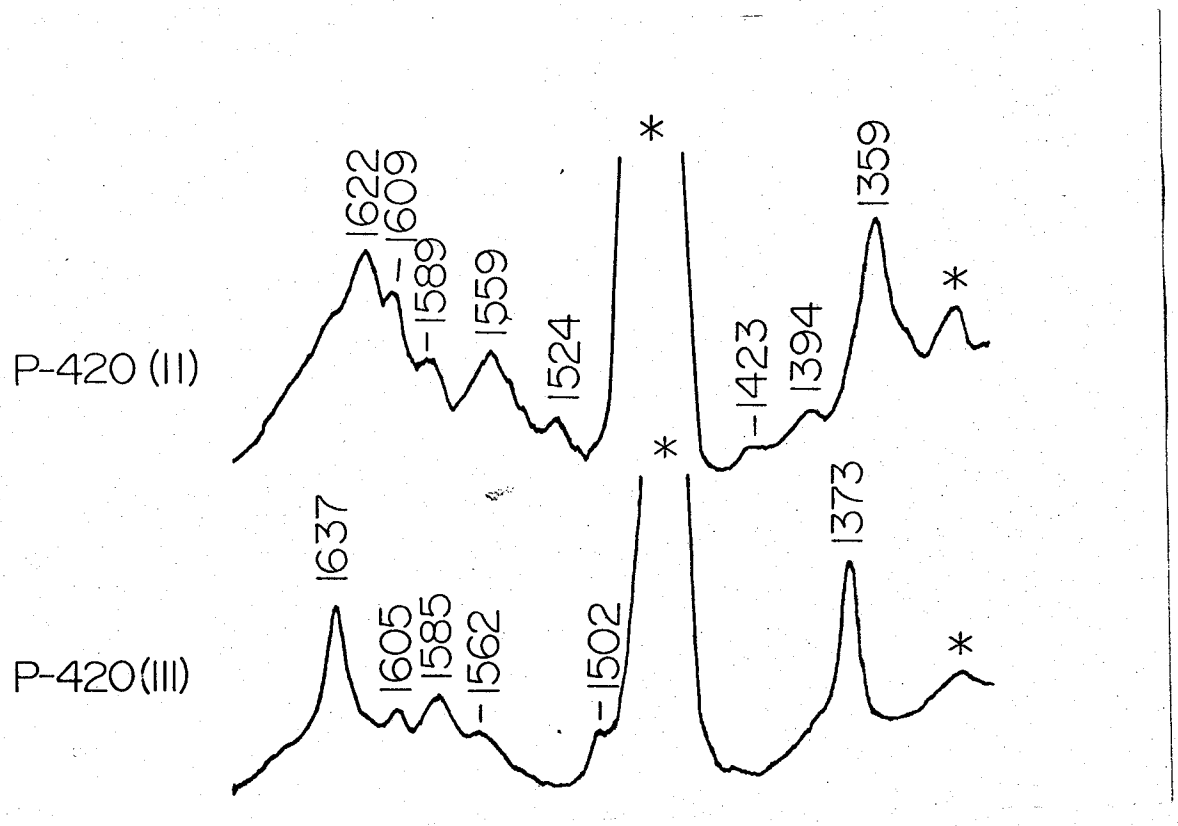

Fig. 8 The resonance Raman spectra of reduced and oxidized PB P-420. Reduced PB P-420 was converted from reduced PB P-450 by the laser illumination for 150 min. Oxidized PB P-420 was obtained by adding KSCN to oxidized PB P-450 and it was confirmed later by absorption spectrum of its heme-CO complex. Two other preparations of oxidized PB P-420 (at pH 7.8 and by laser illumination) gave the identical spectra with the lower one.

DISCUSSION

Reduced P-450 The vibrational assignments of the resonance Raman lines of hemoproteins have been carried out through the normal coordinate calculations for octaethylporphyrinato-Ni(II) [Ni(OEP)] (36). The polarized Raman line of Ni(OEP) corresponding to Band IV of hemoproteins showed definitely the frequency shift upon the ^{15}N substitution of four pyrrole nitrogens but not upon the meso-deuteration (19). The polarization property of Band IV (polarized) indicated that the mode is totally symmetric. Therefore Band IV involves primarily the CN symmetric stretching vibration in which four pyrrole nitrogens must move in-phase along the Fe-N direction (19). As electrons are delocalized to the porphyrin $\pi^*(e_g)$ orbital from the iron d_π orbital in the ferrous low spin state, the CN bond-strength becomes weaker and thus its stretching frequency shifts to lower frequency (18). Consequently the frequency of Band IV can be used as a practical indicator of the amount of electrons delocalized to the porphyrin $\pi^*(e_g)$ orbital.

The Raman spectral features of reduced PB P-450 and PB P-448 resembled those of deoxy Mb (18) and Type a of cytochrome c' (32), indicating the presence of high spin Fe^{2+} ion. This agreed with the results of NMR (8) and Mössbauer studies (9). However, the frequencies of Band IV of reduced P-450 (1341 cm^{-1} for PB P-450, 1347 cm^{-1} for PB P-448, and 1346 cm^{-1} for $P\text{-}450_{cam}$ and MC P-448) were notably lower than those of other ferrous high spin hemoproteins (18,32). Among other hemoproteins only reduced chloroperoxidase gave Band IV at such low frequency (1348 cm^{-1}) (37). This peculiarity would presumably be caused by the strong π basicity of the fifth ligand.

The studies upon the synthetic analogues (10-13) suggested the coordination of RS^- but not RSH to the fifth position of the heme iron of P-450. The difference in coordinations of RS^- and RSH was represented schematically in Fig. 9. Since the neutral sulfur has the electronic structure of $(3s)^2(sp)^4$, two 3p orbitals are used for the covalent bonds (RS and SH). Supposing that the lone pair electrons occupy $3p_z$ orbital, they would coordinate to the d_{z2} or $4p_z$ orbital

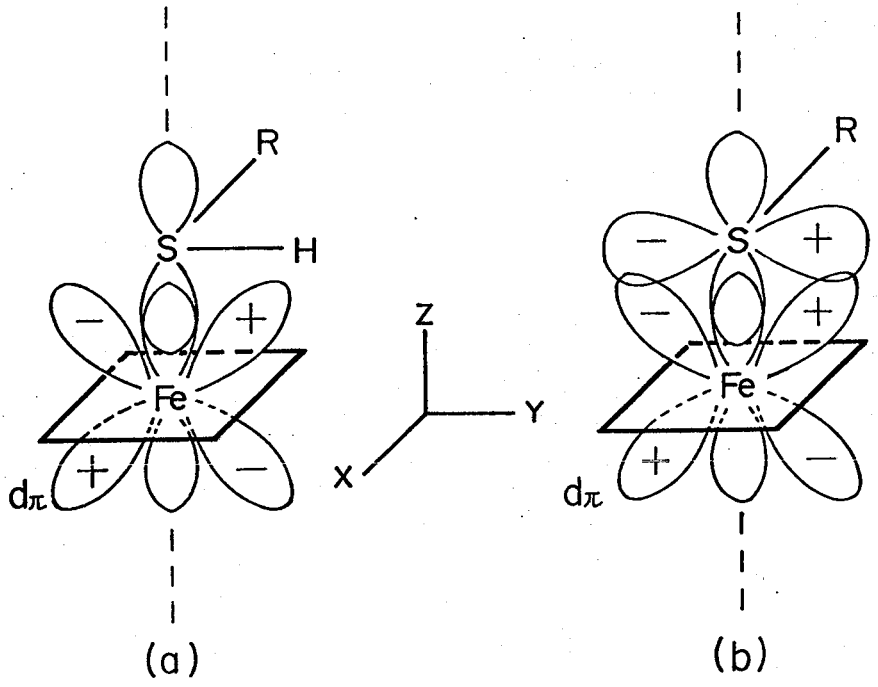

Fig. 9 Schematic representation for the coordinations of RSH (a) and RS^- (b) to the heme iron. 3p orbitals of sulfur and $3d_\pi$ and $3d_{z2}$ orbitals of the heme iron were shown explicitly.

of the heme iron (Fig. 9a). Then the two covalent bonds would parallel the xy plane, although precisely the bond angles of Fe-S-R and Fe-S-H might be larger than 90° due to the sp^3 hybridization. On the other hand, the fact that sulfur anion has one more lone pair orbital, leads to deduce that one of the two lone pairs must parallels the xy plane to interact with d_π(Fe) orbitals while the other is constituting the coordination bond with d_{z2} (Fe) or $4p_z$(Fe) orbital (Fig. 9b).

Since the porphyrin $\pi^*(e_g)$ orbital never interact with the d_{z2}(Fe) and $4p_z$(Fe) orbitals because of different symmetry, the Fe-S bond shown in Fig. 9a would have no paticular influence upon the frequency of Band IV. In fact, the coordination of methionine sulfur to the ferrous heme in reduced cytochrome c did not show any anomàly in the resonance Raman spectra (38). In contrast, the coordination of RS^- anion was expected to provide the significant influence upon the frequency of Band IV because the lone pair electrons in the orbital paralleled with the xy plane might be delocalized into the porphyrin $\pi^*(e_g)$ orbital directly or through the iron d_π orbital. As previously state, the increase of

electrons occupying the porphyrin $\pi^*(e_g)$ orbital would lower the frequency of Band IV. Therefore the unusually low frequency of Band IV seen commonly to reduced P-450 is probably caused by the strong π basicity of the fifth ligand.

Band IV of reduced PB P-450 (1341 cm^{-1}) and PB P-448 with n-pentanol (1342 cm^{-1}), which take low spin state in the oxidized form, was lower than those of reduced PB P-448 (1347 cm^{-1}), MC P-448 (1346 cm^{-1}) and $P\text{-}450_{cam}$ (1346 cm^{-1}), which take high spin state in the oxidized state. This indicated a significant difference in that π basicity of the fifth ligand between the two types of reduced P-450. If the Fe^{2+}-S^- distance is shorter in the former type than the latter, then the larger delocalization of electrons to the porphyrin $\pi^*(e_g)$ orbital was expected and therefore the lower frequency of Band IV of the former could be understood reasonably. The similarities in the frequencies of other Raman lines of reduced PB P-450 and PB P-448 (Fig. 1) implied the resemblance of the rest of structure of heme including the methine-bridges.

Stern and Peisach (10) pointed out, for the porphyrin model compounds, that the dielectric constant of solvent causes the shift of absorption maximum. Since the specificity of the substrate depends upon the apo-protein, the shape and hydrophobicity of the heme pocket would be inherent to the individual P-450. If only the hydrophobicity were different between reduced PB P-450 and PB P-448, both would give the Raman lines with almost same frequencies but different relative intensities (39). It rose against the results shown in Fig. 1. The present observation clarified that their difference in the Raman spectrum is prominent only in the CN stretching frequencies, suggesting that more localized difference is essential to the different λ_{max}.

Band IV of reduced P-450 shifted to the normal frequencies (1360 cm^{-1} for $P\text{-}420_{cam}$ and 1359 cm^{-1} for PB P-420) upon the conversion to P-420 (Fig. 3,4). Collman et al. observed that MCD spectrum of P-420 resembled those of the synthetic models with RSH or N base as the fifth ligand (16). When RS^- of the fifth ligand were protonated upon the P-420 conversion, the $d_\pi(Fe^{2+})$-$p_y(S^-)$-$\pi^*(e_g$, porphyrin) interactions would disappear (see Fig. 9). Therefore Band IV was expected to show high frequency shift to the normal frequency upon the conversion to

P-420. Thus the interpretation of Band IV was completely compatible with the observation by Collman et al (16). However, for the molecular vibrations of porphyrin ring, RSH bound to the heme iron would be indistinguishable from an arbitrary N base with only one lone pair. Detection of Fe-ligand stretching mode would determine the correct choice of the alternatives.

Heme-CO complexes The back donation of electrons from $d_\pi(Fe^{2+})$ to $\pi^*(CO)$ upon the formation of the heme-CO complex decreases the delocalization of $d_\pi(Fe^{2+})$ electrons to $\pi^*(e_g$, porphyrin) orbital, resulting in the higher frequency of Band IV (18). The back-donated electron which occupies the anti-bonding orbital of CO [$\pi^*(CO)$], would weaken the CO bond and thus lower the CO stretching frequency (ν_{CO}). Therefore it was expectable that the lager back donation leads to the higher frequency of Band IV and simultaneously to the lower frequency of ν_{CO} (18) unless the particular interaction exists between CO and the protein.

The frequencies of Band IV of P-450 and P-450·CO were summarized in Table 1. The frequencies of PB P-450·CO and PB P-448·CO are clearly lower than those of HbCO and MbCO (40), indicating that the strong π

Table 1. The frequencies of Band IV of P-450 and some related molecules [cm^{-1}]

	Fe^{2+}	Fe^{2+}·CO	Fe^{3+}
PB P-450	1341	1365	1371
PB P-448	1347	1365	1371
MC P-448	1346		1371
$P\text{-}450_{cam}$	1346		1371
$P\text{-}450_{cam}$·Mp	1358		1371
PB P-420	1359	1371	1372
Hb	1356	1372[a)]	1371[b)]
Mb	1355	1370[a)]	1371[b)]

a) Ref. 40 b) Ref. 18.

basicity of the fifth ligand was still causing the larger delocalization of electrons to the porphyrin $\pi^*(e_g)$ orbital of the heme-CO complexes of PB P-450 and PB P-448. However, Band IV of P-420·CO was identified at 1371 cm^{-1}, the same frequency with HbCO and MbCO. Thus regarding Band IV, the characteristic feature of P-450·CO was lost in P-420·CO.

Hanson et al. (41) interpreted the absorption spectrum of $P\text{-}450_{cam}$·CO single crystal in terms of the p type hyperporphyrin. Its Soret bands at 363 and 446 nm were assumed to result from the mixing of two transitions; $B(\pi - \pi^*)$ and $CT(p^{\#}-\pi^*)$, where $p^{\#}$ involves the contribution from the $\pi(a_{2u})$, $3p_z(S^-)$ and $4p_z(Fe)$. This implicated the orbital mixing of the $\pi(a_{2u})$, $3p_z(S^-)$, and $4p_z(Fe)$ orbitals in the ground electronic state. If the orbital mixing increases the number of electrons occupying the porphyrin $\pi(a_{2u})$ orbital for P-450·CO but not for P-420·CO, then this interaction could be regarded as the origin of the unusual low frequency of Band IV of P-450·CO, because the $\pi(a_{2u})$ orbital is anti-bonding about all eight CN bonds (42). Alternatively, the mixing of the porphyrin $\pi^*(e_g)$ orbital with the $d_\pi(Fe)$ and $p_y(S^-)$ orbitals causes larger delocalization of electrons to the porphyrin $\pi^*(e_g)$ orbital, lowering the frequency of Band IV.

It was unexpected that the CO stretching frequency of PB P-450·CO (Δ_{CO}=1949 cm^{-1}) (43) was as high as that of HbCO (ν_{CO}=1951 cm^{-1}) (44), because the frequency change of Band IV upon the formation of the CO complex [$\Delta=\nu(Fe^{2+}CO)-\nu(Fe^{2+})$] was fairly larger for P-450·CO (Δ=24 cm^{-1}) than for HbCO (Δ=17 cm^{-1}). The apparent inconsistency between Δ and ν_{CO} might be interpreted reasonably if the significance of CO-histidine(distal) interaction of HbCO was considered (45). Without the interaction, ν_{CO} of HbCO might have been higher than the observed one but actually the interaction lowered ν_{CO} of HbCO than as expected only from the back donation.

Oxidized P-450 Oxidized PB P-450, $P\text{-}450_{cam}$·Mp, and $P\text{-}450_{cam}$·Py showed the Raman spectra of the typical ferric low spin type. The Raman lines at 1638 and 1502 cm^{-1} of them were characteristic of ferric low spin hemoproteins (18). The EPR g values (2.4, 2.2, and

1.9) (2) have been the basis of judgement whether the synthetic models were endowed with the characteristic features of P-450. The synthetic analogues with RS^- as the fifth ligand (3-6) satisfied the condition. The similarity in the Raman spectra of PB P-450 and $MbSCH_3$ suppored the coordination of RS^- to the heme iron in oxidized PB P-450, being a less conclusive evidence though.

Band IV oxidized PB P-450 as well as of $MbSCH_3$ did not show any anomaly as seen in the reduced state. Therefore, the Fe^{3+}-S^- interaction is not so strong that the stretching frequencies of the CC and CN bonds of porphyrin ring could be influenced. In such a condition, it seemed unlikely that the CS stretching mode of the fifth ligand appeared in the resonance Raman spectrum, although Champion and Gunsalus took the CS stretching into consideration as a possible origin of the 691 cm^{-1} line of $P\text{-}450_{cam}$.

Spiro and Burke (34) have pointed out that the distortion of heme controled by the apo-protein is most prominet in the ferric high spin state. In fact, the Raman frequencies of aquo Mb (18) differed distinctly from those of ferric high spin iron-porphyrin particularly in the frequency region of 1500-1650 cm^{-1}. The frequencies of a few Raman lines in that frequency region of $P\text{-}450_{cam}$, PB P-448, and MC P-448 were compared with those of other ferric high spin hemoproteins and iron-porphyrins in Table 2. Hemin in 1% SDS solution (32) provided the Raman frequencies similar to those of $P\text{-}450_{cam}$, PB P-448, and MC P-448. Therefore the structure of ferric high spin hemes in the oxidized $P\text{-}450_{cam}$, PB P-448 and MC P-448 was deduced to suffer the protein control little.

Table 2. Comparison of the frequencies of a few Raman lines sensitive to the distortion of hemes in the ferric high spin state [cm^{-1}]

$Fe^{3+}(PP)Cl$[a]	$Fe^{3+}(MP)Cl$[b]	PB P-448	MC P-448	$P\text{-}450_{cam}$[c]	CPO[d]	cyt c'[e]	aquo-Mb[f]
1631(dp)	1632	1629	1630	1623	1627	1631	1613
1589(p)	1588	1587	1588	1584	1588	1583	1581
1572(ap)	1572	1570	1571	1570	1566	1570	1562

a. Iron-protoporphyrin in 1% SDS aqueous solution (ref. 32)

b. Iron-mesoporphyrin dimethylester in CH_2Cl_2 (Ref. 34)

c. Ref. 21

d. Chloroperoxidase (Ref. 37)

e. R. rubrum cytochrome c' (Type II) (Ref. 32)

f. Sperm whale myoglobin at pH 7.0 (Ref. 18)

REFERENCES

1. Sato, R., Satake, H., and Imai, Y. (1973) Drug Metab. Dispos. 1, 6.
2. Stern, J. O., Peisach, J., Blumberg, W. E., Lu, A. Y. H., and Levin, W. (1973) Arch. Biochem. Biophys. 156, 404.
3. Collman, J. P., Sorrell, T. N., and Hoffman, B. M. (1975) J. Am. Chem. Soc. 97, 913
4. Koch. S., Tang, S. C., Holm, R. H., Frenkel, R. B., and Ibers, J. A. (1975) J. Am. Chem. Soc. 97, 916.
5. Tang, S. C., Koch, S., Papaethymiou, G. C., Foner, S., Frankel, R. B., Ibers, J. A., and Holm., R. H. (1976) J. Am. Chem. Soc. 98, 2414.
6. Ogoshi, H., Sugimoto, H., and Yoshida, Z. (1975) Tetrahedron Lett. 2289.
7. Dawson, J. H., Holm, R. H., Trudell, J. R., Barth, G., Linder, R. E., Bunnenberg, E., Djerassi, C., and Tang, S. C. (1976) J. Am. Chem. Soc. 98, 3707.
8. Keller, R. M., Wüthrich, K., and Debrunner, P. G. (1972) Proc. Nat. Acad. Sci. U. S. 69, 2073.
9. Sharrock, M., Münck, E., Debrunner, P. G., Marshall, V., Lipscomb, J. D., and Gunsalus, I. C. (1973) Biochemistry, 12, 258.
10. Stern, J. O. and Peisach, J. (1974) J. Biol. Chem. 249, 7495.
11. Collman, J. P. and Sorrell, T. N. (1975) J. Am. Chem. Soc. 97, 4133.
12. Chang, C. K. and Dolphin, D. (1975) J. Am. Chem. Soc. 97, 5948.
13. Chang, C. K. and Dolphin, D. (1976) Proc. Natl. Acad. Sci. U. S. 73, 3338.
14. Vickery, L., Salmon, A., and Sauer, K. (1975) Biochim. Biophys. Acta, 386, 87.
15. Shimizu, T., Nozawa, T., Hatano, M., Imai, Y., and Sato, R. (1975) Biochemistry, 14, 4172.
16. Collman, J. P., Sorrell, T. N., Dawson, J. H., Trudell, J. R., Bunnenberg, E., and Djerassi, C. (1976) Proc. Nat. Acad. Sci. U. S. 73, 6010.
17. Spiro, T. G. (1975) Biochim. Biophys. Acta, 416, 169.
18. Kitagawa, T., Kyogoku, Y., Iizuka, T., and Saito, M. (1976) J. Am. Chem. Soc. 98, 5169.

19. Kitagawa, T., Abe. M., Kyogoku, Y., Ogoshi, H., Sugimoto, H., and Yoshida, Z. (1977) Chem. Phys. Lett. 48, 55.
20. Peterson, J. A. (1971) Arch. Biochem. Biophys. 144, 678.
21. Shimada, H., Iizuka, T., and Ishimura, Y. in preparation.
22. Imai, Y. and Sato, R. (1974) J. Biochem. 75, 689.
23. Imai, Y. and Sato, R. (1974) Biochem. Biophys. Res. Commun. 60, 8.
24. Ryan, D., Lu, A. Y. H., Kawalek, J., West, S. B., and Levin, W. (1975) Biochem. Biophys. Res. Commun. 64, 1134
25. Haugen, D. A., Coon, M. J. (1976) J. Biol. Chem. 251, 7929.
26. Hashimoto, C., and Imai, Y. (1976) Biochem. Biophys. Res. Commun. 68, 821.
27. Yu. C. A. and Gunsalus, I. C. (1970) Biochem. Biophys. Res. Commun. 40, 1431.
28. Tyson, C. A., Lipscomb, J. D., and Gunsalus, I. C. (1972) J. Biol. Chem. 247, 5777.
29. Yu. C. A. and Gunsalus, I. C. (1974) J. Biol. Chem. 249, 102.
30. Hendra, P. J. and Loader, E. J. (1968) Chem. Ind. 718.
31. Yoshida, Y. and Kumaoka, H. (1975) J. Biochem. 78, 455.
32. Kitagawa, T., Ozaki, Y., Kyogoku, Y., and Horio, T. (1977) Biochim. Biophys. Acta, 495, 1.
33. Mathews, F. S., Levine, M., and Argos, P. (1972) J. Mol. Biol. 64, 449.
34. Spiro, T. G. and Burke, J. M. (1976) J. Am. Chem. Soc. 98, 5482.
35. Champion, P. M. and Gunsalus, I. C.(1977) J. Am. Chem. Soc. 99, 2001.
36. Abe, M., Kitagawa, T., and Kyogoku, Y. (1976) Chem. Lett. 249.
37. Champion, P. M., Remba, R. D., Chiang, R., Fitchen, D. B., and Hager, L. P. (1976) Biochim. Biophys. Acta 446, 486.
38. Kitagawa, T., Kyogoku, Y., Iizuka, T., Ikeda-Saito, M., and Yamanaka, T. (1975) J. Biochem. 78, 719.
39. Kitagawa, T., Ozaki, Y., Teraoka, J., and Kyogoku, Y. (1977) Biochim. Biophys. Acta 494, 100.
40. Rimai, L., Salmeen, I., Petering, D. H. (1975) Biochemistry, 14, 378.

41. Hanson, L. K., Eaton, W. A., Slinger, S. G., Gunsalus, I. C., Gouterman, M., and Connel, C. R. (1976) J. Am. Chem. Soc. 98, 2672.
42. Kashiwagi, H., Obara, S., Takada, T., Miyoshi, E., and Ohno, K. (1978) Intl. J. Quant. Chem. in press.
43. Rein, H., Böhm, S., Jänig, G. -R., and Ruckpaul, K. (1977) Croatica. Chemica. Acta 49, 333.
44. Alben, J. O. and Caughey, W. S. (1968) Biochemistry, 7, 175.
45. Ikeda-Saito, M., Iizuka, T., Yamamoto, H., Kayne, F. J., and Yonetani, T. (1977) J. Biol. Chem. 252, 4882.

Chapter 2.

Raman Study of the Acid-Base Transition of Ferric Myoglobin. Direct Evidence for the Existence of Two Molecular Species at Alkaline pH.

ABSTRACT

Resonance Raman spectroscopy was applied to analyze the spin state equilibrium in the acid-base transition of ferric myoglobin. Direct experimental evidence is presented for the existence of two distinct molecular species of Mb at alkaline pH. The predominant species was the high spin state. The low spin content in the acidic (MbH_2O) and alkaline (MbOH) forms of Mb was estimated to be as large as 6% and 31%, respectively, in good agreement with values deduced from their magnetic susceptibilities. It was shown that both the high and low spin forms of MbOH were structurally different from MbH_2O. It was also found that the intensity ratio of the Raman lines in the lower frequency region [R=I ($\sim$675 cm^{-1})/I($\sim$755 cm^{-1})] is spin state dependent.

INTRODUCTION

The acid and alkaline forms of ferric myoglobin which have been studied extensively (1-6), were characterized by the sixth ligand of the heme iron which is H_2O in the former (MbH_2O) (1) and OH^- in the latter (MbOH) (2). An apparently anomalous magnetic moment of MbOH was explained earlier in terms of three unpaired electrons on the heme iron (3,4), but could also be due to the coexistence of both high (S=5/2) and low spin (S=1/2) forms in thermal equilibrium at alkaline pH (2). Using resonance Raman spectroscopy the direct experimental evidence to support the existence of two distinct forms of MbOH was presented in this Chapter and the predominant form as the high spin species was identified. It was also shown that high spin form of MbOH is different from MbH_2O. Previous applications of resonance Raman scattering have demonstrated the sensitivity of the method to the identity of the sixth ligand (7,8), and to the oxidation and spin

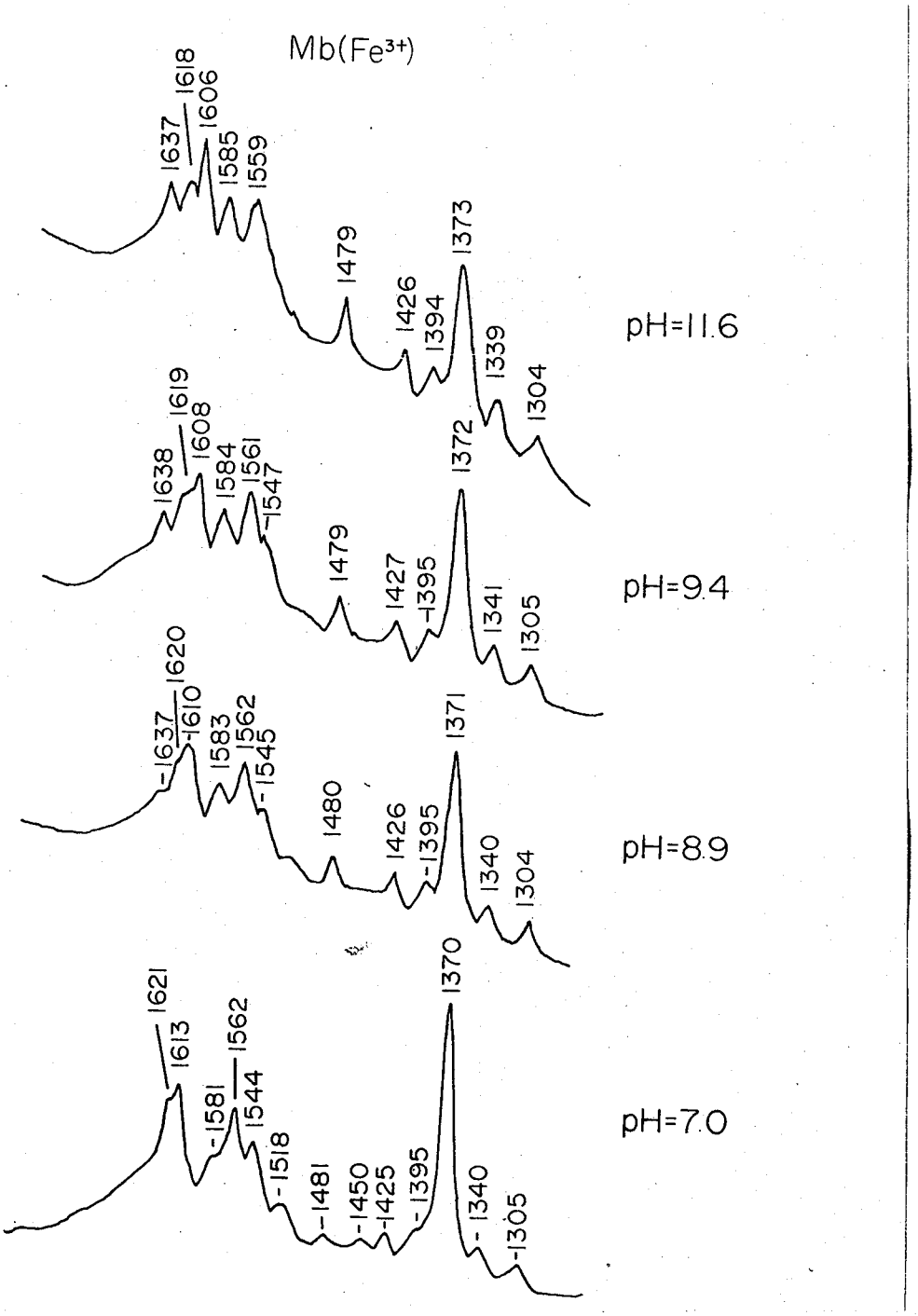

Fig. 1 Resonance Raman spectra (448.0 nm excitation) of ferric myoglobin (equine) at several pH values. Instrumental conditions; power, 200 mW; time constant, 0.5 sec; sensitivity, 1000 counts full scale; rate, 0.25 sec; slit width, 5 cm^{-1}; scanning speed, 20 cm^{-1}/min.

states of the heme iron (9-11).

EXPERIMENTAL

Equine skeletal muscle myoglobin (Sigma type I) was purified on CM-cellulose column just before the measurement of the Raman spectra and its pH values were adjusted with HCl and NaOH. MbF, MbSCN, MbN_3, MbIm (Im; imidazole), and MbCN were obtained by adding 50-fold excesses of NaF, KSCN, NaN_3, imidazole, and KCN, to 0.7 mM solution of Mb, respectively.

Raman spectra were measured with the use of a JEOL-02AS Raman spectrometer and an Ar^+-Kr^+ mixed laser (Spectra physics model 164-02). Absorption spectra were recorded with a Hitachi 124 recording spectrophotometer.

RESULTS AND DISCUSSION

The resonance Raman spectra of Mb, as shown in Fig. 1, varied appreciably with pH. An intensity increase of the Raman line at 1637 cm^{-1}, which was the band characteristic of the ferric low spin state of hemoproteins (12) and was mainly associated with methine-bridge stretching vibrations (13,14), clearly indicated an increase in the concentration of ferric low spin molecules with increasing pH. However, the Raman lines at 1618, 1606, 1559, and 1479 cm^{-1} at pH 11.6 implied simultaneously the presence of ferric high spin species (12).

The pH dependence of absorbance at 580 nm, as shown in Fig. 2a, indicated a pK of 8.9 for the equilibrium between equine MbH_2O and MbOH, in good agreement with the pK for sperm whale Mb (6). The fraction of MbOH [c] at an arbitrary pH was given therefore by the expression

$$[c] = 1/(1 + 10^{8.9-pH}) \qquad (i)$$

A plot of [c] against pH was given in Fig. 2b. At pH 11.6, it was calculated that the equilibrium mixture should contain 99.8% of Mb in the alkaline form even though Raman lines characteristic of both high and low spin states coexist in the resonance Raman spectra (Fig. 1).

Previously Yamamoto *et al.* (9) pointed out that the intensity

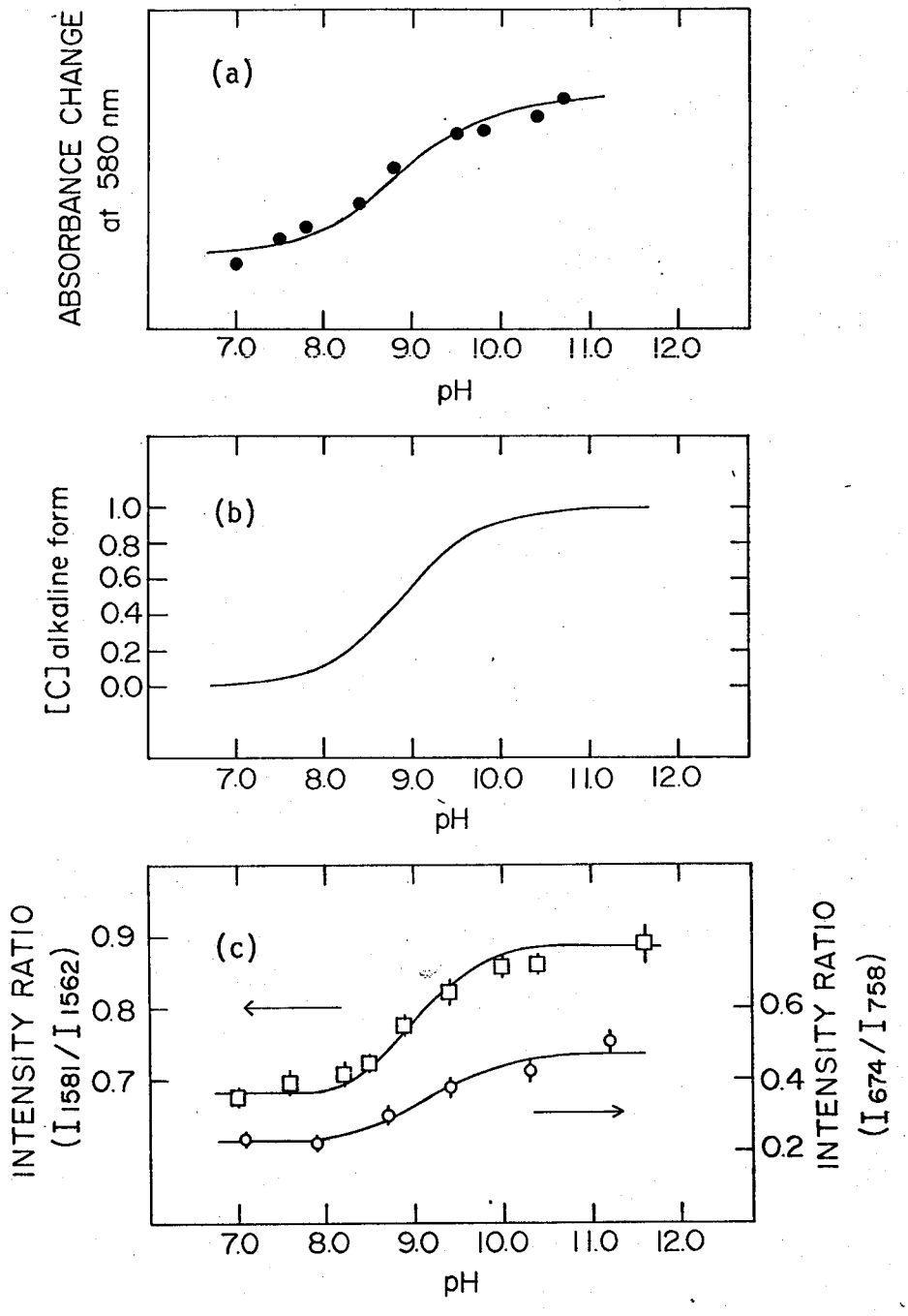

Fig. 2 The pH dependence of equine ferric myoglobin. (a) Absorbance at 580 nm. (b) Concentration of the alkaline form (see text). (c) Intensity ratios of Raman lines; (□) I(1581 cm^{-1})/I(1562 cm^{-1}); (o) I(674 cm^{-1})/I(758 cm^{-1})

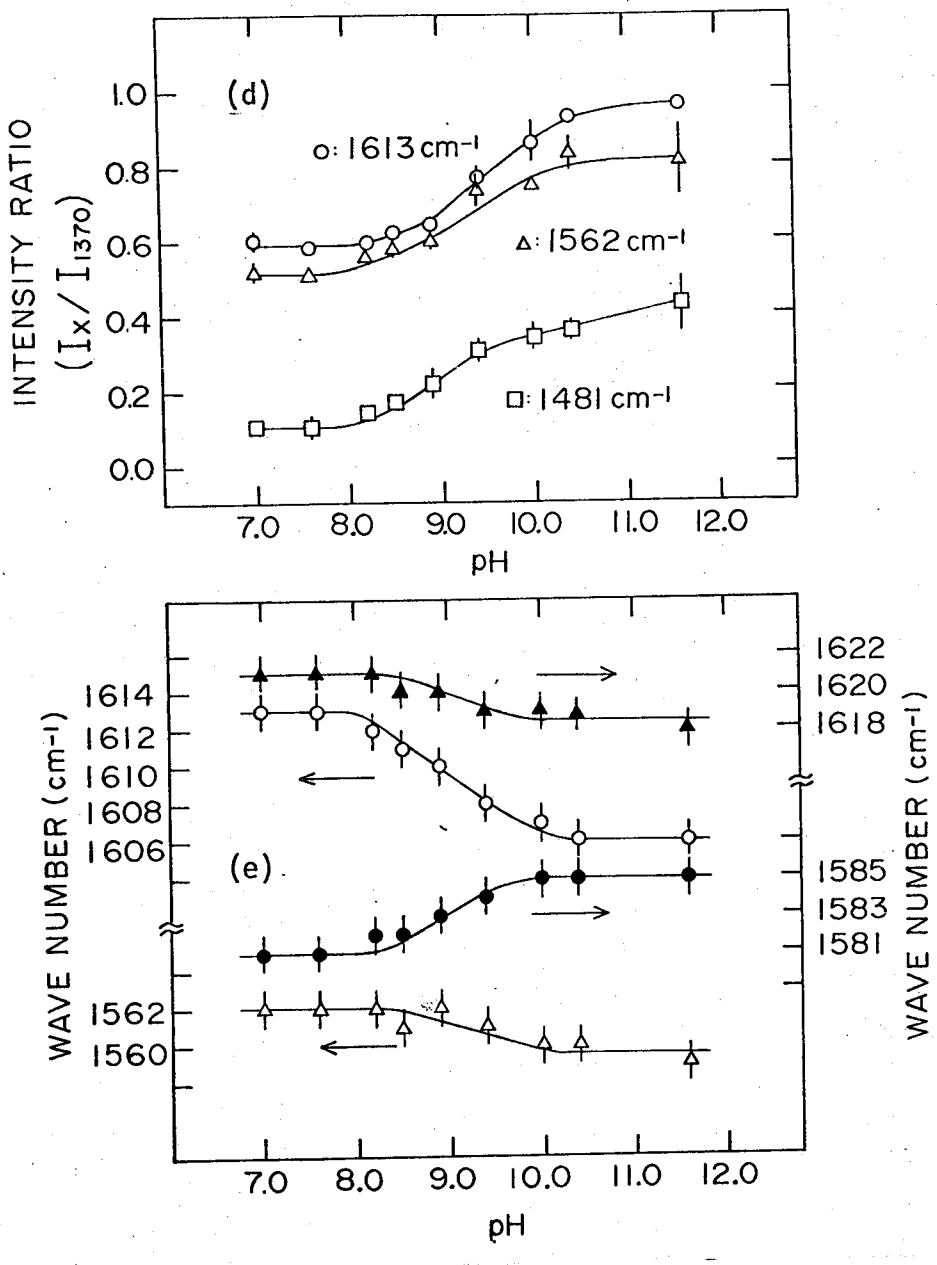

Fig. 2 (d) Raman peak intensities relative to the 1370 cm^{-1} band. (e) Frequency shifts of Raman lines.

ratio of the two Raman lines [R_s=I(1585 cm^{-1})/I(1560 cm^{-1})] reflected the relative concentration of low and high spin states of the heme iron. This ratio was confirmed to be larger for Mb derivatives in the ferric low spin state, such as MbCN, MbN_3, and MbIm, while it was smaller for ferric high spin derivatives such as MbF, MbOCN, and MbH_2O, when all resonance Raman spectra were excited by the 488.0 nm line. The pH dependence of this ratio for Mb, as shown in Fig. 2c, was consistent with the expected increase of the low spin species at higher pH, deduced from NMR (5,6) and magnetic susceptibility measurements (15). Therefore it was clear that the change in R_s with pH was due to the same factors governing the changes observed in NMR (6) and absorption spectra.

The intensity ratio [$R_s(x)$] at pH x can be approximated in terms of a sum of contribution from low (R_s^l) and high spin (R_s^h) species as

$$R_s(x) = \alpha R_s^l + (1-\alpha)R_s^h \qquad \text{(ii)}$$

where α is the mol fraction of low spin species. Assuming R_s^l =1.45 and R_s^h=0.64 (16), as the limiting values for purely low and high spin states, respectively, one obtained α=0.3 at pH 11.6 and α=0.06 at pH 7.0 for Mb. These results agreed closely with the values deduced from magnetic susceptibility measurements, namely α=0.31 (MbH_2O) and α=0.08 (MbOH) (15). This implied that 69% of Mb is in the high spin state at pH 11.6 although 99.8% of Mb is in the alkaline form.

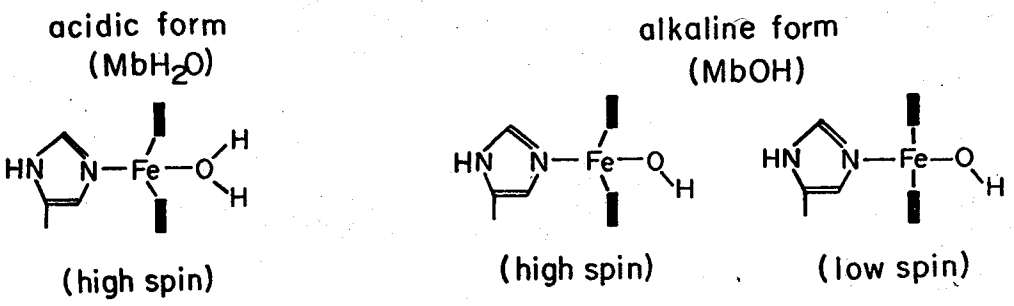

Fig. 3 Acidic and alkaline forms of ferric Mb.

It was emphasized here that the high spin species at pH 11.6 (MbOH, h.s.) is evidently different from the high spin species at pH 7.0 (MbH_2O) (Fig. 3). Figs. 2d and 2e illustrated the pH dependence of selected Raman frequencies and relative intensities of Mb. The relative intensities of the Raman lines at 1613, 1562, and 1481 cm^{-1}, characteristic of the high spin state increase as pH was raised, in spite of the expected decrease in concentration of MbH_2O (Eq. i). The frequency shifts of ring stretching vibrations shown in Fig. 2e, suggested a slight difference between MbOH, h.s. and MbH_2O in bond strength and/or structure of the heme groups. The existence of two kinds of high spin species in the alkaline solution was not taken into consideration in the recent analysis of the pH dependence of the NMR hyperfine shift of Mb (5,6).

It was also found that the intensity ratio of the Raman lines in the lower frequency region [$R=I(674\ cm^{-1})/I(758\ cm^{-1})$] is spin state dependent. Raman spectra in this frequency region for various derivatives of Mb were shown in Fig. 4, where (A) and (B) included those derivatives known to be mainly in the high and low spin states, respectively. This intensity ratio for Mb varies also with pH as illustrated in Fig. 2c, yielding larger values as the fraction of low spin species is increased. Since this ratio is small in square planar metallo-octaethylporphyrin [M(OEP)] and low spin Fe(OEP) but large for high spin Fe(OEP), irrespective of the axial ligand (17), it may also be dependent upon the planarity of the heme group.

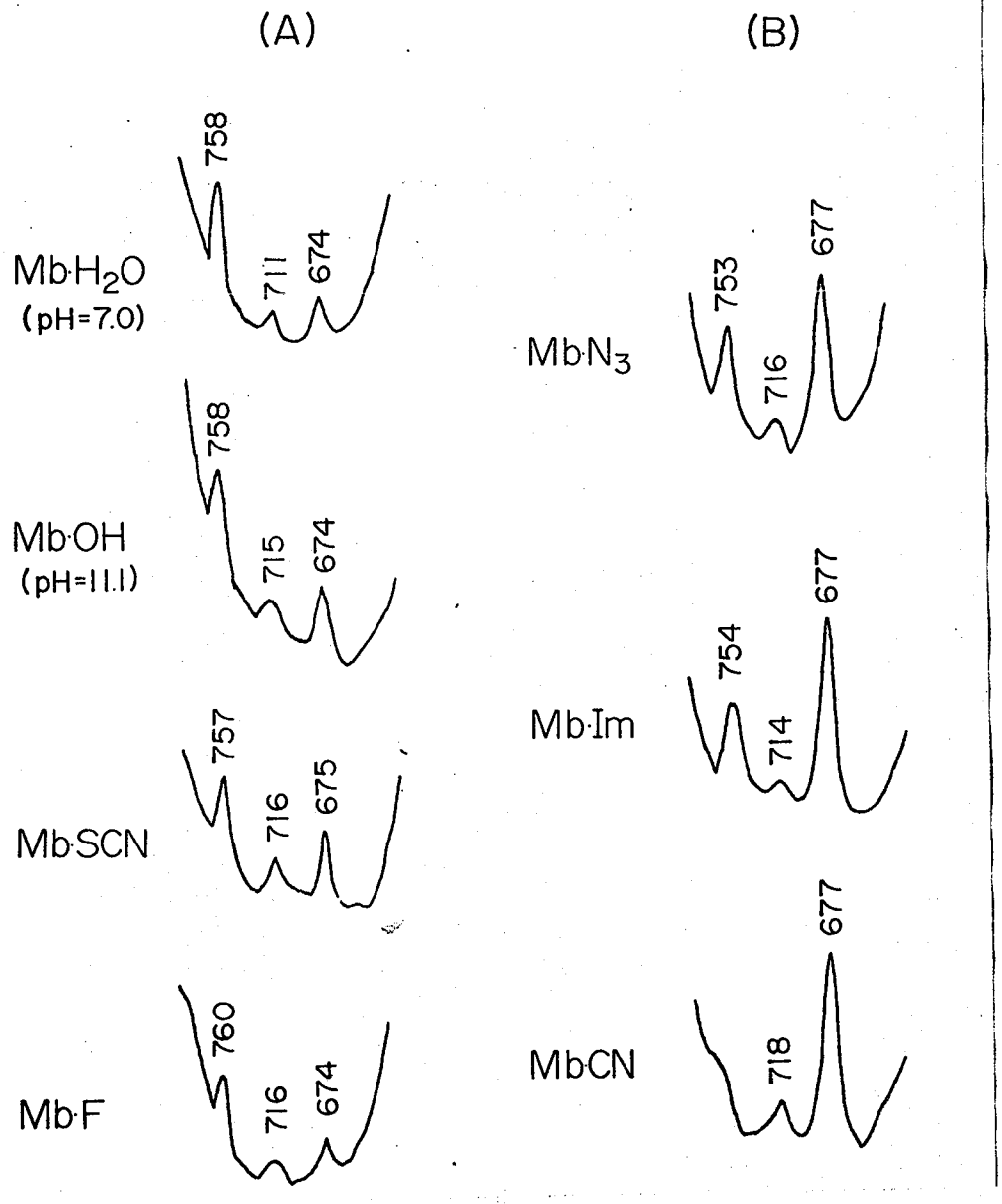

Fig. 4 Resonance Raman spectra in the region of 600-800 cm^{-1} of several high spin (A) and low spin (B) derivatives of ferric myoglobin.

REFERENCES

1. Stryer, L., Kendrew, J. C., and Watson, H. C. (1964) J. Mol. Biol. 8, 96.
2. George, P., Beetlestone, J., and Griffith, J. (1961) "Hematin Enzyme" (Falk, J. E., Lemberg, R., and Morton, R. K., eds.) 105, Pergamon Press, New York.
3. Coryell, C. D., Stitt, F., and Pauling, L. (1937) J. Am. Chem. Soc. 59, 633.
4. Theorell, H. and Ehrenberg, A. (1951) Acta Chem. Scand. 5, 823.
5. Morishima, I. and Iizuka, T. (1974) J. Am. Chem. Soc. 96, 5279.
6. Iizuka, T. and Morishima, I. (1975) Biochim. Biophys. Acta 400, 143.
7. Ikeda-Saito, M., Kitagawa, T., Iizuka, T., and Kyogoku, Y. (1975) FEBS Lett. 50, 233.
8. Rimai, L., Salmeen, I. T., and Petering, D. H. (1975) Biochemistry, 14, 378.
9. Yamamoto, T., Palmer, G., Gill, D., Salmeen, I. T., and Rimai, L. (1973) J. Biol. Chem. 248, 5211.
10. Brunner, H. and Sussner, H. (1973) Biochim. Biophys. Acta 310, 20.
11. Spiro, T. G. and Strekas, T. C. (1974) J. Am. Chem. Soc. 96, 338.
12. Kitagawa, T., Iizuka, T., Saito, M., and Kyogoku, Y. (1975) Chem. Lett. 849.
13. Kitagawa, T., Ogoshi, H., Watanabe, E., and Yoshida, Z. (1975) Chem. Phys. Lett. 30, 451.
14. Stein, P., Burke, J. M., and Spiro, T. G. (1975) J. Am. Chem. Soc. 97, 2304.
15. Beetlestone, J. and George, P. (1964) Biochemistry, 3, 707.
16. These values were derived from resonance Raman spectra for MbF (R_s^h) and MbCN (R_s^l), respectively. One may note that these values are applicable only to the Raman spectra excited by the 488.0 nm line because of resonance effect.
17. Kitagawa, T., Abe, M., Kyogoku, Y., Ogoshi, H., Watanabe, E., and Yoshida, Z. (1976) J. Phys. Chem. 80, 1181.

Chapter 3.

Resonance Raman Study of the Classification of Various C-Type Cytochromes

ABSTRACT

Resonance Raman spectra of cytochromes c, c_2, c_3, c-551, c-552, c-555, and f were measured in reduced and oxidized states. The assignment of several Raman lines which are used as structural monitors were established. The frequencies of the oxidation state marker showed that the sixth ligand binds to the heme iron mainly through the σ type interaction in the reduced C-type cytochromes. On the basis of relative intensity of Raman lines in the reduced state, the cytochromes were apparently classified into two groups; c-type (cyt c, cyt c_2, cyt c-551) and f-type (cyt f, cyt c-555, cyt c-552). The excitation profiles of the representatives of two groups revealed that the difference of Raman spectra was attributable to the position of α-absorption band which influenced strongly the apparent intensity of Raman lines. The relative intensity of two Raman lines around 750 cm^{-1} and around 680 cm^{-1} were aligned in order of the wavelength of α-band. It might be concluded that vibrational-spectroscopically there is no large difference between two groups, although the extra Raman lines were observed for f-type cytochromes upon excitation at shorter wavelength. The relative intensity of two Raman lines around 1585 and 1563 cm^{-1} of oxidized cytochromes suggested that the hemes of f-type cytochromes have slightly more hydrophobic environment than those of c-type cytochromes.

INTRODUCTION

The Raman spectra of a number of hemoproteins have been reported (1-3) and the correlations between the positions of Raman lines and the structural parameters of the heme (oxidation state, spin state, etc.) have been well established. Recent Raman studies revealed that two types binding interaction between the heme iron and the axial ligand in ferrous

low spin state could be classified by the Raman line called the oxidation state marker (4). The frequencies of this Raman line was unusually low for the reduced cytochrome P-450 (5) and chloroperoxidase (6). Our previous study have shown that there is another type of ligand sensitive Raman line (7). The Raman lines around 1565 cm^{-1} (ferric) and around 1540 cm^{-1} (ferrous) were sensitive to the replacement of the sixth ligand of heme iron (7). In addition, according to the detailed model compound study, the pH induced changes of the resonance Raman spectra observed for the C-type cytochromes were interpreted in terms of the replacement of axial ligands and the changes of hydrophobicity around the heme moieties (7).

Excitation profiles of hemoproteins and thier model metallo-porphyrins were examined carefully (1,2). When the Raman spectra of hemoproteins were excited at shorter wavelength than 500 nm, the intense Soret band dominates the scattering mechanism (8-10), while upon excitation about 500 nm the α and β bands dominate the scattering (11,12). The enhanced vibrational modes are all totally symmetric in the former case, whereas non-totally symmetric modes are strongly enhanced in the latter case. Spiro et al. showed that the intensity of the non-totally symmetric Raman bands reaches maximum at the center of the α band (8,11), and within the β band. The latter maximum,however, shifts systematically to shorter wavelength with increasing vibrational frequency of the Raman band (11).

Many kinds of C-type cytochromes were found and classification of them has been extensively investigated (12,13). It has been pointed out previously by Yamanaka et al. that the f-type cytochrome differs considerably from c_2-type cytochrome in the reactivity with Pseudomonus cytochrome oxidase [EC 1,9,3,2] ; the f-type cytochromes react fairly rapidly with the enzyme whereas the c_2-type cytochromes do scarcely (14). The f-type cytochromes have an asymmetric α-peak, a high ratio (about 7) of A_γ(reduced)/A_α(reduced) and considerably small value of millimolar extinction coefficient of the α band (about 22) (12,13). On the contrary, in the c_2-type cytochromes the α band is symmetric, the ratio of A_γ/A_α is about 5, and millimolar extinction at α peak is comparable to that of mammalian cytochrome c (cyt c) (about 28) (12,13). Therefore it

seems interesting to study the Raman spectral properties of the c_2- and f-type cytochromes in comparison with their absorption spectral properties. Rhodospirillum rubrum cytochrome c_2 (cyt c_2) and Pseudomonas aeruginosa cytochrome c-551 (cyt c-551) were taken up as the c_2-type cytochrome and Spirulina platensis cytochrome f (cyt f), Chlorobium thiosulphatophilum cytochrome c-555 (cyt c-555) and Thermus thermophilus HB8 cytochrome c-552 (cyt c-552) were taken up as the f-type cytochrome. Horse heart cyt c which has similar to the c_2-type cytochromes in absorption spectrum and Desulfovibrio vulgaris cytochrome c_3 (cyt c_3) were also studied.

EXPERIMENTAL

Horse heart cyt c was purchased from Sigma Chemical Company (type VI) and used without further purification. Rhodospirillum rubrum cyt c_2 and Pseudomonas aeruginosa cyt c-551 were generously provided by Prof. T. Horio (Institute for Protein Research, Osaka University). Desulfovibrio vulgaris cyt c_3 was highly purified by the method given in Ref. (15). Purification procedures for Chlorobium thiosulphatophilum cyt c-555 (14) and Spirulina platensis cyt f (16) were described elsewhere. Thermus thermophilus HB8 cyt c-552 was generously provided by Dr. H. Kihara (Jichi Medical College), Dr. H. Hon-nami and Dr. T. Oshima (Institute for Life Science, Mitsubishi Kasei Company). To obtain the Raman spectra of oxidized or reduced cytochromes a small amount of potassium ferricyanide or sodium dithionite was added to solutions of cytochromes, respectively.

Resonance Raman spectra were excited by an argon ion laser (Spectra Physics Model 164) and were recorded on a JEOL-400 D Raman spectrometer equipped with a HTV-R 649 photomultiplier. The frequency calibration of the spectrometer was performed with indene (17) within $\pm$ 1 cm^{-1} of uncertainty.

Upon the measurements of Raman spectra 200 µl of 0.5 mM (oxidized) or 0.1 mM (reduced) cytochrome solution was put in a cylindrical cell and the scattered light was collected at right angle to the excitation light. The absorption spectra were measured with

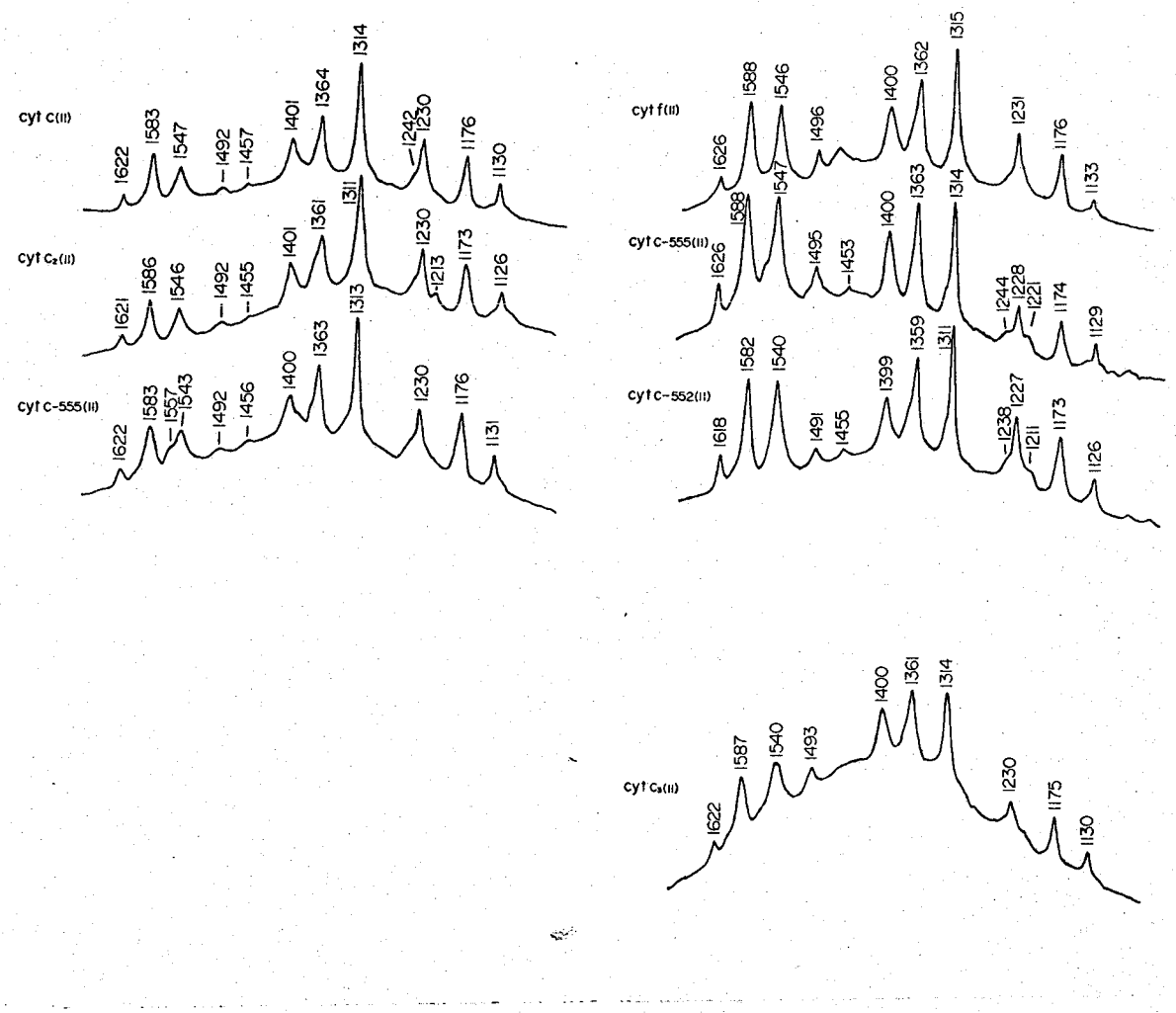

Fig. 1 Resonance Raman spectra of various reduced C-type cytochromes. Instrumental conditions: laser, 514.5 nm; power 180 mW at laser out put; slit width, 2 cm^{-1}; time constant, 3.2 sec; scan speed, 25 cm^{-1}/min; sample temperature, 10°C.

a Hitachi 124 recording spectrophotometer at 25°C.

RESULTS

Fig. 1. shows the resonance Raman spectra of reduced cyt c, c_2, c-551, c_3, c-552, c-555, and f in the frequency region of 1100-1700 cm^{-1}. The observed Raman lines were named tentatively as A, B, C, etc. as shown Fig. 1. The oxidation state marker Raman lines (G) were found between 1359 and 1364 cm^{-1}. The spin state marker Raman lines (A,D) were found between 1618 and 1626 cm^{-1} and between 1491 and 1496 cm^{-1}, respectively. The ligand sensitive Raman lines (C) were observed at 1546 or 1547 cm^{-1} for reduced cyt c, cyt c_2, cyt c-555, and cyt f, at 1543 cm^{-1} for reduced cyt c-551, and at 1540 cm^{-1} for reduced cyt c_3 and cyt c-552. The frequencies of Raman lines of cyt c-555 were close to those of cyt f and were higher than those of the others. The Raman lines of reduced cyt c-552 lie at especially lower frequencies in comparison with the others. An extra Raman line was clearly recognized at 1557 cm^{-1} for cyt c-551 and at 1563 cm^{-1} for cyt c-555. The relative intensities of Raman lines distinguished the two types of cytochromes and are shown in Table 1 where the peak hight ratios to that of G are

Table 1. Relative intensity ratio of Raman bands (X/G) G; 1360 cm^{-1}

	B/G	C/G	D/G	H/G	J/G	K/G
cyt c	0.9	0.5	0.1	2.0	0.8	0.5
cyt c_2	0.8	0.6	0.2	1.9	0.9	0.5
cyt c-551	0.8	0.6	0.2	1.9	1.1	0.5
cyt f	1.0	0.9	0.3	1.5	0.5	0.2
cyt c-555	1.2	1.2	0.3	1.3	0.4	0.2
cyt c-552	1.0	0.9	0.2	1.4	0.6	0.3
cyt c_3	0.9	0.7	0.2	1.4	0.7	0.4

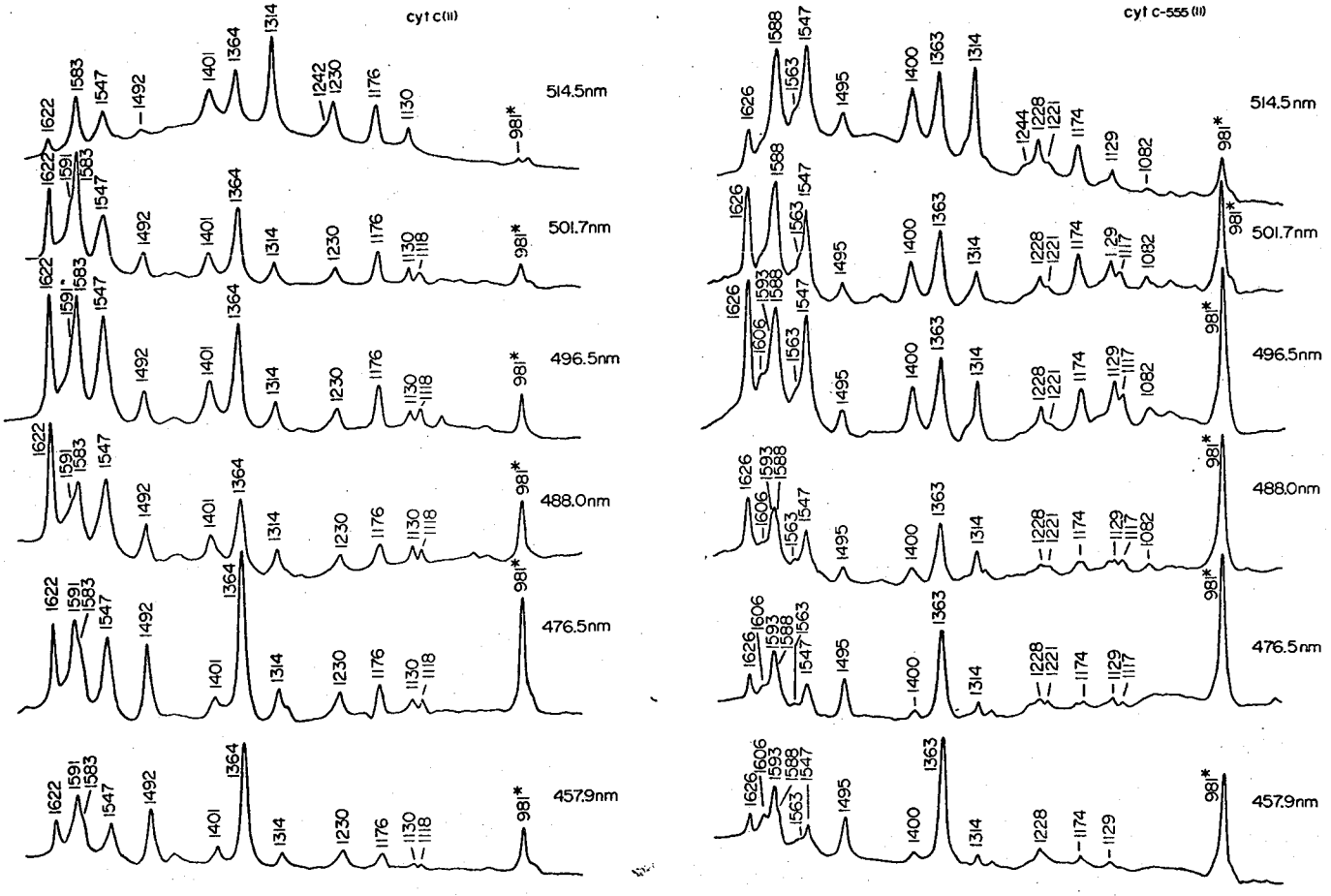

Fig. 2 (a) Resonance Raman spectra of reduced cyt c and cyt c-555 for various excitation lines of argon ion laser. The Raman line with an asterisk is due to the sulfate peak from $(NH_4)_2SO_4$ which was used for internal standard of Raman intensities. Instrumental conditions were similar to those of Fig. 1 without laser line and power.

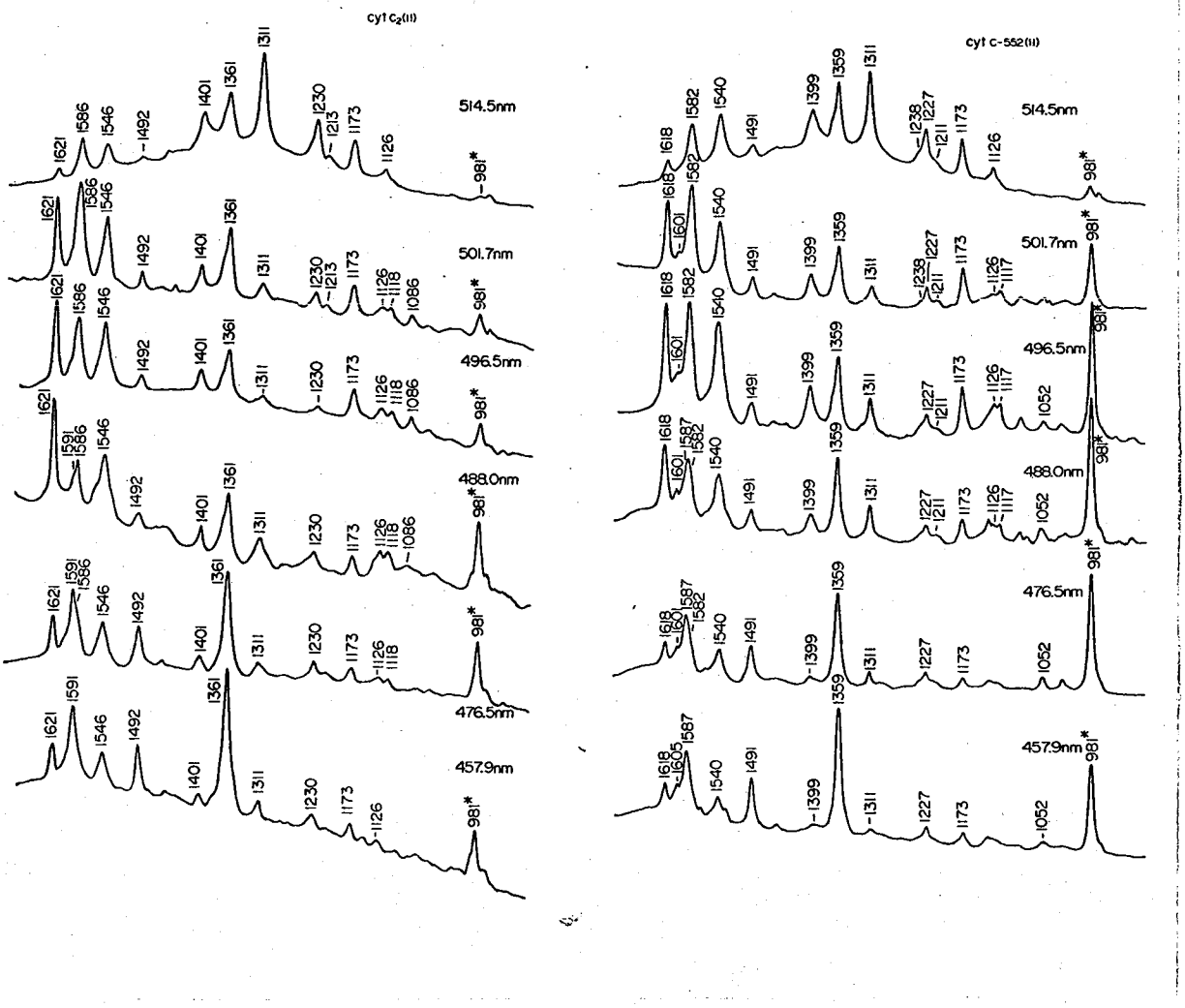

Fig. 2 (b) Resonance Raman spectra of reduced cyt c_2 and cyt c-552 for various excitation lines of argon ion laser.

listed. The relative intensities of Raman lines of cyt c, cyt c_2, and cyt c-551 were alike to each other and those of cyt f, cyt c-555, and cyt c-552 were also close to each other.

Fig. 2. shows the Raman spectra of reduced cyt c, cyt c_2, cyt c-552, and cyt c-555 for various wavelengths of excitation. The Raman spectrum of cyt c resembled closely that of cyt c-552 at every excitation wavelength. The Raman spectrum of cyt c or cyt c_2 excited by the 457.9 nm line was similar to that of cyt c-555 or cyt c-552 excited by the 476.5 nm line. The Raman spectrum of cyt c or cyt c_2 excited by the 476.5 nm line was also similar to that of cyt c-555 or cyt c-552 excited by the 488.0 nm line. In an analogous way to above the Raman spectrum of cyt c or cyt c_2 excited by one of the lines of argon ion laser was similar to that of cyt c-555 or cyt c-552 excited by the next longer wavelength line of argon ion laser. A few new Raman lines were observed by the excitation at shorter wavelength. For cyt c and cyt c_2 the intensity of the Raman lines at 1591 and 1592 cm^{-1} got stronger and stronger at shorter wavelength and for cyt c-555 and cyt c-552 the 1593 and 1587 cm^{-1} lines did. However for the latter group of cytochromes another Raman line could be detected clearly at 1606 and 1601 cm^{-1}, respectively, upon the excitation at shorter wavelengh.

Fig. 3. shows the Raman spectra of reduced cyt c, cyt c_2, cyt c-551, cyt c_3, cyt c-552, cyt c-555, and cyt f in the region of 650-850 cm^{-1}. The relative intensity of the Raman lines near 750 and 690 cm^{-1} clearly depended upon the position of a α absorption band; cyt c which gives rise to the α band at 550 nm yielded a weak Raman line at 689 cm^{-1}, whereas cyt c-555 which gives rise to the α band at 555 nm yielded the strong Raman line at 686 cm^{-1}. The longer the wavelength of α band, the stronger the intensity of Raman line at 685 cm^{-1}. The absorption maxima of electronic spectra was shown in Table 2.

Fig. 4. shows the Raman spectra of the oxidized cyt c, cyt c_2, cyt c-551, cyt f, cyt c-555, cyt c-552, and cyt c_3. Similar characteristics of Raman frequencies as in the reduced state were observed in the oxidized state. The frequencies of Raman lines of oxidized cyt c-555 were very close to those of oxidized cyt f and higher than those of the others. The Raman lines of oxidized cyt c-552 was located at

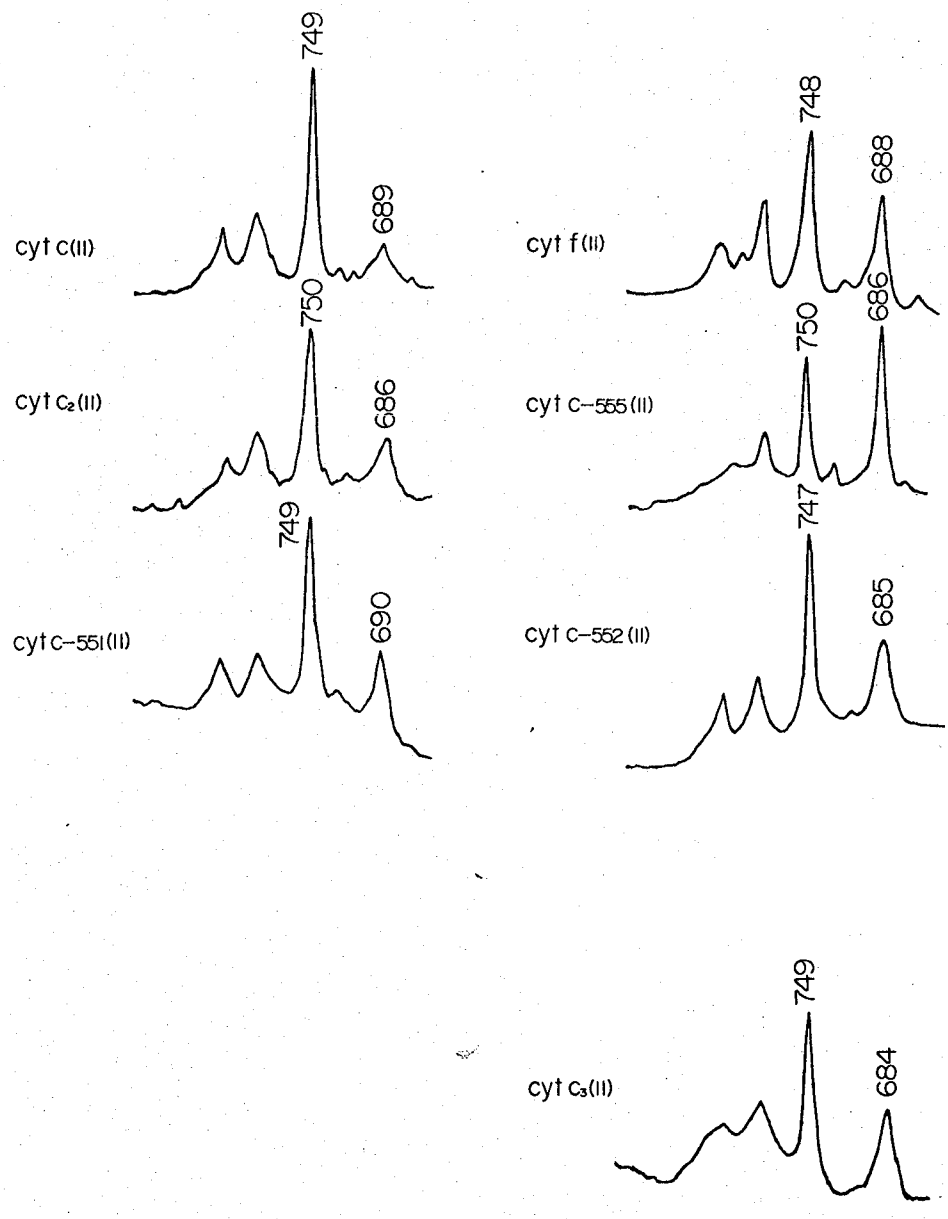

Fig. 3 Resonance Raman spectra of various reduced C-type cytochromes in the region of 650-850 cm^{-1}. Instrumental conditions: slit width; 3 cm^{-1}, other conditions were similar to those of Fig. 1.

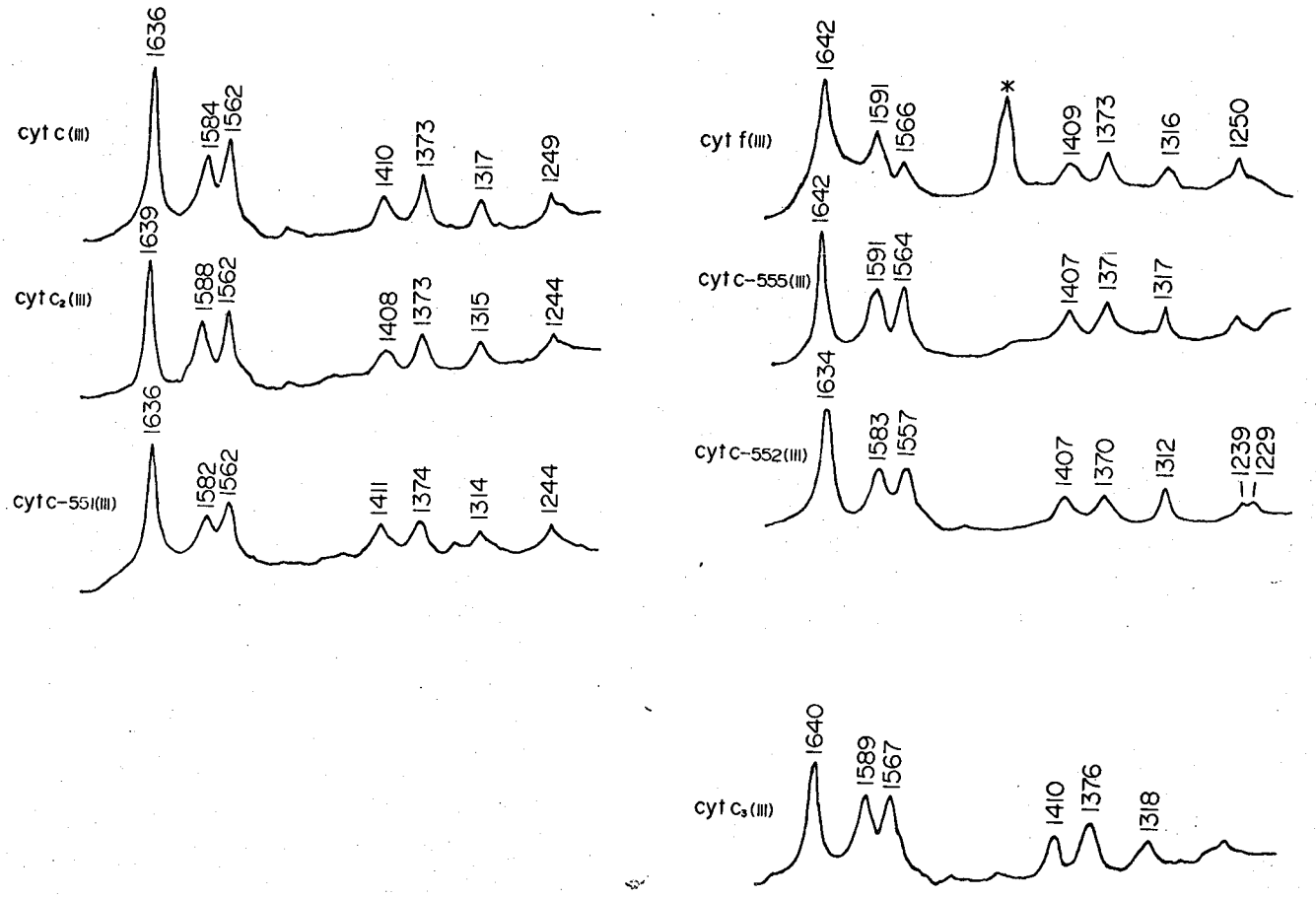

Fig. 4 Resonance Raman spectra of various oxidized C-type cytochromes. The Raman line with asterisk was due to solvent of cyt f. Instrumental conditions: slit width; 3 cm^{-1}, other conditions were similar to those of Fig. 1.

Table 2. The absorption maxima of electronic spectra

	α	β (reduced)	γ	γ (oxidized)	A_γ/A_α (reduced)
cyt c	550	520	415	409	4.8
cyt c_2	550	522	417	413	5.1
cyt c-551	551	521	416	409	5.3
cyt f	553.6	523	416		6.45
cyt c-555	555	523	417	411	7.1
cyt c-552	552	522	417	408	8.1
cyt c_3	552	523	419	410	6.3

lower frequency in comparison with the others. The remarkable difference of the relative intensity was observed only about two Raman line around 1585 and 1563 cm^{-1}. The latter Raman lines were stronger than the former in cyt c, cyt c_2, and cyt c-551. On the contrary for the others the latter lines were weaker than or equal to the former lines.

DISCUSSION

Reduced form The assignments of Raman lines of hemoproteins were fairly established by experimental studies upon the Raman spectra of metallo-octaethylporphyrins [M(OEP)], their meso-deuterated compounds [M(OEP)-d_4] (18), and ^{15}N-enriched metallo-octaethylporphyrins [M(OEP)-$^{15}N_4$] (19) and also by theoretical studies upon the normal coordinated calculation of metallo-octaethylporphyrins (20). The Raman lines A, B, and D were mainly due to the methine-bridge stretching vibrations (18), and the Raman line C involved the out-of-phase stretching motion of the four CC bonds of pyrrole ring (18). The oxidation state marker (G) was associated with the CN symmetric stretching vibration (19). The frequencies of the G lines showed that the sixth ligand binds to the heme iron mainly through the σ type

interaction in the reduced C-type cytochromes.

The resonance Raman spectra of various C-type cytochromes were apparently classified into two groups as shown in Fig. 1, Fig. 4, and Table 1 (hereafter they will be referred to as c-type [cyt c, cyt c_2, and cyt c-551] and f-type [cyt f, cyt c-555, and cyt c-552]). The Raman spectrum of reduced cyt c_3 showed the intermidiate nature between the two types. The relative intensity of Raman lines of reduced cyt c_2 resembled closely that of reduced cyt c. In addition the frequency of the oxidation state marker, spin state marker, ligand sensitive Raman line was very close to each other. Probably the structure of the heme and its surroundings of reduced cyt c_2 was similar to that of reduced cyt c. The Raman spectrum of reduced cyt c-551 was also close to that of reduced cyt c or cyt c_2 except for the frequency of Raman line C. The excess Raman line at 1557 cm^{-1} of reduced cyt c-551 might indicate the existence of high spin component. The Raman spectrum of reduced cyt c-555 was quite close to that of reduced cyt f for both the frequencies and intensities, although the excess Raman line was detected at 1563 cm^{-1} for reduced cyt c-555. This result obtained by Raman scattering could confirm that cyt c-555 is a f-type cytochrome (14). The characteristics of the Raman spectra of reduced cyt c-552 (21) and cyt c_3 (7) were described in detail elsewhere.

The results obtained in Fig. 2 and 3 suggested that the relative intensities of Raman lines of reduced cytochromes depended strongly upon the position of the α band. Thus, we performed the analysis of the excitation profile for reduced cyt c and cyt c-555. The relative intensities of three depolarized ($\sim$1400, $\sim$1547, and $\sim$1625 cm^{-1}), two anomalously polarized ($\sim$1130 and $\sim$1314 cm^{-1}) and one polarized ($\sim$1364 cm^{-1}) lines of reduced cyt c and cyt c-555 to 981 cm^{-1} line of $(NH_4)_2SO_4$ are plotted against the excitation wavelength in Fig. 5. The anomalously polarized and polarized Raman lines were highly intensified at 514.5 nm.

The formulation developed by Albrecht (22) and modified later Tang and Albrecht (23) was used for the present analysis of excitation profile. For non-totally symmetric vibrations Albrecht's B term is considered to be the main term for Raman intensity, while for totally symmetric vibrations Albrecht's A term is considered to be the main

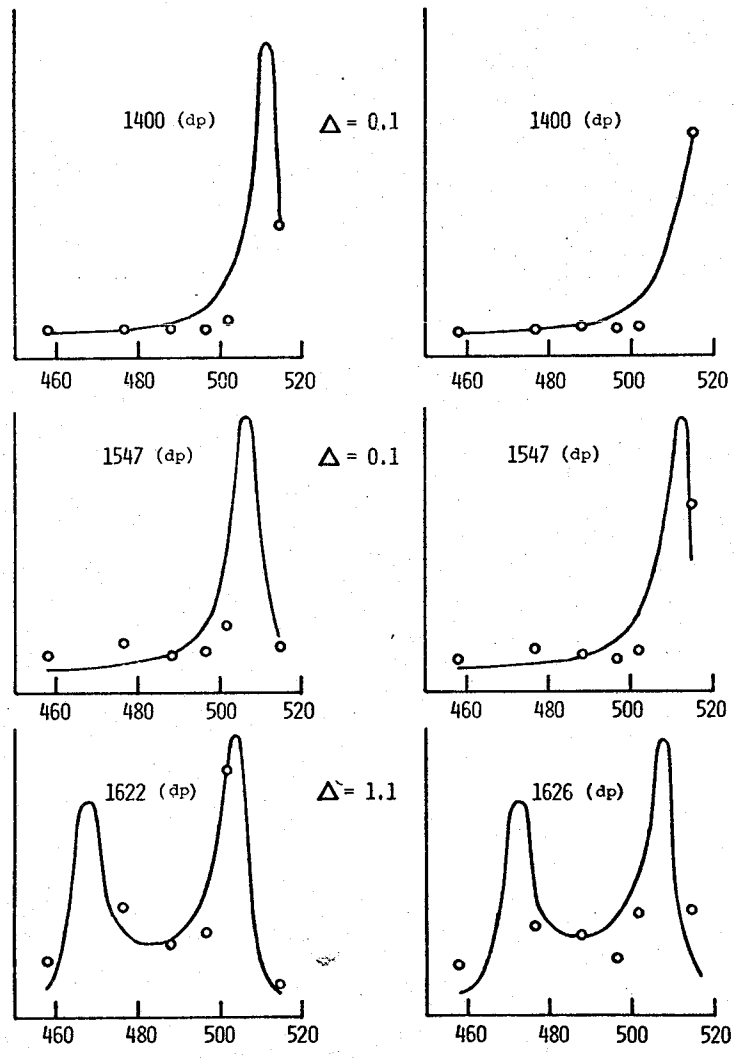

Fig. 5 The excitation profiles observed and calculated of reduced cyt c and cyt c-555. Open circles indicate the relative to that of the 981 cm^{-1} line of $(NH_4)_2SO_4$. Curves show the calculated excitation wavelength dependence of the Raman intensity.

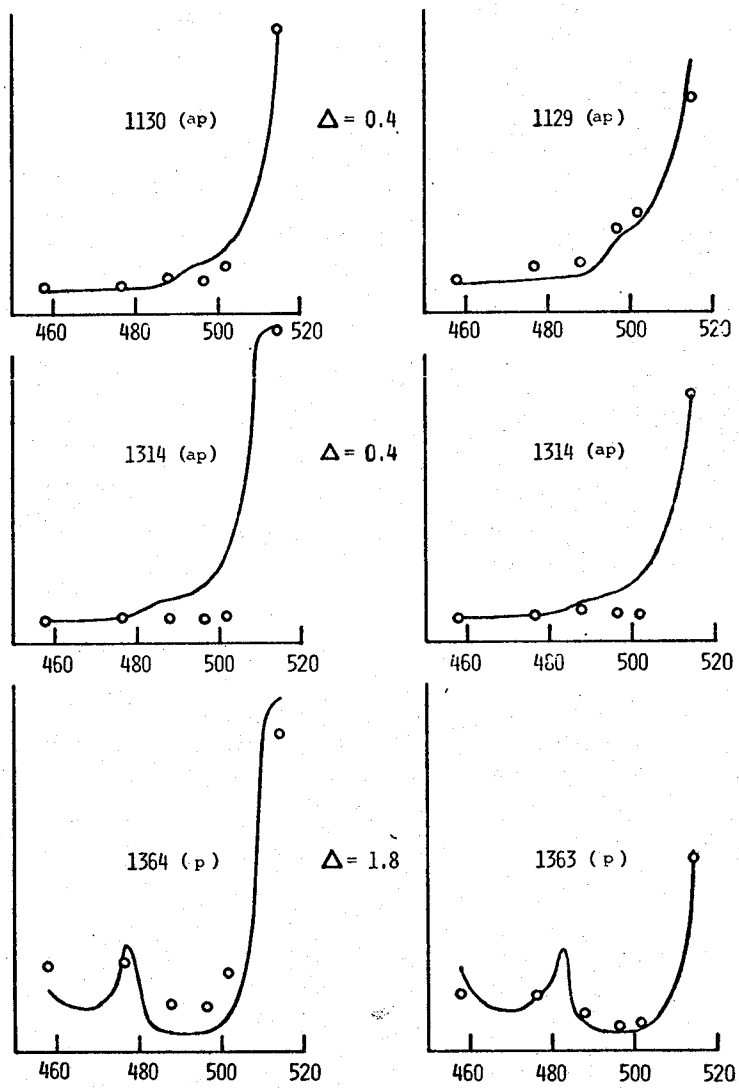
1130 (ap)
Δ = 0.4
1129 (ap)
460
480
500
520
1314 (ap)
Δ = 0.4
1314 (ap)
1364 (p)
Δ = 1.8
1363 (p)

term. The intensity of the anomalously polarized Raman lines could be attributed mainly to the B term. In Fig. 5 the solid lines show the calculated excitation profile of the Raman intensity. The best fitted Δ (the separation between the equilibrium position of the ground and excited states) was chosen commonly for both cytochromes. The experimental results of the excitation profiles of reduced cyt c and cyt c-555 were explained by the calculated curves. This fact suggested that the apparent difference in intensity between the c- and f-type cytochromes reflected the difference of the characteristics of electronic absorption spectra. The observed relative intensity of two Raman lines around 750 and 688 cm^{-1} could be clearly interpreted by the calculated relative intensity as shown in Fig. 6. It might be concluded that there is no large difference in vibrational frequencies between the two groups. The fact that the extra Raman lines were observed at 1606 and 1601 cm^{-1} for reduced cyt c-555 upon excitation at shorter wavelength and cyt c-552 might indicate the lower symmetry of hemes of f-type cytochromes which show the asymmetric α band and high intensity ratio of A_γ/A_α .

Oxidized state Since the interaction between heme and apoprotein was unusally weak in the oxidized form, the difference of the Raman spectra between c-type and f-type was not always clear. The relative intensity and frequencies of Raman lines of oxidized cyt c_2 was close to those of cyt c. Even in the oxidized state the structure of heme and heme environment of cyt c_2 resemble those of cyt c. Those of cyt c-551 was also similar to those of cyt c and cyt c_2. In the preceiding paper (7), the hydrophobicity of heme environment was examined according to the model compound study. It was concluded from the relative intensity of two Raman lines around 1585 cm^{-1} and 1565 cm^{-1} that oxidized cyt b_5 is more hydrophobic than that of oxidized cyt c. The fact that the relative intensity of the Raman line around 1585 cm^{-1} was stronger in f-type cytochromes suggested that f-type cytochrome imply the slightly more hydrophobic environment of the heme than c-type cytochrome.

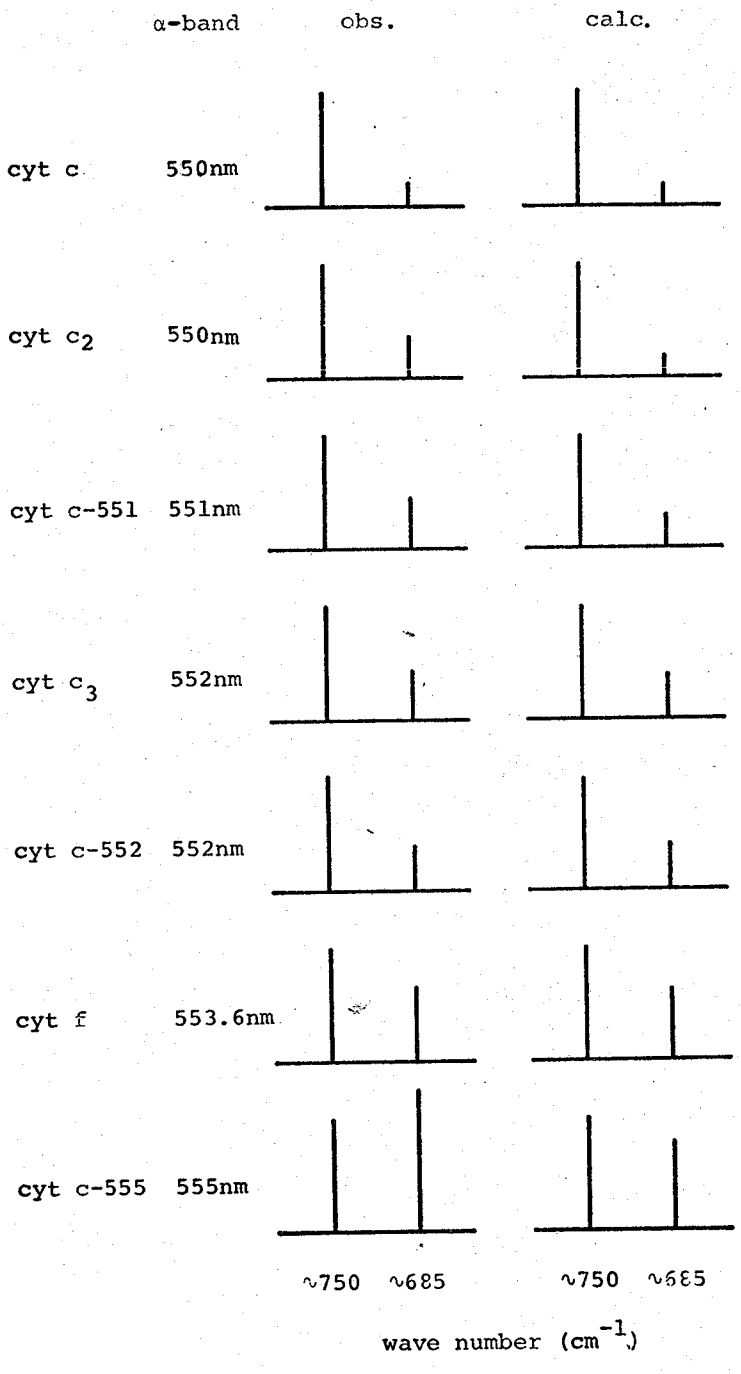

Fig. 6 The observed and calculated intensities of the Raman lines around 750 cm^{-1} and 685 cm^{-1} of reduced C-type cytochromes. The intensity of the Raman line around 750 cm^{-1} was normalized.

ACKNOWLEDGEMENT

The author would like to express his gratitude to Dr, H. Kihara, Jichi Medical College and Dr. T. Oshima and Dr. H. Hon-nami, Institute for Life Science, Mitsubishi Kasei Company for the courtesy of providing him with Thermus thermophilas HB8 cyt c-552.

REFERENCES

1. Spiro, T. G. (1975) Biochim. Biophys. Acta 416, 169.
2. Spiro, T. G. (1976) "Vibrational Spectra and Structure" (Durig, J. R. ed.) Vol. 5, p 101, Elsevier Scientific Publishing Company, Amsterdam.
3. Spiro, T. G. and Gaber, B. P. (1977) Ann. Rev. Biochem. 46, 553.
4. Kitagawa, T., Kyogoku, Y., Iizuka, T., and Ikeda-Saito, M. (1976) J. Am. Chem. Soc. 98, 5169.
5. Ozaki, Y., Kitagawa, T., Kyogoku, Y., Shimada, H., Iizuka, T., and Ishimura, Y. (1976) J. Biochem. 80, 1447; Ozaki, Y., Kitagawa, T., Kyogoku, Y., Imai, Y., Hashimoto-Yutsudo, C., and Sato, R., submitted to J. Am. Chem. Soc.
6. Champion, P. M., Remba, R. D., Chiang, R., Fitchen, D. B., and Hager, L. P. (1976) Biochim. Biophys. Acta 446, 486.
7. Kitagawa, T., Ozaki, Y., Teraoka, J., Kyogoku, Y., and Yamanaka, T. (1977) Biochim. Biophys. Acta 494, 100.
8. Strekas, T. G. and Spiro, T. G. (1973) J. Raman Spectrosc. 1, 197.
9. Nafie, L. A., Pezolet, M., and Peticolas, W. L. (1973) Chem. Phys. Lett. 20, 563.
10. Freidman, J. M. and Hochstrasser, R. M. (1973) Chem. Phys. 1, 457.
11. Spiro, T. G. and Strekas, T. C. (1972) Proc. Natl. Acad. Sci. U. S. 69, 2622.
12. Lemberg, R. and Barrett, J. (1972) "Cytochromes" Academic Press, New York.
13. Yamanaka, T. and Okunuki, K. (1974) "Microbial Iron Metabolism" (Neilands, J. B. ed.) p 394, Academic Press, New York.
14. Yamanaka, T. and Okunuki, K. (1968) J. Biochem. 63, 341.
15. Yagi, T. and Maruyama, K. (1971) Biochim. Biophys. Acta 243, 214.
16. Yamanaka, T. unpublished
17. Hendra, P. J. and Loader, E. J. (1968) Chem. Ind. 718.
18. Kitagawa, T., Ogoshi, H., Watanabe, E., and Yoshida, Z. (1975) J. Phys. Chem. 79, 2629.
19. Kitagawa, T., Abe, M., Kyogoku, Y., Ogoshi, H., Sugimoto, H., and Yoshida, Z. (1977) Chem. Phys. Lett. 48, 55.

20. Abe, M., Kitagawa, T., and Kyogoku, Y. (1976) Chem. Lett. 249.
21. Kihara, et al. in preparation,
22. Albrecht, A. C. (1961) J. Chem. Phys. 34, 1476.
23. Tang, J. and Albrecht, A. C. (1970) "Raman Spectroscopy" Vol. 2, (Szymanski, ed.) Plenum Press, New York.

Chapter 4.

The pH Dependence of the Resonance Raman Spectra of Various C-Type Cytochromes. Replacement of the Sixth Ligand and Structural Alterations at Heme Moieties.

ABSTRACT

The pH dependence of resonance Raman spectra were studied for ferrous and ferric cytochromes c, c_2, c-551, and c-555. The frequencies of the 1565 cm^{-1} (ferric) and 1539 cm^{-1} lines (ferrous) were sensitive to the replacement of the sixth ligand. The titration curve for the 1565 cm^{-1} line of cytochrome c was parallel with that for the 695 nm band. The Raman spectrum of ferric cyt c·CH_3NH was almost identical with that of native alkaline cyt c. The present results of Raman spectra would be reasonably interpreted if an arbitrary N-base such as lysine or histidyl imidazole were coordinated as the sixth ligand in the alkaline form of the native cyt c. For ferric cyt c-551, it was deduced that the replacement of the axial ligand occurred at about pH 11.5. The relative intensities of three Raman lines at 1639, 1587, and 1561 cm^{-1} of ferric protoporphyrin bis-imidazole complex were found, from its Raman spectra measured in the presence or absence of detergents, to depend upon the hydrophobicity in the environment of the heme and the relative intensities of the corresponding three Raman lines of cytochromes suggested that the heme pocket of ferric cytochrome b_5 is more hydrophobic than that of ferric cytochrome c.

INTRODUCTION

The dependence of the resonance Raman spectra of hemoproteins upon the oxidation and spin states of the heme iron was well documented (1,2). The Raman line called as the oxidation state marker appears at the frequencies between 1355 and 1362 cm^{-1} and between 1369 and 1375 cm^{-1} for the reduced and oxidized states, respectively. Recent Raman studies revealed that the frequencies of the oxidation state marker band was unusually low for the reduced cytochrome P-450_{cam} (1346 cm^{-1})

(3) and reduced chloroperoxidase (1348 cm^{-1})(4) but unusually high (1382 cm^{-1}) for the compound II of horseradish peroxidase [HRP-comp (II)](5,6). This Raman line was pointed out as a possible indicator of two types of binding interaction between the heme iron and the axial ligand (7).

On the other hand it may be overlooked that there is another type of ligand-sensitive Raman line. The previous investigation have shown that the Raman line around 1540 cm^{-1} of ferrous carboxymethyl-methionyl cytochrome c (alkyl c) was shifted sensitively with pH despite the negligible change of the oxidation state marker or other bands (8,9). The change in the Raman spectrum was not associated with the possible ionization of histidine-18 of the fifth ligand but its implications have not been studied throughly in relation with the changes of the heme-linked properties. It was the purpose of this Chapter to establish an empirical rule which related the pH induced changes of the resonance Raman spectra of various C-type cytochromes with the structure changes around their heme moieties.

The existence of two distinct forms of ferric cytochrome c [cyt c(Fe^{3+})] in an alkaline solution was now in general agreement, though the sixth ligand of the alkaline form was unknown. The 695 nm band (10-14) and NMR methyl signal of the coordinated methionine (Met-80)(15,16) of cyt c(Fe^{3+}) suggested that the transition with pK 9.3 was associated with the replacement of the Met-80 to some other strong field ligand. Thus cyt c(Fe^{3+}) was a sutable material to identify the Raman spectral change caused by the replacement of the sixth ligand. The pH dependent structural alterations at heme moieties of another C-type cytochromes were not always well known.

Therefore,in this Chapter, the pH dependence of the resonance Raman spectra were examined carefully for various C-type cytochromes including cytochromes c, c_2, c-551, and c-555. To investigate the effect of the hydrophobicity in the heme pocket upon the resonance Raman spectra, ferrous and ferric protoporphyrin with various axial ligands were subjected to Raman spectroscopy in the presence and absence of detergents. The pH induced changes of the resonance Raman spectra observed for the C-type cytochromes were interpreted in terms of the replacement of the

axial ligands and the change of hydrophobicity around the heme moieties.

EXPERIMENTAL

Rhodospirillum rubrum cytochrome c_2 (cyt c_2) and Pseudomonas aeruginosa cytochrome c-551 (cyt c-551) were generously provided by Dr. T. Horio (Institute for Protein Research, Osaka University). Purification procedures for Chlorobrium thiosulphatophilum cytochrome c-555 (cyt c-555) were described elsewhere (17). Horse heart cytochrome c (cyt c) (Sigma Type VI), bovine hemin (Sigma Type I), sodium dodecyl sulfate (SDS) (Nakarai chemicals) and cetyltrimethylammonium bromide (CTAB) (Wako chemicals) were purchased and used without further purification.

Raman spectra were excited by the 514.5 nm line of Ar^+ ion laser (Spectra Physics Model 164) and recorded on a JEOL-400D Raman spectrometer equipped with HTV-R649 photomultiplier. The frequency calibration of the spectrometer was performed with indene (18) within $\pm$ 1 cm^{-1} of uncertainly. For the measurements of the Raman spectra 200µl of 0.7 mM (ferric) or 0.1 mM (ferrous) cytochrome solution was put in a cylindrical cell and the scattered light at angle to the excitation light (~50 mW at sample point) was collected. The pH of the solution was adjusted with concentrated HCl or NaOH and was determined after the Raman measurement with Hitachi-Horiba M-5 pH meter.

For every experiment upon iron-protoporphyrin derivatives [Fe(PP)L or $Fe(PP)L_2$], a fresh solution of hemin was prepared to protect it from self-association as follows; 20 mg of hemin was dissolved in 0.3 ml of 0.1 M NaOH solution and then diluted to 3 ml with H_2O. For imidazole (Im) derivatives, 212 mg of Im (44 times of the equivalence) was added to the solution first but otherwise 5µl of the solution was diluted to 300µl with H_2O or detergent solution of certain concentration. Reduction of the hemin as well as cytochromes was performed with small amount of solid dithionite. The reduction under the reduced pressure was carried out as follows. The degassed solution of $Fe^{3+}(PP)Cl$ was frozed and then solid dithionite was placed on a frozen solution. Before melting, the cell was evacuated again until 0.1 mmHg after one cycle of degassing,

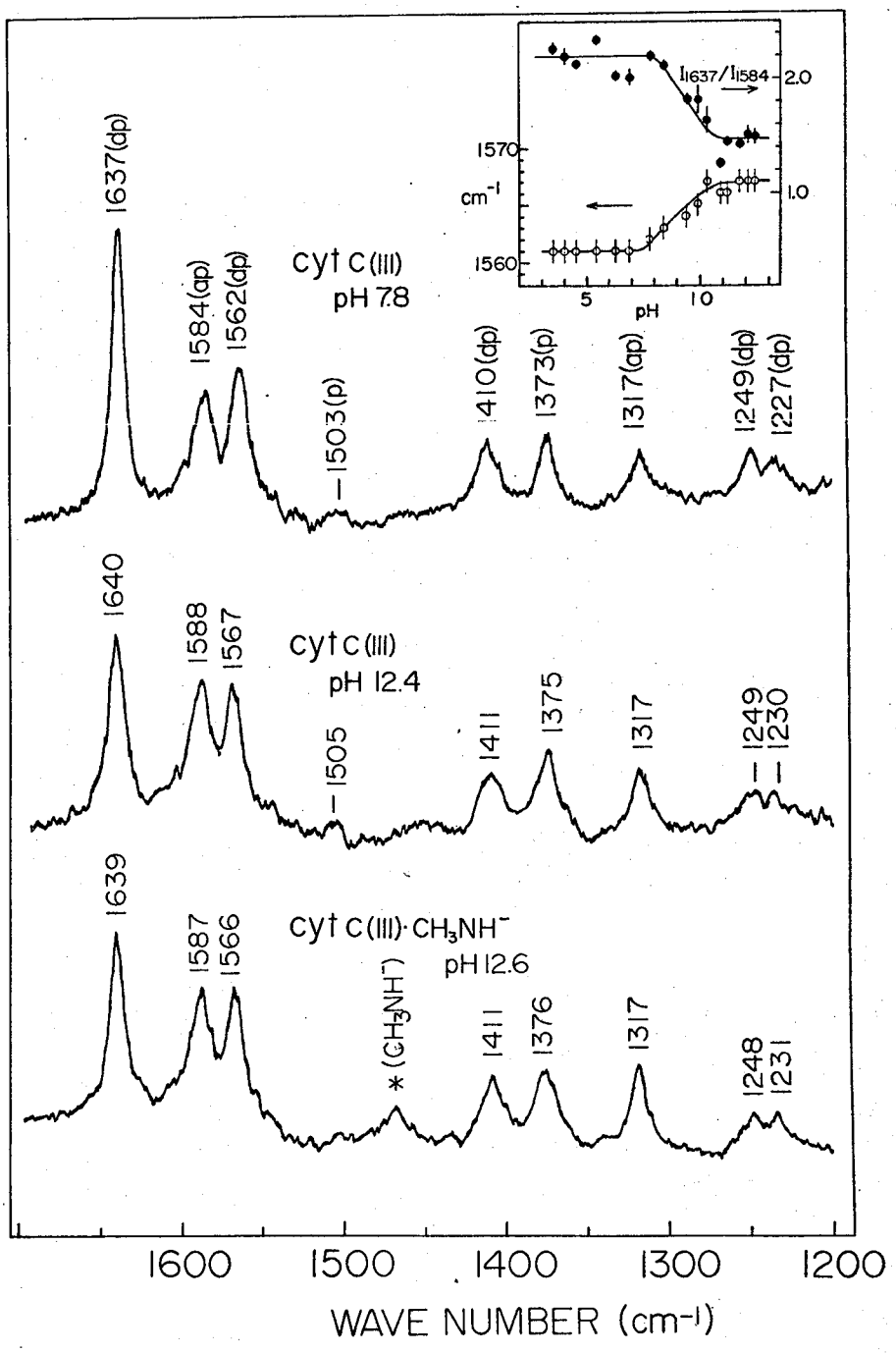

Fig. 1 The resonance Raman spectra of ferric cytochrome c at pH 7.8 and 12.4 and its methylamine complex at pH 12.6 excited at 514.5 nm. Numbers beside the peaks denote the frequency (cm^{-1}) and p, dp, and ap mean the polarized, depolarized, and anomalously-polarized lines, respectively. The insertion represents the pH dependence of the relative peak intensity I(1637 cm^{-1})/I(1584 cm^{-1})(•) and the frequency of the 1565 cm^{-1} line (o).

the Raman spectrum was measured under the condition.

Iron-protoporphyrin dimethylester [Fe^{3+}(PPDM)] was kindly given by Dr. H. Ogoshi (Kyoto University) and its bis-imidazole complex [Fe^{3+}(PPDM)Im_2] was obtained by refluxing it in benzene in the presence of excess Im. The crystal of Fe^{3+}(PPDM)$Im_2$was dissolved in CH_2Cl_2 to get Raman spectrum.

RESULTS

The resonance Raman spectra of cyt c(Fe^{3+}) at pH 7.8 and 12.4 were shown in Fig. 1, where polarization properties of the Raman lines (p, polarized; dp, depolarized; ap, anomalously-polarized) were also indicated beside the peak frequency (cm^{-1}). The prominent differences between the Raman spectra of the neutral and alkaline forms were demonstrated in the insertion of Fig. 1, where the frequencies of the depolarized lines around 1565 cm^{-1} and relative peak intensities of two Raman lines, 1636 cm^{-1}/1584 cm^{-1}, were plotted against pH. It was evident that the change of the Raman spectra (midpoint is at pH 9.4) corresponds to the transition with pK 9.3 detected previously with other methods (10-16). There was no additional change observed in the Raman spectra although with NMR spectroscopy small transitions caused by the ionization of tyrosine residue (15) and further replacement of the axial ligand to hydroxyl anion (16) were found above pH 11. The Raman spectra of methylamine-cytochrome c complex [cyt c(Fe^{3+})·CH_3NH], shown at the bottom of Fig. 1, was quite close to that of native alkaline form, while the complex formation was found in the NMR spectroscopy (16).

The general pattern of Raman spectra of other ferric cytochromes were similar to those in Fig. 1 as shown in Fig. 2a, 2b, and 2c. The frequencies of several Raman lines of cyt c, cyt c_2. cyt c-551, and cyt c-555 are plotted against pH in Fig. 3a, 3b, 3c, and 3d. Although two axial ligands of the heme iron at neutral pH are all histidine and methionine for cyt c_2(Fe^{3+}) (19), cyt c-551(Fe^{3+}) (20), and cyt c (Fe^{3+})(21), the frequency change of their Raman lines occurred in the defferent pH region.

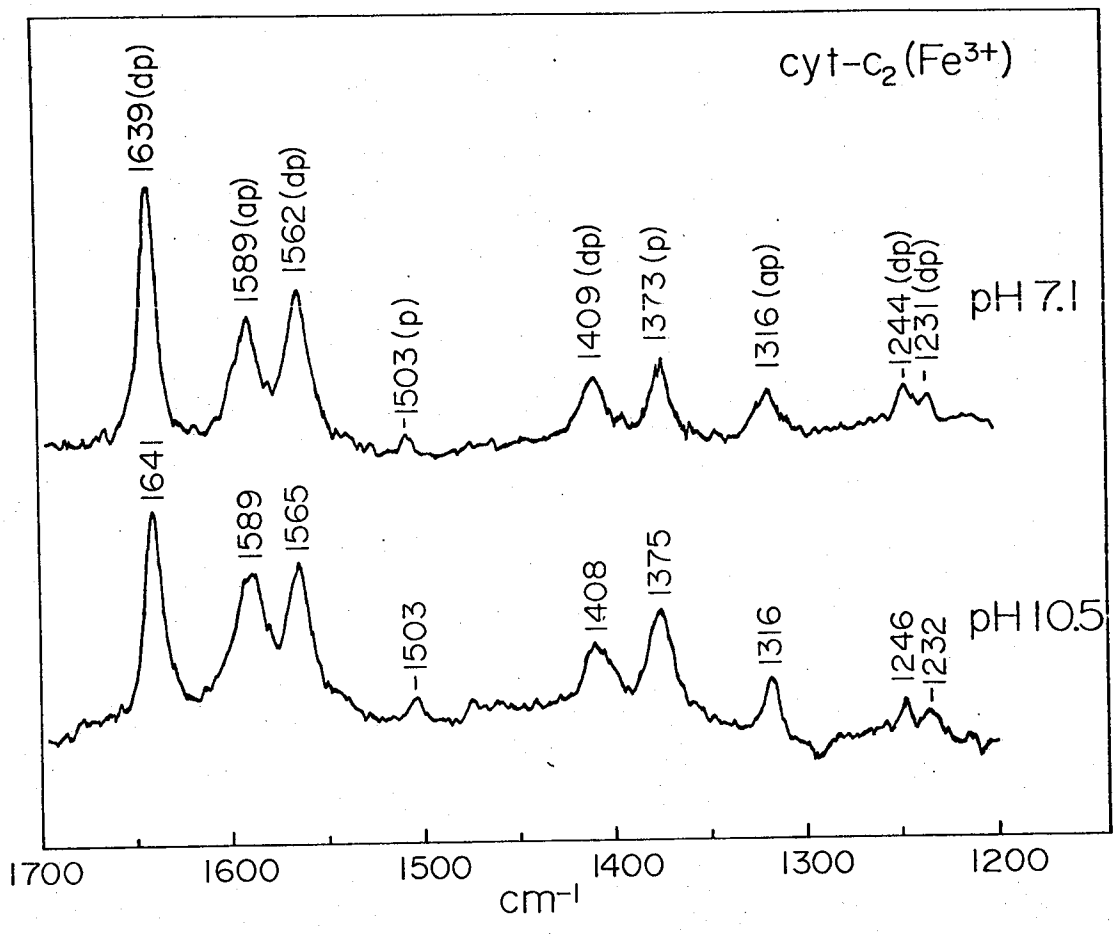

Fig. 2 The resonance Raman spectra of ferric cyt c_2 at pH 7.1 and 10.5.

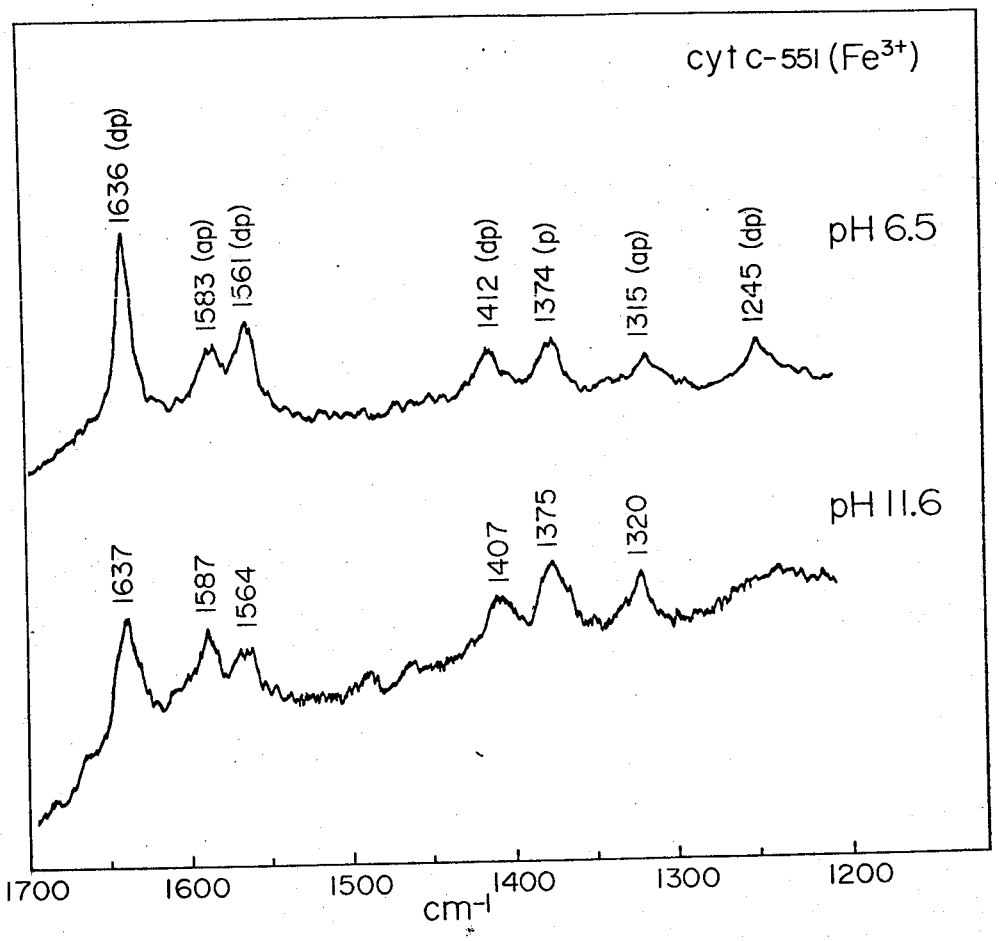

Fig. 2 (continued)

The resonance Raman spectra of ferric cyt c-551 at pH 6.5 and 11.6.

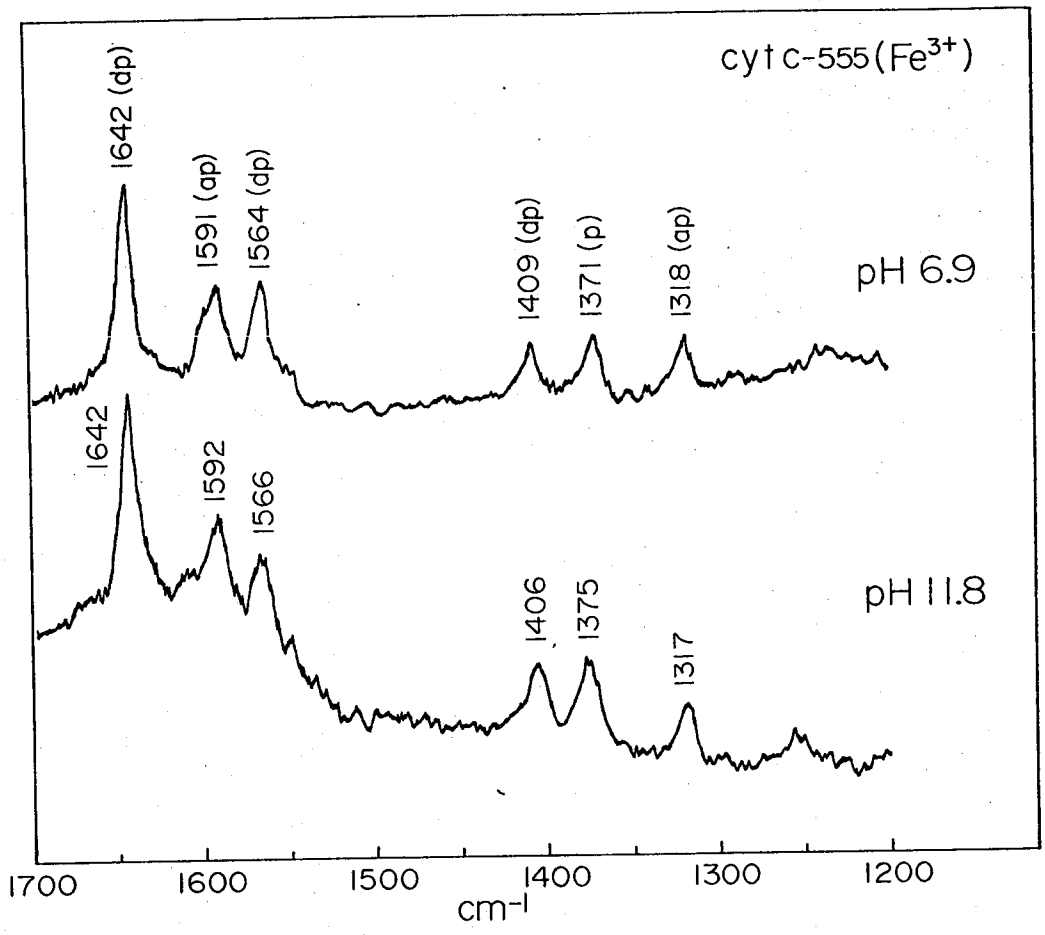

Fig. 2 (continued)

The resonance Raman spectra of ferric cyt c-555 at pH 6.9 and 11.8.

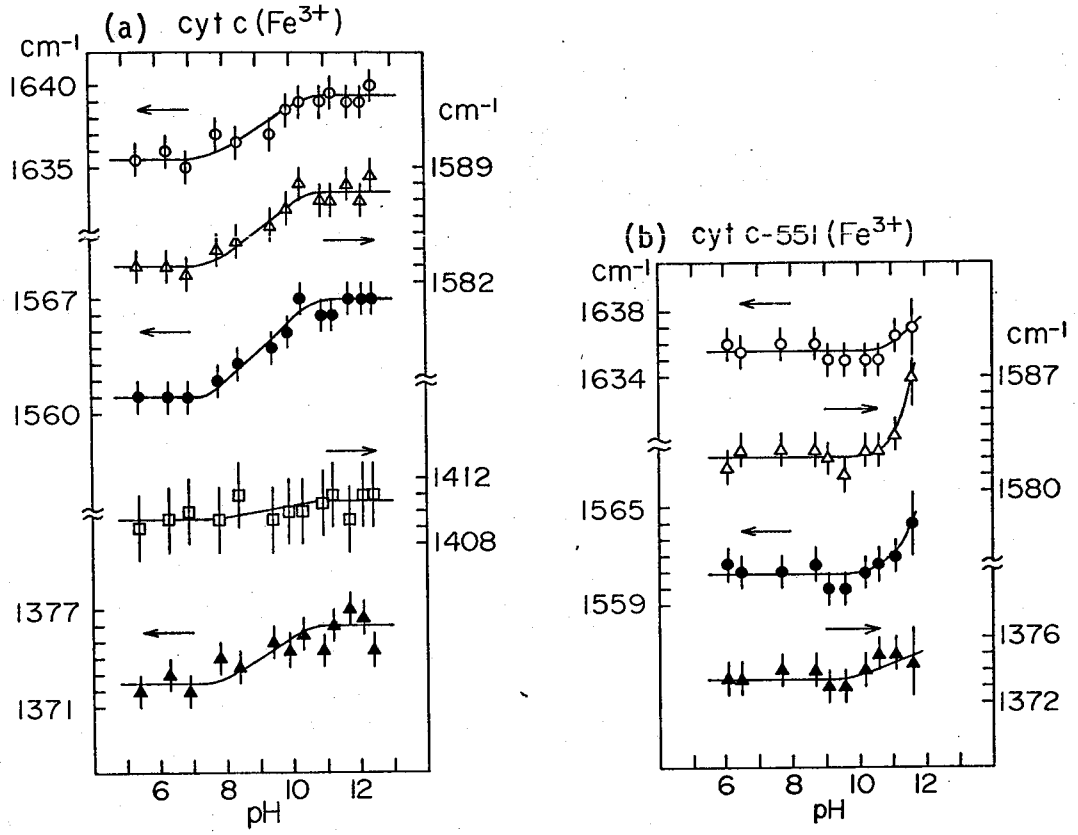

Fig. 3 The pH dependence of the frequencies of the resonance Raman lines of oxidized cyt c (a), cyt c-551 (b), cyt c_2 (c), and cyt c-555 (d).

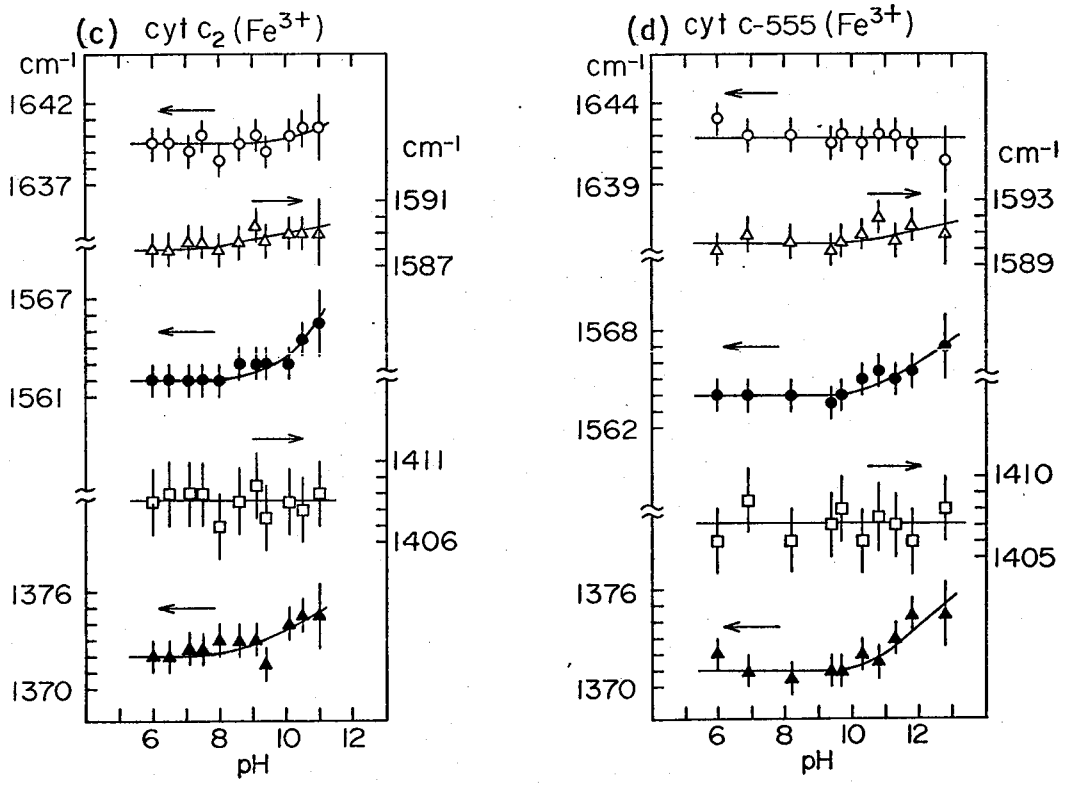

Fig. 3 (continued)

Fig. 4 illustrated the Raman spectra of bis-imidazole complex of iron-protoporphyrin [$Fe^{3+}(PP)Im_2$] under various conditions. The relative peak intensities of three Raman lines at 1639, 1587, and 1561 cm^{-1} of $Fe^{3+}(PP)Im_2$ at pH 12.1 resembled those of cyt c(Fe^{3+}) in Fig. 1. The Raman spectra of $Fe^{3+}(PP)Im_2$ at pH 7.8 and 13.5 (not shown) were alike and therefore the intensities and frequencies of the Raman lines of $Fe^{3+}(PP)Im_2$ were unaffected by pH.

When detergents were added to the $Fe^{3+}(PP)Im_2$ solution, the relative intensities of those Raman lines were altered with the concentration of the detergents. The Raman spectra at 0.002% and 2.5% CTAB were represented as the second and third curves of Fig. 4. The fourth curve, obtained in the presence of 2.0% SDS, was close to the third curve and therefore the spectral alteration was not dependent upon whether the detergent was cationic (CTAB) or anionic (SDS). In the presence of detergents, higher concentration of Im was necessary for completeness of the complex formation. The relative peak intensities of the three Raman lines of $Fe^{3+}(PPDM)Im_2$ in CH_2Cl_2 were closer to those of $Fe^{3+}(PP)Im_2$ in the presence of detergents rather than to those in their absence. For comparison, the Raman spectrum of rabbit liver cytochrome b_5 [cyt $b_5(Fe^{3+})$], in which the two axial ligands of the heme iron are histidyl imidazole (22), was reproduced at the bottom in Fig. 4 (9). It was noticeable that the relative intensities of the three Raman lines of cyt $b_5(Fe^{3+})$ were closer to those of $Fe^{3+}(PP)Im_2$ in the presence of detergents and to those of $Fe^{3+}(PPDM)Im_2$ in an organic solvent rather than to those of $Fe^{3+}(PP)Im_2$ in the absence of detergents.

It is noted that the frequencies of the Raman lines of ferrous cytochromes studied including cyt c(pH 3.0-pH 12.6), cyt c_2 (pH 5.3-pH 12.1), cyt c-551 (pH 4.0-pH 10.5), and cyt c-555 (pH 2.5-pH 12.5) did not vary with pH even for the 1539 cm^{-1} line.

Fig. 5 exhibited the Raman spectra of $Fe^{2+}(PP)L_2$ (L=cyanide, imidazole, and methylamine). These Raman spectra were not pH dependent in the alkaline region and their general pattern were similar to those of ferrous cytochromes. However, it should be emphasized that the depolarized line of $Fe^{2+}(PP)L_2$ corresponding to the ligand sensitive line of ferrous cytochromes appeared at 1530 cm^{-1} for L=methylamine,

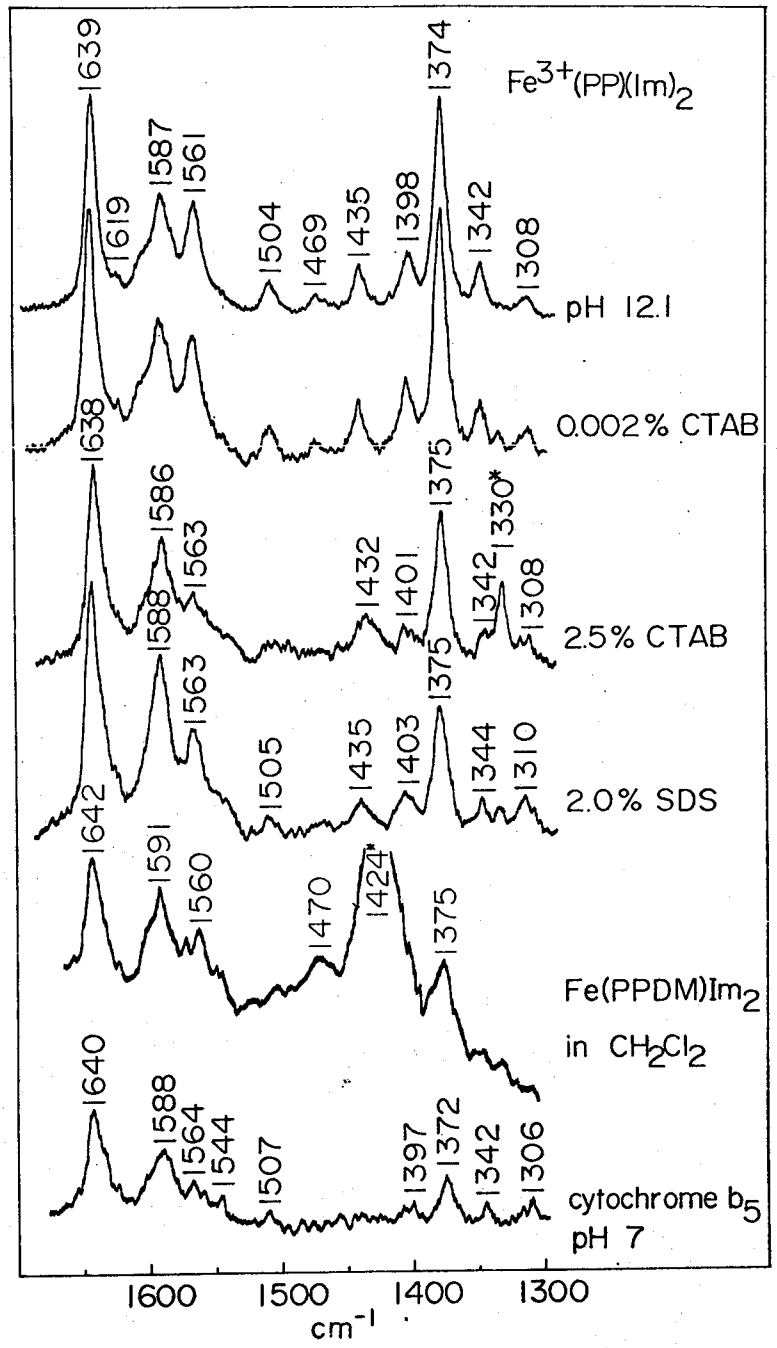

Fig. 4 The Raman spectra of ferric protoporphyrin bis-imidazole complex [$Fe^{3+}(PP)Im_2$] at pH 12.1 in the absence of detergent, in the presence of 0.002% CTAB, 2.5% CTAB, and 2.0% SDS, and those of ferric protoporphyrin dimethylester bis-imidazole complex in CH_2Cl_2 and cyt b_5 at pH 7. The Raman lines at 1330 and 1424 cm^{-1} (marked with asterisk) are due to free imidazole and CH_2Cl_2, respectively.

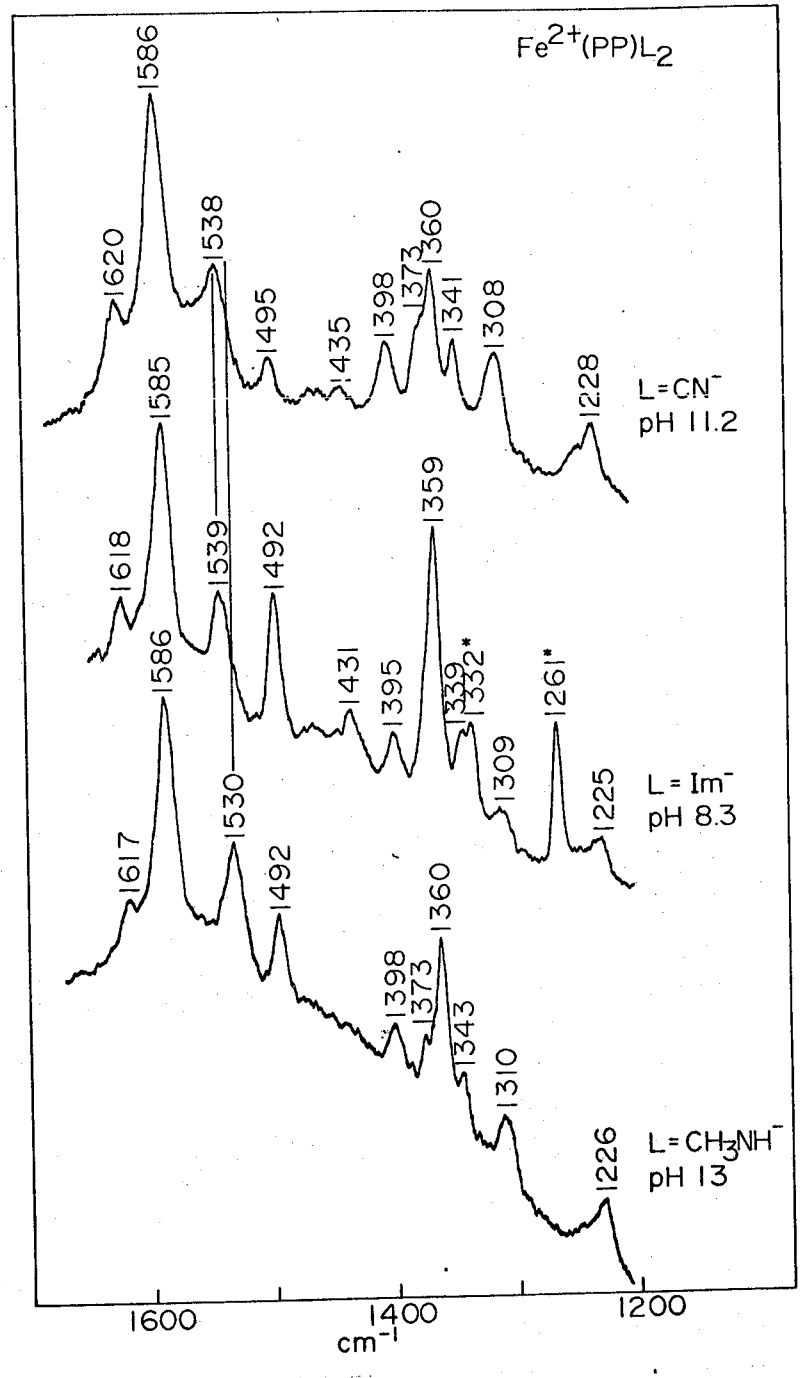

Fig. 5 The resonance Raman spectra of ferrous protoporphyrin bis-cyanide, bis-imidazole, and bis-methylamine complexes upon the excitation at 514.5 nm.

at 9 cm^{-1} lower frequency than those for L=cyanide and imidazole.

When CTAB was added to $Fe^{2+}(PP)Im_2$, the 1539 cm^{-1} line shifted slightly to lower frequency (1537, 1535, 1535, and 1535 cm^{-1} in 0.0025, 0.025, 0.25, and 2.5% CTAB, respectively). Upon the addition of SDS, the almost identical change with the case of CTAB was observed. The intensity of the 1539 cm^{-1} line of $Fe^{2+}(PP)Im_2$ relative to that of the 1585 cm^{-1} line decreased as the increase of the CTAB concentration, though less distinctly than the case of $Fe^{3+}(PP)Im_2$.

DISCUSSION

Raman frequencies and axial ligand of ferric cytochromes If an extremely narrow slit width could be used, the Raman spectra of cyt c (Fe^{3+}) around pH 9 should have shown, in principle, two Raman lines at 1561 and 1568 cm^{-1} and the intensity ratio of the two Raman lines should have been plotted against pH. Actually, however, the present resolution was not enough to dissolve the two lines and therefore the apparent frequency of the composite peak was plotted against pH in Figs. 1 and 3. The midpoint of the titration curve should denote the correct pK only when the two Raman lines possessed an equal intensity. Phenomenally the frequency change of the 1565 cm^{-1} line of cyt c(Fe^{3+}) parallels the titration curves obtained from the 695 nm band (10-14) or the NMR methyl signal of Met-80 (15,16), and thus is caused presumably by the replacement of the sixth ligand from Met-80 to other strong field ligand, though the residue is unknown.

The coordination of hydroxyl anion in the alkaline form (13,14) was less likely because cyt c(Fe^{3+}) at pH 12.7 did not show the Raman characteristics of alkaline myoglobin (23) in which the hydroxyl anion is known to be bound to the heme iron. The NMR paramagnetic shift of the peripheral methyl signals suggested the coordination of lysine in the alkaline form (15,16), although the disappearance of the 695 nm band occurred even to the modified cytochrome c in which no free lysine was identified (13,14). Since the Raman spectrum of cyt c(Fe^{3+})·CH_3NH was almost identical with that of native alkaline cyt c(Fe^{3+})(Fig. 1), the present results would be reasonably interpreted if an arbitrary

N-base such as lysine or histidyl imidazole were coordinated as the sixth ligand in the alkaline form of the native cyt c(Fe^{3+}).

The sensitivity of the oxidation state marker to the electronic property of the axial ligand (L) was previously discussed (7). When L is strong π donor, the delocalization of π electrons to the porphyrin $\pi^*(e_g)$ orbital becomes more significant and as a result, the frequencies of ferrous cytochrome $P\text{-}450_{cam}$ (3) and ferrous chloroperoxidase (4) decrease more than the usual case of ferrous high spin hemoproteins. In contrast, the frequency of HRP-comp(II) was higher than those of Fe^{3+} hemoproteins, because of $Fe^{4+}\text{-}L^-$ structure (5,6). Fig. 3 demonstrated that the pH induced frequency change of the 1565 cm^{-1} line was parallel with the change of the oxidation state marker ($\sim$1375 cm^{-1}). It may imply a common feature for the origin of the frequency change.

However there were other features which indicated the different sensitivity to the axial ligand between the 1565 cm^{-1} line and the oxidation state marker. When the sixth ligand of cyt c(Fe^{3+}) was replaced by exogeneous ligands such as N_3^- [cyt c(Fe^{3+})$\cdot N_3$] and Im [cyt c(Fe^{3+})$\cdot$Im], the corresponding Raman line appeared at 1563 and 1567 cm^{-1}, respectively, although both gave the oxidation state marker at the same frequency (1374 cm^{-1})(9). In the resonance Raman spectra of HRP-comp(II), the 1565 cm^{-1} line was missing although those corresponding to the 1640, 1587, and 1372 cm^{-1} lines of cyt c(Fe^{3+}) appeared clearly at 1644, 1590, and 1382 cm^{-1}(see Fig. 3 of ref. 5).

The oxidation state marker is associated mainly with the $C_\alpha N$ symmetric stretching vibration and the four pyrrole nitrogens are displaced toward the iron ion in-phase during the vibration (24). On the other hand, according to the normal coordinate analysis, the 1565 cm^{-1} line involves the out-of-phase stretching motion of the four $C_\beta C_\beta$ bonds, corresponding to the mode for the 1576 cm^{-1} (B_{1g}) of octaethylporphyrinato Ni(II) (25). In the case of bis-imidazole heme a(Fe^{3+}), the Raman line appeared at 1555 cm^{-1} but shifted to 1564 cm^{-1} upon the formation of cyanhydrin or bisulfite adduct (26). This change was not accompanied with the frequency shift of the oxidation state marker. The corresponding Raman line in the substituted ferrous cytochrome b_5 was identified at 1545, 1538, and 1548 cm^{-1} for deutero-,

proto-, and meso-hemes, respectively (27). These facts may imply that the 1565 cm^{-1} line is more sensitive to the peripheral groups of the porphyrin ring. Thus it might be likely that the oxidation state marker indicates more sensitively a change of the $C_\alpha N$ bonds and thus reflects the change transfer from the axial ligand to the π^*(porphyrin)(e_g) orbital through the heme iron in the ground electronic state (25) and that the 1565 cm^{-1} line indicates preferably a status change of the $C_\beta C_\beta$ bonds. If, in the C-type cytochromes, some effects caused by the conformation change of the peptide chain upon the replacement of the axial ligand, were transmitted to the heme through thioether bridges and/or the change of Fe-L interactions upon the replacement of L particularly perturbed the electronic state of the $C_\beta C_\beta$ bonds, the 1565 cm^{-1} line could be more sensitive to L than the oxidation state marker ($\sim$1375 cm^{-1}).

The frequencies , 1568 cm^{-1} for cyt c(Fe^{3+})(pH 12,7) and 1566 cm^{-1} for cyt c_3(Fe^{3+})(9) were close to 1567 cm^{-1} of cyt c(Fe^{3+})·Im (9) and 1566 cm^{-1} of cyt c(Fe^{3+})·CH_3NH, presumably due to the common property of L=N-base. On the other hand, 1562 cm^{-1} of cyt c(Fe^{3+})(pH 6.8), 1562 cm^{-1} of cyt c_2(Fe^{3+})(pH 7), and 1561 cm^{-1} of cyt c-551(Fe^{3+})(pH 6.3) were alike in accord with the facts of L=S (methionine) in cyt c (Fe^{3+})(21), cyt c_2(Fe^{3+})(19), and cyt c-551(Fe^{3+})(20).

The pH induced frequency-change of the 1565 cm^{-1} of cyt c_2(Fe^{3+}) (Fig. 3) started around pH 9 and the titration curve is not always parallel with that obtained from the 697 nm band of Rhodospirillum rubrum cyt c_2(Fe^{3+})(28). However, the titration curve for the 404 nm band of the cyt c_2(Fe^{3+}) showed two transitions with pK 9 and pK 11 (28) and the present Raman titration curve may possibly represent the latter transition.

Recently, for cyt c-551(Fe^{2+} and Fe^{3+}) in neutral pH region, the coordination of methionine-61 to the heme iron was confirmed through the observation of the NMR methyl signal of the coordinated methionine (29), although its pH dependence was not reported. So far as deduced from the Raman spectra, the replacement of the axial ligand occurred at about pH 11.5. The similar frequency change of the Raman line was also observed at above pH 12 for ferric cytochrome c-552 from Thermus

thermoplilus HB8 and it was parallel with the titration curve for the disappearance of the 690 nm band (30). In concluding, it became evident that the frequency of the 1565 cm^{-1} line of oxidized C-type cytochromes could practically be used as a possible indicator for the identity of the sixth ligand, and frequency change due to the replacement of the sixth ligand occurs in the characteristic pH region of the individual protein even though the sixth ligand is commonly methionine.

The Raman frequency and axial ligand of the ferrous cytochromes

The Raman line corresponding to the 1565 cm^{-1} line of ferric cytochromes was recognized at around 1540 cm^{-1} in the ferrous state (Fig. 4). The Raman line of alkyl c(Fe^{2+}) appeared at 1545 cm^{-1} at pH 3.9 and 1533 cm^{-1} at pH 9.7 (8). In the case of cyt c_3(Fe^{2+}), the 1541 cm^{-1} line disappeared at pH 9 and instead the 1536 cm^{-1} line appeared in the alkaline region (31).

This type of frequency change could not be identified upon the pH change or change of hydrophobicity at the heme moieties for the $Fe^{2+}(PP)Im_2$. However, it did occur upon the change of the axial ligand. When two axial ligands were imidazoles, the Raman line appeared at 1539 cm^{-1} but at 1530 cm^{-1} when they were methylamines (Fig. 5). If $Fe^{2+}(PP)Im_2$ and $Fe^{2+}(PP)(CH_3NH)_2$ were considered as the models for the hemes coordinated by two histidines and lysines (ε-N), respectively, the frequency drop of the Raman line of cyt c_3(Fe^{2+}) upon the increase of pH might imply the replacement of the axial ligand from histidine to lysine.

Since the coordination of histidine following to the thioether bridge would be unaltered, the replacement of the axial ligand would be limitted to the sixth ligand. Assuming that the apparent peak position of the Raman line of cyt c_3(Fe^{2+}) was the superposition of two Raman lines at 1541 and 1536 cm^{-1} with equal intensity, it could be interpreted that the two step transition shown in Ref. 31 by Teraoka et al. consisted of the stepwise replacement of the sixth ligands of the four hemes. The four heme irons would be coordinated by eight histidines at pH 6 as deduced from NMR spectroscopy (32,33). At the first transition two of the four hemes were altered. In other words, two kinds of hemes

coexisted between pH 7 and 8 where two of the four hemes were left unchanged as they were at pH 6 but the other two were same with those at pH 9. Finally above pH 9, all of four hemes possess the same set of two axial ligands which were different from those at pH 6.

Raman intensity and hydrophobicity around the heme moiety The intensity ratio of two Raman lines, 1587 cm^{-1}/1561 cm^{-1}, was pointed out as the indicator to the spin states of the heme iron (34), although the values were rather scattered among the low spin hemoproteins. On the other hand the dependence of the Raman intensity ratio upon the surroundings of heme was clearly demonstrated in Fig. 4. In the 2.5% CTAB (69 mM) and 2% SDS (63 mM) solutions, which were much higher than their CMC ($\sim$1 mM for CTAB and $\sim$7 mM for SDS)(38), the mole ratio of heme/detergents was 1/300 and thus the heme was thought to be placed in a fairly hydrophobic environment. Therefore it was reasonable that the Raman spectra of $Fe^{3+}(PP)Im_2$ in 2.5% CTAB or 2% SDS solution resembled that of the $Fe^{3+}(PPDM)Im_2$ in CH_2Cl_2 (ε_r=7.77 at 10°C; ε_r, relative dielectric constant)(35). Under this condition the intensity ratio 1587 cm^{-1}/1561 cm^{-1} became larger than 2 but in the absence of detergents the ratio was nearly unity. The direct factors which produced this difference would be the difference in absorbance of visible bands and vibronic coupling terms (36). However, empirically, it could be deduced from Fig. 4 that the heme of cyt $b_5(Fe^{3+})$ is placed in much more hydrophobic environment than that of cyt c at pH 6.8. This conclusion was consistent with the fact that the replacement of the sixth internal ligand with an exogeneous ligand such as N_3^- and Im was easy for cyt $c(Fe^{3+})$ even at neutral pH (37) but was impossible for neutral cyt $b_5(Fe^{3+})$, because such exogeneous ligands were supposed to be transported to the heme iron by water.

The replacement of the sixth ligand of cyt $c(Fe^{3+})$ with the exogeneous ligands did not change the relative intensity (9). The replacement of it with other amio acid residues of the peptide chain would be accompanied by the conformational change of the protein, resulting in the change of the environment of the heme. The change of the relative intensity of the Raman lines of cyt $c(Fe^{3+})$ with pH

represented in Fig. 1, indicated the slightly more hydrophobic environment of the heme in alkaline cyt c(Fe^{3+}) than in neutral one. In the case of cyt c_2(Fe^{3+}), cyt c-551(Fe^{3+}), and cyt c-555(Fe^{3+}), it was likely that the similar change of the environment of the heme occurred with pH change (Fig. 2).

REFERENCES

1. Spiro, T. G. (1975) Biochim. Biophys. Acta 416, 169.
2. Spiro, T. G. and Strekas, T. C. (1974) J. Am. Chem. Soc. 96, 338.
3. Ozaki, Y., Kitagawa, T., Kyogoku, Y., Shimada, H., Iizuka, T., and Ishimura, Y. (1976) J. Biochem. 80, 1447.
4. Champion, P. M., Remba, R. D., Chiang, R., Fitchen, D. B., and Hager, L. P. (1976) Biochim. Biophys. Acta 446, 486.
5. Felton, R. H., Romans, A. Y., Yu, N. T., and Schonbaum, G. R. (1976) Biochim. Biophys. Acta 434, 82.
6. Rakhit, G., Spiro, T. G., and Uyeda, M. (1976) Biochem. Biophys. Res. Commun., 71, 803.
7. Kitagawa, T., Kyogoku, Y., Iizuka, T., and Ikeda-Saito, M. (1976) J. Am. Chem. Soc. 98, 5169.
8. Ikeda-Saito, M., Kitagawa, T., Iizuka, T., and Kyogoku, Y. (1975) FEBS Lett. 50, 233.
9. Kitagawa, T., Kyogoku, Y., Iizuka, T., Ikeda-Saito, M., and Yamanaka, T. (1975) J. Biochem. 78, 719.
10. Greenwood, C. and Palmer, G. (1965) J. Biol. Chem. 240, 3660.
11. Davis, L. A., Schejter, A., and Hess, G. P. (1974) J. Biol. Chem. 249, 2624.
12. Lambeth, D. O., Campbell, K. L., Zand, R., and Palmer, G. (1973) J. Biol. Chem. 248, 8130.
13. Pettigrew, G. W., Aviram, I., and Schejter, A. (1976) Biochem. Biophys. Res. Commun. 68, 807.
14. Stellwagen, E., Babul, J., and Wilgus, H. (1975) Biochim. Biophys. Acta 405, 115.
15. Gupta, R. K. and Koenig, S. H. (1971) Biochem. Biophys. Res. Commun. 45, 1134.
16. Morishima, I., Ogawa, S., and Iizuka, T. to be published.
17. Yamanaka, T. and Okunuki, K. (1968) J. Biochem. 63, 341.
18. Hendra, P. J. and Loader, E. J. (1968) Chem. Ind. 718.
19. Salemme, F. R., Freer, S. T., Xuong, Ng. H., Alden, R. A., and Kraut, J. (1973) J. Biol. Chem. 248, 3910.
20. Dickerson, R. E., Timkovich, R., and Almassy, R. J. (1976) J. Mol.

Biol. 100, 473.
21. Takano, T., Kallai, O. B., Swanson, R., and Dickerson, R. E. (1973) J. Biol. Chem. 248, 5234.
22. Mathews, F. S., Levine, M., and Argos, P. (1972) J. Mol. Biol. 64, 449.
23. Ozaki, Y., Kitagawa, T., and Kyogoku, Y. (1976) FEBS Lett. 62, 369.
24. Kitagawa, T., Abe, M., Kyogoku, Y., Ogoshi, H., Sugimoto, H., and Yoshida, Z. (1977) Chem. Phys. Lett. 48, 55.
25. Abe, M., Kitagawa, T., and Kyogoku, Y. (1976) Chem. Lett. 249.
26. Kitagawa, T., Kyogoku, Y., and Orii, Y. (1977) Arch. Biochem. Biophys. 181, 228.
27. Ader, F. (1975) Arch. Biochem. Biophys. 170, 644.
28. Pettigrew, G. W. and Schejter, A. (1974) FEBS Lett. 43, 131.
29. Keller, R. M. and Wüthrich, K. (1976) FEBS Lett. 180.
30. Kihara, H., Honnami, H., Ooshima, T., and Kitagawa, T. to be published.
31. Kitagawa, T., Ozaki, Y., Teraoka, J., Kyogoku, Y., and Yamanaka, T. (1977) Biochim. Biophys. Acta 494, 100.
32. McDonald, C. C., Phillips, W. D., and LeGall, J. (1974) Biochemistry, 13, 1952.
33. Dobson, C. M., Hoyle, N. J., Geraldes, C. F., Bruschi, M., LeGall, J., Wright, P. E., and Williams, R. J. P. (1974) Nature 249, 425.
34. Yamamoto, T., Palmer, G., Gill, D., Salmeen, I. T., and Rimai, L. (1973) J. Biol. Chem. 248, 5211.
35. In "Handbook for Chemistry" (Japanese Chemical Society ed.) (1966) p. 708 for CMC and p. 1006 for ε_r, Maruzen, Tokyo.
36. Albrecht, A. C. (1961) J. Chem. Phys. 34, 1476.
37. Ikeda-Saito, M. and Iizuka, T. (1975) Biochim. Biophys. Acta 393, 335.

Chapter 5.

Resonance Raman Study of the pH-Dependent and Detergent-Induced Structual Alterations around the Heme Iron-Ligand Bonding of *R. rubrum* Cytochrome c'.

ABSTRACT

The resonance Raman spectra and the structures of the heme moiety of *Rhodospirillum rubrum* cytochrome c' were studied for its five states characterized by absorption spectra; Types *a* and *n* of the reduced form and Types I, II, and III of the oxidized form. The frequency of the ligand sensitive Raman line suggested the coordination of lysine (N_ε) at the sixth position of the heme iron of Type *n*. The sixth ligand of Type III was deduced to be either lysine or histidine but would not be methionine. Type *a* and Type II gave the Raman spectra of rather normal high spin type but Type I was unusual in the sense that the frequencies of the Raman lines associated primarily with methine -bridge CC-stretching vibrations were relatively high in comparison with those of other high spin hemoproteins. Type I was converted directly to Type III upon the addition of SDS or 2-propanol but the conversion occurred *via* Type II when pH was increased. Structual difference around the heme iron-ligand bonding between the high spin hemes of Type I and Type II was investigated and the reason why the frequencies of the methine-bridge CC-stretching modes were widely spread among the high spin hemes was discussed in detail.

INTRODUCTION

Cytochrome c' (1), found in some of purple photosynthetic bacteria and denitrifying bacteria, contains one or two C-type hemes but gives rise to the hemoglobin-like absorption spectrum at physiological pH and the cytochrome c-like one at extremely alkaline pH (2). The structural characterization of the spectral alterations of cytochrome c' has currently been a matter of physicochemical concerns. There are two and three, at least, spectroscopically distinguishable forms in the

reduced and oxidized states, respectively (3)(Fig. 1) (Hereafter, in accord with Ref. 3, they are called as Types a or n and Types I, II, or III for the reduced and oxidized forms, respectively).

The Mössbauer (4) and magnetic susceptibility data (5,6) revealed the existence of high spin ferrous heme in Type a, while Type n is in typical ferrous low spin state. Type I characterized by the Soret band at 390 nm corresponds to the species that Maltempo (7) previously interpreted as the quantum mechanical admixture of mid spin (S=3/2) and high spin states (S=5/2) because of the facts that its EPR (8), Mössbauer (4), and magnetic susceptibility data (5,6) were significantly different from those of acid metmyoglobin (S=5/2). Type II characterized by the split Soret bands at 402 and 370 nm, gives the highest value of the magnetic susceptibility among the five states(6) and Type III with the Soret band at 407 nm is in typical low spin state. The interconversions of the five states were examined by Imai et al (3) with the visible absorption spectra.

Previously Strekas and Spiro reported the resonance Raman spectra of Rhodopseudomonas palustris cytochrome c' (9). They found an anomaly that the oxidized form at pH 6.9 gave the Raman spectrum of low spin type despite magnetically in high spin state, interpreting it in terms of an distorted structure of heme with possible intermediate spin state, though there was no experimental foundation for the proposed distortion of the heme. The pH dependence of the resonance Raman spectra of various hemoproteins have previously investigated (10-12) and the Raman features of the status changes of the heme moiety such as the alteration of the hydrophobicity around the heme and the replacement of the axial ligand of the heme iron about several C-type cytochromes were elucidated (13). In this Chapter, the resonance Raman spectra of Rhodospirillum rubrumcytochrome c' and the structure changes around the heme iron-ligand bonding upon the pH change and additions of detergent or alcohols were interpreted on the basis of the previous results.

The R. rubrum cytochrome c' consists of two equivalent monoheme subunits (M_w=26,000)(2). The amino acid sequence of Cys-X-Y-Cys-His present near the C-terminal of the polypeptide chain (14) provides

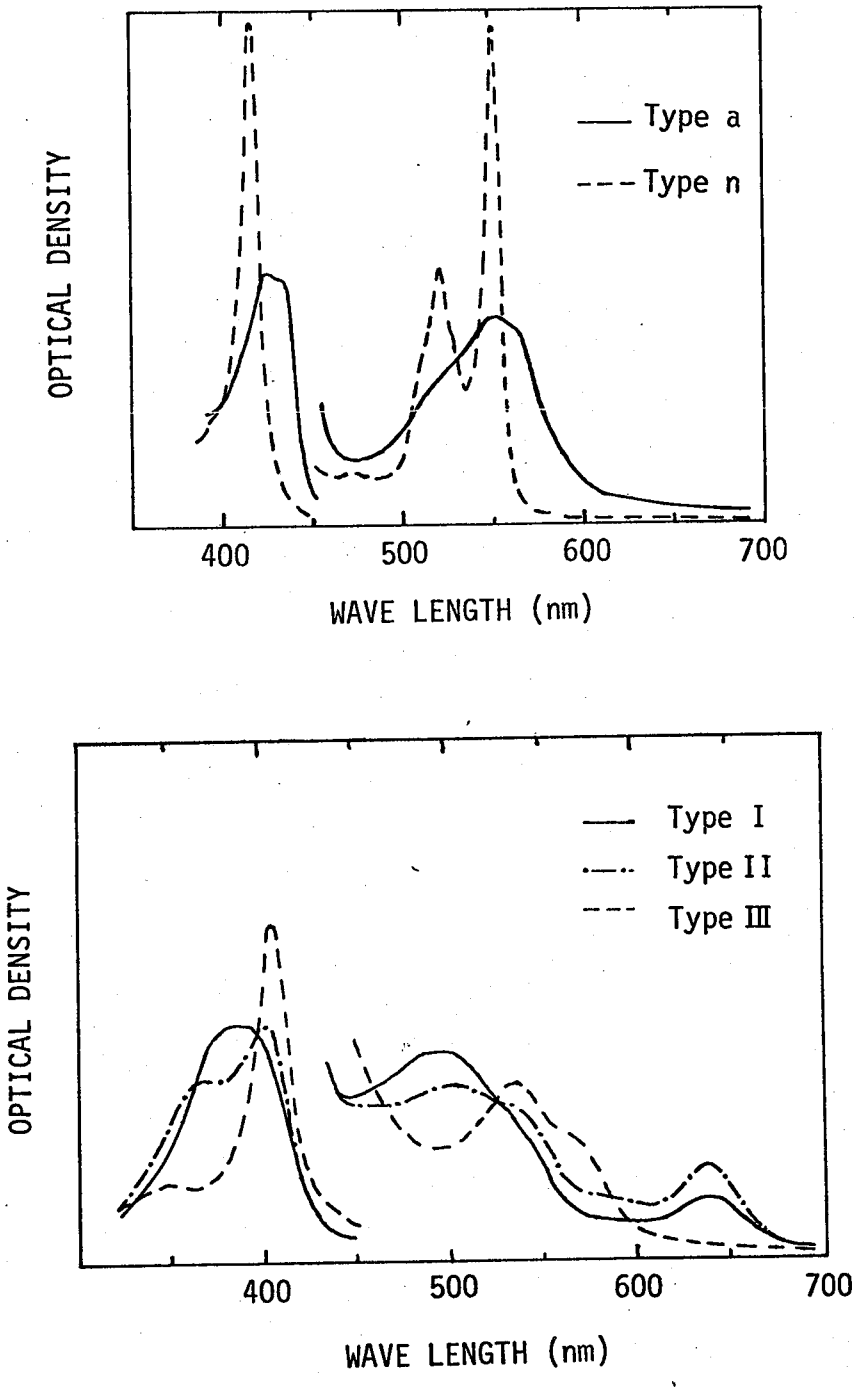

Fig. 1 The absorption spectra of the five types of R. rubrum cytochrome c'

presumably the thioether linkage between the heme and apoprotein and the coordination of histidine to the fifth position of the heme iron as in other C-type cytochromes (15). Simple anionic ligands such as N_3^- and CN^- are not bound even to the heme irons of Type I and II (16), although they are known to react with metmyoglobin (17) and oxidized cytochrome c (18).

EXPERIMENTAL

R. rubrum cytochrome c' purified with the method described previously (19), was dissolved in 0.01 M phosphate buffer at pH 7 and its concentration was determined spectroscopically on the basis of ε_{mM}=7.39 at 638 nm (2) with the use of a Hitachi-124 spectrophotometer. The pH of the solution was adjusted with concentrated HCl or NaOH and was determined after Raman experiments with Hitachi-Horiba M-5 pH meter. Cytochrome c (horse heart, Sigma, Type VI), hemin (bovine, Sigma, Type I), sodium dodecyl sulfate (SDS) (Nakarai chemicals), and 2-propanol (Katayama chemicals) were purchased and used without further purification.

Raman spectra were excited by the 514.5 nm line of an Ar^+ ion laser (Spectra physics, Model 164) and were recorded on a JEOL-400D Raman spectrometer equipped with a HTV-R649 photomultiplier. The frequency calibration was performed with indene (20). All the spectra were measured at 10°C with a longitudinal type cell (0.3 ml).

RESULTS

The polarized Raman spectra of Types a (pH 6.9) and n (pH 12.4) of the reduced form and Types I (pH 7.3), II(pH 10.8), and III (pH 13.3) of the oxidized form are shown in Fig. 2, where solid lines and broken lines denote the parallel ($I_{\parallel}$) and perpendicular ($I_{\perp}$) components, respectively. The intensity ratio of the two polarizations ($\rho_1=I_{\perp}/I_{\parallel}$) determines the polarization properties of Raman lines; polarized (p, $\rho_1<3/4$), depolarized (dp, $\rho_1=3/4$), and anomalously-polarized (ap, $\rho_1>3/4$),

The Raman spectra of Types a and n were generally close to those of deoxy myoglobin and ferrous cytochrome c observed under the same

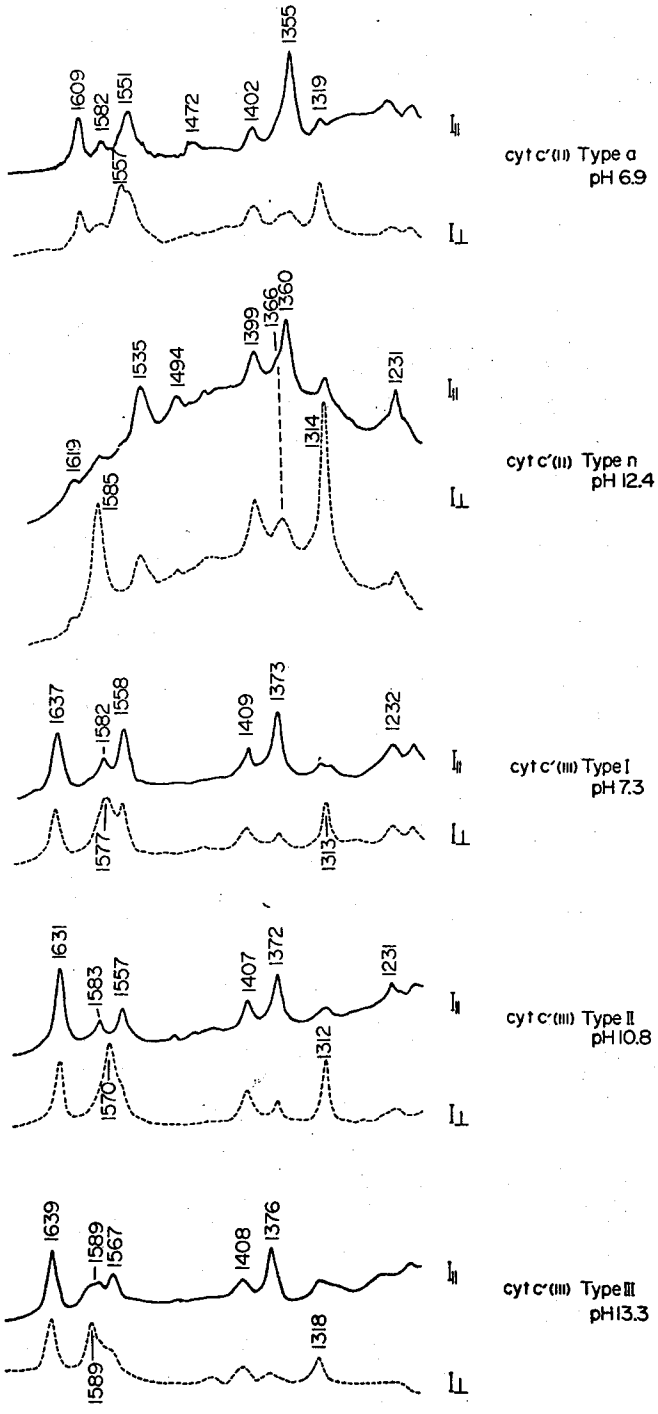

Fig. 2 The polarized Raman spectra of the five types of R. rubrum cytochrome c, upon the excitations at 514.5 nm. Solid lines and broken lines denote the electric vector of the scattered radiation to be parallel ($I_{\parallel}$) and perpendicular ($I_{\perp}$) to that of the excitation light, respectively.

experimental conditions, respectively. The same relationships of resemblance were found in their absorption spectra (2). However, one distinct difference between the Raman spectra of Type a and deoxy myoglobin is noted for the frequencies of the ap lines 1319 cm^{-1} of Type a and at 1302 cm^{-1} of deoxy myoglobin. It is caused by the difference in the peripheral substituents at 2 and 4 positions of porphyrin ring (11,21).

The Raman line (p) called as the oxidation state marker (22-25) appeared between 1355 and 1360 cm^{-1} in the reduced state of this cytochrome and it appeared between 1372 and 1376 cm^{-1} in the oxidized state. Since the oxidation state marker of ferrous high spin state is expected at around 1345 cm^{-1} when the fifth ligand is a strong π donor (26,27), the frequency 1355 cm^{-1} of Type a may implicate the histidine coordination at the fifth position. The 1360 cm^{-1} of Type n indicates that the sixth ligand binds to the heme iron mainly through the σ type interaction (25), because the Raman line should be located at frequencies higher than 1372 cm^{-1} when the π back donation to the axial ligand is significant.

The dp line, previously noticed as being ligand sensitive (10,13), was identified at 1535 cm^{-1} for Type n. This frequency is close to that of reduced carboxymethyl-methionyl cytochrome c at alkaline pH (1533 cm^{-1})(10), in which the sixth ligand is supposed to be lysine (28), but is definitely lower than that of reduced cytochrome c (1547 cm^{-1})(29), in which the sixth ligand is methionine (28). The corresponding Raman line of ferrous low spin derivatives of iron-protoporphyrin showed clear frequency drop by 9 cm^{-1} upon the replacement of the axial ligands from imidazole to methylamine (13). The former and latter may serve as model for the hemes coordinated by histidyl imidazoles and N_{ε} of lysines, respectively. The frequency of the ligand sensitive Raman line of Type n (1535 cm^{-1}) thus suggests the coordination of lysine as the sixth ligand of its heme iron. The Raman spectra of Type II and III were of typical high spin and low spin types, respectively, although the spectrum of Type I was unusual in the sense that the frequencies of the highest dp (1637 cm^{-1}) and highest ap (1577 cm^{-1}) lines were too high in comparison with those of other high spin hemoproteins. The

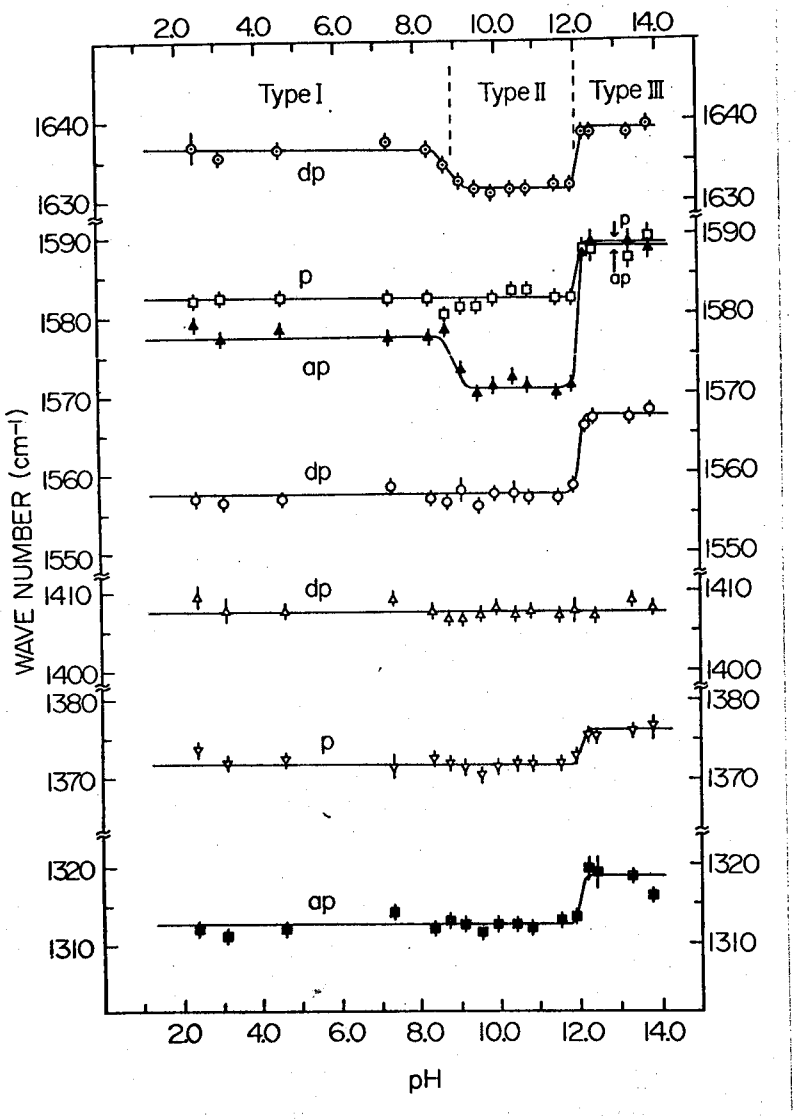

Fig. 3 The pH dependent frequency changes of the representative resonance Raman lines of R. rubrum cytochrome c'(oxidized form). P, dp, and ap indicate the polarized, depolarized, and anomalously -polarized lines, respectively.

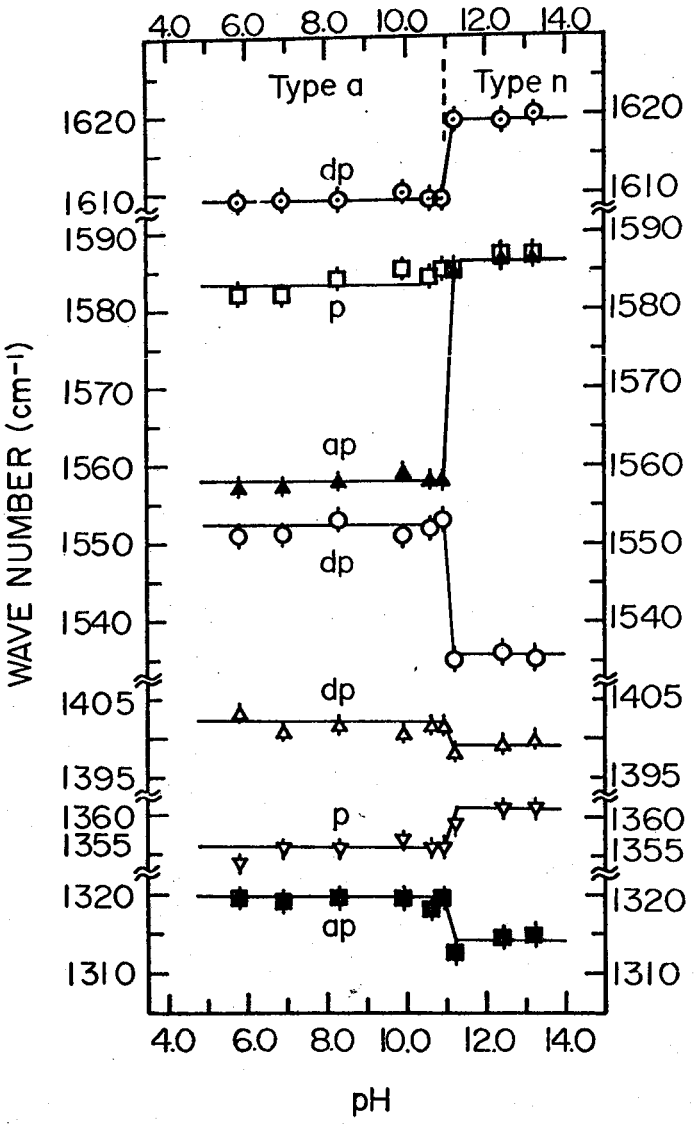

Fig. 3 (continued)
The pH dependent frequency changes of the representative resonance Raman lines of R. rubrum cytochrome c' (reduced form).

implications of these spectra of the oxidized form will be discussed in detail later.

The pH dependence of the frequencies of several Raman lines are shown in Fig. 3. These plots clarify the states of R. rubrum cytochrome c' as follows: Type a, 5<pH<11,1; Type n, 11,1<pH; Type I, 2<pH<8.4; Type II, 9.3<pH<12.1; Type III, 12.1<pH. The present specification is consistent with the previous one obtained from the absorption spectra (3). One may note that the transitions between Type a and Type n and between Type II and Type III are extremely sharp but the transition between Type I and Type II is gradual. Furthermore, as to the transition between Type I and Type II, the frequency changes were detected for only a few Raman lines in contrast with other two cases. It may imply a minor difference in geometrical structures of the hemes of Type I and Type II.

When SDS was added to Type I solution to yield 0.05% (W/W) SDS solution at fixed pH (pH 7.5), the Raman spectrum was almost identical with that of Type III. At an appropriate concentration, Type I and Type III were coexistent but their Raman lines were not observed separately because of poor resolution. Instead, as the change of populations of Type I and Type III, the apparent peak frequencies were shifted and they are plotted against the SDS concentration in Fig. 4(a). The transition from Type I to Type III occurred around the concentration of 0.02% which is much lower than its CMC [0.2% (W/W) at 20°C for SDS]. This type of Raman spectral change was not recognized for the addition of cetyltrimethyl-ammonium bromide (CTAB)(cationic detergent) or Triton X-100 (neutral detergent), while the Raman spectra of ferric iron-protoporphyrin-bis-imidazole complex was altered upon the additions of both SDS and CTAB (13).

Addition of an arbitrary alcohol to the solution of Type I at the fixed pH (pH 7.5) again changed its Raman spectrum to that of Type III. The frequencies of selected Raman lines of cytochrome c' are plotted against the concentration of 2-propanol in Fig 4(b). So far as deduced from Raman spectrum, Type I was completely converted to Type III when 30% (V/V in final concentration) of 2-propanol was added. At the transient state the molecule did not pass through Type II and it was

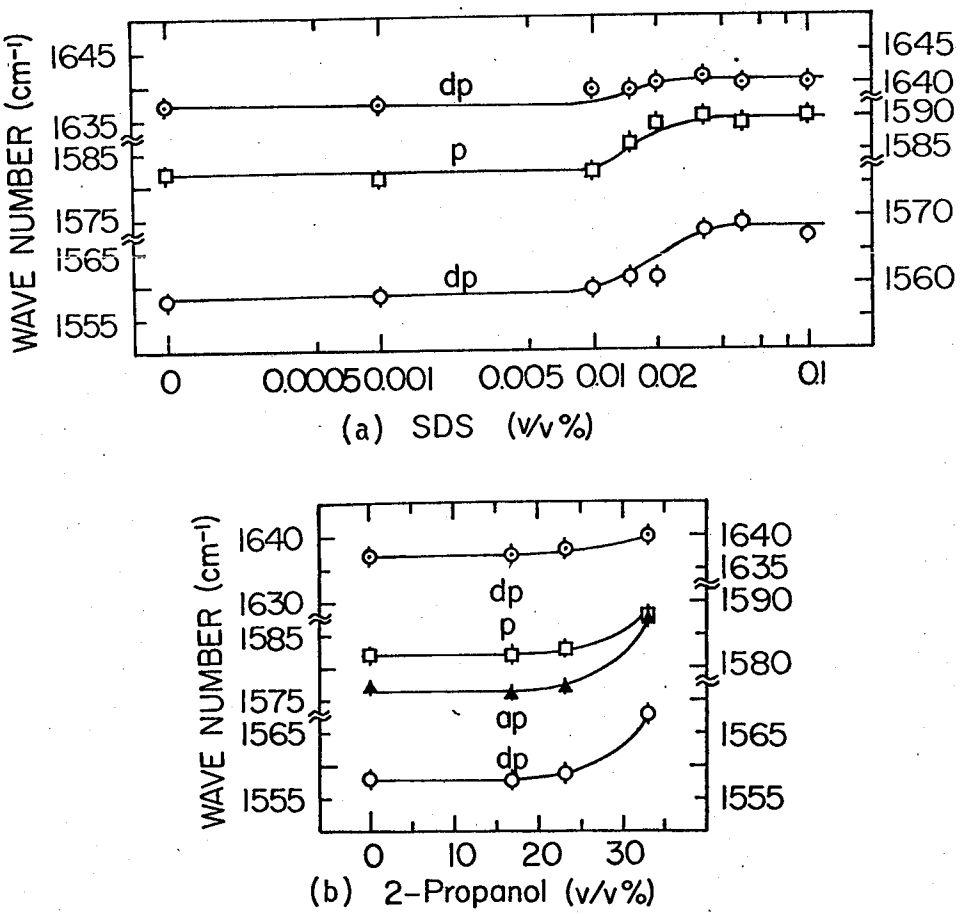

Fig. 4 Frequency changes of the resonance Raman lines of of the oxidized R. rubrum cytochrome c' upon addition of SDS (upper figure) and 2-propanol (lower figure) to the solution of Type I at fixed pH of 7.5.

also true in the case of the addition of SDS. Since the Raman spectral change was parallel with that of visible absorption spectra (3), other organic reagents which caused the identical changes of the visible absorption spectra with 2-propanol, are thought to induce the Raman spectral changes similar to those which 2-propanol induced.

The Raman spectrum of hemin in 2.0% SDS solution was typical high spin type and was not varied upon the addition of 35% 2-propanol. Therefore, even if 2-propanol were bound to the heme iron of cytochrome c', the resulting heme would not give rise to the Raman spectrum of low spin type. In other words, the transition from Type I to Type III upon the addition of SDS or 2-propanol can not be attributed to the direct interaction of the heme iron with SDS or 2-propanol. Probably SDS or 2-propanol might relax the structure of the apoprotein of Type I, allowing the coordination of an arbitrary strong-field ligand to the sixth coordination position of the heme iron in Type III.

In Fig. 2 the prominent differences between the Raman spectra of Type 1 and Type II were recognized in the frequency region of 1500-1650 cm^{-1}. Accordingly the polarized Raman spectra of the appropriate model systems in that frequency region are shown in Fig. 5. Oxidized cytochrome c at pH 1.0, which is known to be in the high spin state through the disappearance of NMR hyperfine-shifted lines (30), gave the Raman spectrum of high spin type but its Raman frequencies were not coincident with those of Type I or Type II. Hemin in 1.0% SDS solution showed the Raman spectrum similar to that of Type II. The frequencies of the Raman lines of Type I and Type II in this frequency region are compared with those of other high spin hemes in Table 1.

A mixture of hemin with KCN yielded thermal mixture of low spin and high spin states when their mole ratio (hemin/KCN) was about 1/100. As shown in third curve of Fig. 5, the Raman spectrum of the thermal mixture contains the Raman lines characteristic of high spin species (1631 and 1568 cm^{-1}) and low spin species (1637 and 1588 cm^{-1}). The Raman spectrum of Type I lacks this characteristics, that is, coexistence of two sets of Raman lines. Thus Type I can not be regarded as the thermal mixture of the high spin and low spin species, although the magnetic susceptibility of Type I is smaller than that of Type II.

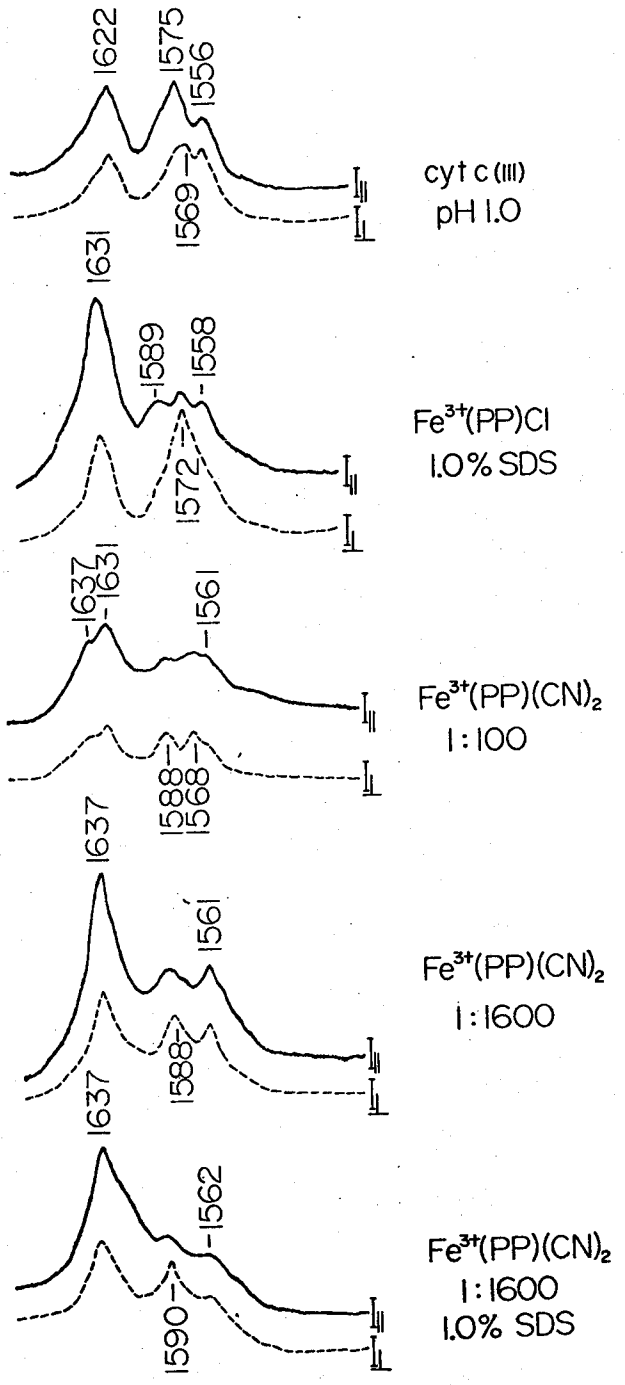

Fig. 5 The polarized Raman spectra in the frequency region between 1500-1650 cm^{-1} of several model systems. cyt c(III); horse heart cytochrome c(Fe^{3+}) at pH 1.0. Fe^{3+}(PP)Cl; bovine hemin in 1.0% SDS solution. $Fe^{3+}(PP)(CN)_2$; ferric iron-protoporphyrin bis-cyanide complex. When mole ratio of Fe^{3+}(PP)Cl/KCN is 1/100, the spectrum contains the Raman lines of both Fe^{3+}(PP)Cl and $Fe^{3+}(PP)(CN)_2$ but when it is 1/1600, the Raman spectrum is of purely low spin type. The bottom curve indicates the Raman spectrum of $Fe^{3+}(PP)(CN)_2$ in the presence of 1.0% SDS.

Table 1. Frequencies of the four Raman lines of high spin ferric hemes (cm^{-1})

	Type I	Type II	Fe(OEP)Cl	Fe(PP)Cl	cyt c	MbH_2O
dp	1637	1631	1629	1631	1622	1614
p	1582	1583	1582	1589	1575	1585
ap	1577	1570	1568	1572	1569	1560
dp	1558	1557	1545	1558	1556	1544

Fe(OEP)Cl; octaethylporphyrinato-Fe(III)(Ref. 32).
Fe(PP)Cl; hemin in 1% SDS.
cyt c; horse heart cytochrome c(Fe^{3+}) at pH 1.0.
MbH_2O, sperm whale myoglobin at pH 7 (Ref. 25).

This conclusion is consistent with that Strekas and Spiro reached previously (9).

The Raman spectrum of iron-protoporphyrin-bis-cyanide complex (fourth curve) was similar to that of Type III except for the frequency of the ligand sensitive line (1561 cm^{-1} for the model compound and 1567 cm^{-1} for Type III). The intensity of the 1561 cm^{-1} line diminished upon the addition of 1% SDS (mole ratio of porphyrin/SDS is 1/18) and the identical intensity change was observed for iron-protoporphyrin-bis -imidazole complex. This intensity change was previously attributed to the change of hydrophobicity around the heme (13). On the basis of these facts, the relative intensity of the 1567 cm^{-1} line of Type III (Fig. 1) may suggest that the hydrophobicity of the heme of Type III is similar to that of iron-porphyrin complexes in the absence of detergents. The measurements of the Raman spectrum of cytochrome c' at lower temperature were impossible of the increased fluoresence as decreasing of temperature.

DISCUSSION

Polarization properties of Raman lines specify the symmetry of the vibrational modes. When the effective symmetry of the heme group are approximated to D_{4h} group, the polarized and anomalously-polarized

resonance Raman lines correspond to the A_{1g}, B_{1g} or B_{2g}, and A_{2g} species, respectively. The vibrational modes of those species in the frequency region of 1000-1650 cm^{-1} of symmetric metalloporphyrin were described elsewhere (31-33).

The frequency of the second highest B_{1g} mode, which is associated primarily with $C_\beta C_\beta$-stretching vibrations (31), was previously noticed to be sensitive to the identity of the sixth ligand of the low spin heme iron in C-type cytochromes (13). The corresponding frequency of Type III (1567 cm^{-1}) is close to those of cytochrome c at pH 12.4 (1567 cm^{-1}) and methylamine-cytochrome c complex (1566 cm^{-1})(13), imidazole-cytochrome c complex (1566 cm^{-1})(11), and cytochrome c_3 (1566 cm^{-1}), but is notably higher than those of neutral cytochrome c (1562 cm^{-1}) and other C-type cytochromes with methionine as the sixth ligand (13). The sixth ligand of cytochrome c_3 at pD 8.0 was deduced to be histidine with NMR spectroscopy (34). Accordingly the sixth ligand of the heme iron in Type III would presumably be a strong-field N-base such as N_ε of lysine or histidyl imidazole but would not be methionine.

One of the arguments in discussing the structural characteristics of Type I and Type II may be present in difference of temperatures at which the magnetic and Raman experiments were performed. However, Maltempo (35) reported that the visible absorption spectra of Chromatium cytochrome c' was essentially temperature independent between 293 and 77 K. Champion et al. (36) pointed out that temperature dependence of Raman frequencies was insignificant to cytochrome c in the temperature region between 280 and 68 K where the visible absorption spectrum of cytochrome c was substantially unaltered except for slight sharpening of the vibronic bands at lower temperatures. These facts may allow to use the magnetic data at low temperature for discussion of the Raman data at room temperature.

Tasaki et al. (6) observed the magnetic susceptibility of R. rubrum cytochrome c', reporting n_{eff}=5.2 (Type I) and n_{eff}=6.4 (Type II) at 150 K (n_{eff}: effective number of Bohr magneton). In comparison of these values with n_{eff}=5.92, 3.87, and 1.73 expected theoretically for S=5/2, S=3/2, and S=1/2, respectively, Type II is considered to be essentially

in high spin state. The Raman frequencies of Type II represented in Table 1, are close to those of high spin model compounds such as octaethylporphyrinato iron (III) in CH_2Cl_2 solution (32) and hemin in 1.0% SDS aqueous solution but are clearly different from those of myoglobin in ferric high spin state (25). Accordingly the heme of Type II seems to have less strain by the apoprotein than those of Type I and myoglobin.

The pH alteration upon freezing of buffer solution (37) may result in the contamination of other molecular species of different pH but, in the case of cytochrome c', the low n_{eff} value of Type I can not be ascribed to the contamination of Type II with larger n_{eff} value, As described previously the Raman spectrum of Type I implicated the existence of only one kind of molecular species. The magnetic susceptibility of Type I (n_{eff}=5.2 at 150 K) is not so far from those of high spin hemoproteins (n_{eff}=5.89 in acid-metmyoglobin at 77 K (38) and n_{eff}=4.5 in methemoglobin at pH 6 at 150 K (6)). Thus the heme of Type I is deduced to be in a peculiar high spin state possibly caused by the strain from polypeptide chain.

When the Raman spectrum of Type I is compared with those of other high spin hemoproteins, the frequencies of the highest B_{1g} (1637 cm^{-1}) and highest A_{2g} modes (1577 cm^{-1}) are puzzling, because the corresponding frequencies have never exceeded 1631 and 1572 cm^{-1}, respectively, in other high spin ferric hemoproteins and iron-porphyrins. Strekas and Spiro (9), therefore, suggested the intermediate spin state with moderately domed structure of heme for R. palustris cytochrome c' at neutral pH. However, it is only square planar ferrous porphyrin with no axial ligand that has been proved experimentally to be in the intermediate spin state (39,40). It would be unlikely to assume that the histidine of the fifth ligand dissociates at pH 8.5 only in the oxidized state. On the other hand, the reduced hemin in 2.5% CTAB or 2.0% SDS solutions gave the Raman spectra of ferric low spin type (13) and accordingly it belongs to the category which Spiro and Burke assigned to the ferrous heme with the intermediate spin state (41). Then the hemin in 2.0% SDS is also expected to be in the intermediate spin state of the ferric iron. Nevertheless, its Raman spectrum was not close to

that of Type I. Therefore it seems unlikely to assign the heme of Type I to the intermediate spin state.

Since the highest B_{1g} and highest A_{2g} modes are associated mainly with the methine-bridge CC-stretching vibrations (31,32), these frequencies are considered to be affected sensitively by the stretching force constants of the CC bonds. Regarding the electronic state of the porphyrin ring, the highest occupied π orbital in the a_{2u} species [$\pi(a_{2u})$] is bonding about the methine-bridge CC bonds (42). The increase of electron occupation in this orbital would raise the bond order of the methine-bridge CC bonds and thus would result in the larger force constants of the CC bonds. Accordingly the vibrational frequencies of the CC-stretching mode could be higher as the increase of electron occupation in the $\pi(a_{2u})$ orbital. On the basis of the results of the normal coordinate calculations of metalloporphyrin (31), it is expected that the increase of the methine-bridge CC-stretching force constants by 0.1 mdyne/A without the changes of other force constants would bring about the increase of the frequencies of the B_{1g} and A_{2g} modes by ca. 8 cm^{-1} and an A_{1g} mode ($\sim$1500 cm^{-1}, not recognized in Fig. 1) by ca. 4 cm^{-1} but other frequencies would be almost unaltered. This manipulation would reproduce the Raman spectral difference between Type I and Type II; the frequencies of the B_{1g} and A_{2g} modes of Type I are higher by 6 and 7 cm^{-1} than those of Type II, respectively (see Fig. 1) and the frequencies of other Raman lines are alike between Type I and Type II.

Since the $\pi(a_{2u})$ orbital belongs to the same symmetry species with the empty $4p_z$ orbital of the heme iron which would presumably interact with lone pair of the fifth ligand, the $\pi(a_{2u})$, $4p_z$(Fe), and lone pair orbitals would constitute molecular orbitals of the a_{2u} species (Fig. 6). This consideration is also applied to the case of domed structu (C_{4v} symmetry) where the subscript g and u should be deleted. Therefore, the electron occupation in the $\pi(a_{2u})$ orbital would depend upon the charge transfer among the heme iron, the fifth ligand, and the porphyrin ring. Even a slight change in the distance between the heme iron and the fifth ligand would affect appreciably the amount of the charge transfer and thus alter the methine-bridge CC-stretching frequencies.

The heme irons are generally located out of the porphyrin plane in the high spin state and the exact distance between the heme iron and the fifth ligand might be inherent in individual hemoproteins. Accordingly the present model would explain, without assuming any special distortion of heme, the reason why the frequencies of the methine-bridge CC-stretching modes are widely spread among the high spin hemes including those of Type I and Type II (see Table 1). Simultaneously the change of electron distribution among the heme iron, porphyrin ring, and the fifth ligand may possibly change the effective value of the magnetic susceptibility.

Since the helix content of the polypeptide chain has no correlation with the conversion among the three types of the oxidized cytochrome c' (43), the change of secondary structure of the polypeptide chain would not be essential to the conversions. Thus it is attempted to speculate that Type III takes normal low spin state with lysine as a likely sixth ligand of the heme iron and that Type I and Type II possess a similar domed structure of heme with histidine as the fifth ligand but the interaction between the heme iron and the fifth ligand is slightly different between the two states presumably due to the strain caused by the apoprotein.

REFERENCES

1. Kennel, S. J., Meyers, T. E., Kamen, M. D., and Bartsch, R. G. (1972) Proc. Nat. Acad. Sci. U. S. 69, 3432.
2. Horio, T. and Kamen, M. D. (1961) Biochim. Biophys. Acta 48, 266.
3. Imai, Y., Imai, K., Sato, R., and Horio, T. (1969) J. Biochem. 65, 225.
4. Moss, T. H., Bearden, A. J., Bartsch, R. G., and Cusanovich, M. A. (1968) Biochemistry 7, 1583.
5. Ehrenberg, A. and Kamen, M. D. (1965) Biochim. Biophys. Acta 102, 333.
6. Tasaki, A., Otsuka, J., and Kotani, M. (1967) Biochim. Biophys. Acta 140, 284.
7. Maltempo, M. M. (1974) J. Chem. Phys. 61, 2540.
8. Maltempo, M. M., Moss, T. H., and Cusanovich, M. A. (1974) Biochim. Biophys. Acta 342, 290.
9. Strekas, T. C. and Spiro, T. G. (1974) Biochim. Biophys. Acta 351, 237.
10. Ikeda-Saito, M., Kitagawa, T., Iizuka, T., and Kyogoku, Y. (1975) FEBS Lett. 50, 233.
11. Kitagawa, T., Kyogoku, Y., Iizuka, T., Ikeda-Saito, M., and Yamanaka, T. (1975) J. Biochem. 78, 719.
12. Ozaki, Y., Kitagawa, T., and Kyogoku, Y. (1976) FEBS Lett. 62, 369.
13. Kitagawa, T., Ozaki, Y., Teraoka, J., Kyogoku, Y., and Yamanaka, T. (1977) Biochim. Biophys. Acta 494, 100.
14. Ambler, R. P. (1975) "Handbook of Biochemistry and Molecular Biology" (3rd ed.)(Fasman, G. D. ed.).
15. Dickerson, R. E., Timkovich, R., and Almassy, R. J. (1976) J. Mol. Biol. 100, 473.
16. Taniguchi, S. and Kamen, M. D. (1963) Biochim. Biophys. Acta 74, 438.
17. Antonini, E. and Brunori, M. (1971) "Hemoglobin and Myoglobin in their Reactions with Ligands" North Holland, Amsterdam.
18. Ikeda-Saito, M. and Iizuka, T. (1975) Biochim. Biophys. Acta 393, 335.

19. Bartsch, R. G., Kakuno, T., Horio, T., and Kamen, M. D. (1971) J. Biol. Chem. 246, 4489.
20. Hendra, P. J. and Loader, E. J. (1968) Chem. Ind. 718.
21. Ader, F. and Frecinska, M. (1974) Arch. Biochem. Biophys. 165, 570.
22. Yamamoto, T., Palmer, G., Gill, D., Salmeen, I. T., and Rimai, L. (1973) J. Biol. Chem. 248, 5211.
23. Spiro, T. G. and Strekas, T. C. (1974) J. Am. Chem. Soc. 96, 338.
24. Kitagawa, T., Iizuka, T., Saito, M., and Kyogoku, Y. (1975). Chem. Lett. 849.
25. Kitagawa, T., Kyogoku, Y., Iizuka, T., and Ikeda-Saito, M. (1976) J. Am. Chem. Soc. 98, 5169.
26. Ozaki, Y., Kitagawa, T., Kyogoku, Y., Shimada, H., Iizuka, T., and Ishimura, Y. (1976) J. Biochem. 80, 1447.
27. Champion, P. M., Remba, R, D., Chiang, R., Fitchen, D. B., and Hager, L. P. (1976) Biochim. Biophys. Acta 446, 486.
28. Dickerson, R. E., Takano, T., Kallai, O. B., and Samson, L. "Structure and Function od Oxidation-Reduction Enzyme" (Akesson, A. and Ehrenberg, A. eds.) p 69, Pergamon Press, Oxford.
29. Strekas, T. C. and Spiro, T. G. (1972) Biochim. Biophys. Acta 278, 188.
30. Gupta, K. K. and Koenig, S. H. (1971) Biochem. Biophys. Res. Commun. 45, 1134.
31. Abe, M., Kitagawa, T., and Kyogoku, Y. (1976) Chem. Lett. 249.
32. Kitagawa, T., Ogoshi, H., Watanabe, E., and Yoshida, Z. (1975) Chem. Phys. Lett. 30, 451; (1975) J. Phys. Chem. 79, 2629.
33. Kitagawa, T., Abe, M., Kyogoku, Y., Ogoshi, H., Sugimoto, H., and Yoshida, Z. (1977) Chem. Phys. Lett. 48, 55.
34. McDonald, C. C., Phillips, W. D., and LeGall, J., (1974) Biochemistry 13, 1952.
35. Maltempo, M. M. (1976) Biochim. Biophys. Acta 434, 513.
36. Champion, P. M., Collins, D. W., and Fitchen, D. B. (1976) J. Am. Chem. Soc. 98, 7114.
37. Orii, Y. and Morita, M. (1977) J. Biochem. 81, 163.
38. Iizuka, T. and Kotani, M (1969) Biochim. Biophys. Acta 194, 351.

39. Collman, J. P., Hoard, J. L., Kim, N., Lang, G., and Reed, C. A. (1975) J. Am. Chem. Soc. 97, 2676.
40. Dolphin, D., Sama, J. R., Tsin, T. B., Wong, K. T. (1976) J. Am. Chem. Soc. 98, 6971.
41. Spiro, T. G. and Burke, J. M. (1976) J. Am. Chem. Soc. 98, 5482.
42. Kashiwagi, H., Obara, S., Takada, T., Miyoshi, E., and Ohno, K. to be published.
43. Imai, Y., Imai, K., Ikeda, K., Hamaguchi, K., and Horio, T. (1969) J. Biochem. 65, 629.

Chapter 6.

Resonance Raman Spectra of Metallo-trans-octaethylchlorins

ABSTRACT

As a series of studies for vibrational spectra of metallo-porphyrins, resonance Raman spectra have been measured for metallo-trans-octaethylchlorins [M(OEC), M=Cu^{2+}, Ni^{2+}, Fe^{3+}], ^{15}N substituted Cu(OEC), and γ,δ-dideuterated Cu(OEC). The vibrational frequencies of M(OEC) were close to those of the corresponding derivatives of metallo-octaethylporphyrin [M(OEP)]. The methine-bridge stretching vibrations and the ring vibrations of pyrrole were assigned on the basis of frequency shift upon the isotope substitutions. Dependence of Raman intensities upon the excitation wavelength were clearly different between M(OEC) and M(OEP) in accord with the difference in their absorption spectra. The intensity enhancement of Raman lines around 1100-1300 cm^{-1} was particularly notable for M(OEC) upon excitation at 568.2 nm but was not so for M(OEP). The Raman lines due to iron-ligand (L) stretching vibrations of Fe(OEC)L were identified at 608 cm^{-1} for L=F and at 361 cm^{-1} for L=Cl while L-Fe-L symmetric stretching mode of $Fe(OEC)L_2$ was found at 303 cm^{-1} when L=imidazole.

INTRODUCTION

Resonance Raman studies of metallo-porphyrin complexes have revealed the vibrational spectra of the porphyrin skeleton with various peripheral substituents, the metal dependence of their vibrational frequencies and the excitation profile of Raman scattering intensity (1-20). The assignment of the resonance Raman lines of metallo-porphyrins has been established on the basis of the observed frequency shifts upon the meso-deuteration, ^{15}N substitution of the four pyrrole nitrogens and the normal coordinate calculations (21-25). These studies on model compounds have provided a basic knowledge for the analysis of the resonance Raman spectra of various hemoproteins.

Recently the resonance Raman spectra of chlorophylls were also

reported by Lutz et al. (26-29). Although empirical assignments of several Raman bands of chlorophylls were previously given, model compounds study is still required to confirm them. Since the chromophore of chlorophyll consists of magnesium chlorin, in which one of four $C_\beta C_\beta$ bonds of the porphyrin skeleton is saturated, the analysis of the resonance Raman spectra of metallo-trans-octaethylchlorin [M(OEC)] may give rise to useful information for analyzing the resonance Raman spectra of chlorophyll. Furthermore Fe(OEC) derivatives may serve as model compounds of heme d which is a prothetic group of cytochrome CD (30).

It is also interesting to see how the vibrational frequencies and resonance Raman intensities are perturbed by saturation of one of the conjugated double bonds. Accordingly the resonance Raman study of M(OEC) has been undertaken. To assign the vibrational modes, deuterium substitution of the methine hydrogen atoms at γ and δ positions and, ^{15}N substitution of the four pyrrole nitrogens were performed. Considering the appearance of Fe-L stretching band in the resonance Raman spectra of Fe(OEP)L and $Fe(OEP)L_2$ (13,31), we tried to find the Fe-L stretching band for Fe(OEC)L and $Fe(OEC)L_2$.

For the purpose of comparison, metallo-octaethylporphyrin [M(OEP)] was subjected to the Raman measurement again under the same experimental conditions as for M(OEC). Thus the similarity and difference between the resonance Raman spectra of M(OEC) and M(OEP) is discussed in this paper.

EXPERIMENTAL

The procedures for the preparation of M(OEC), its γ,δ-deuterated derivative [$M(OEC)-d_2$] and M(OEP) were reported previously (32,33). Complete deuterium substitution only at γ,δ positions of free base chlorin was confirmed by disappearance of ^1H-NMR peak at 8.86 p.p.m. and presence of peak at 9.87 p.p.m. However mass spectrum of its cupper complex indicated presence (30%) of monodeuterated Cu(OEC) besides di-deuterated one, although the incorporation of cupper ion was performed in deuterated solvent including C_6D_6 and CH_3OD. $Fe^{3+}(OEP)Cl-^{15}N_4$ was synthesized according to the method reported in our previous papers

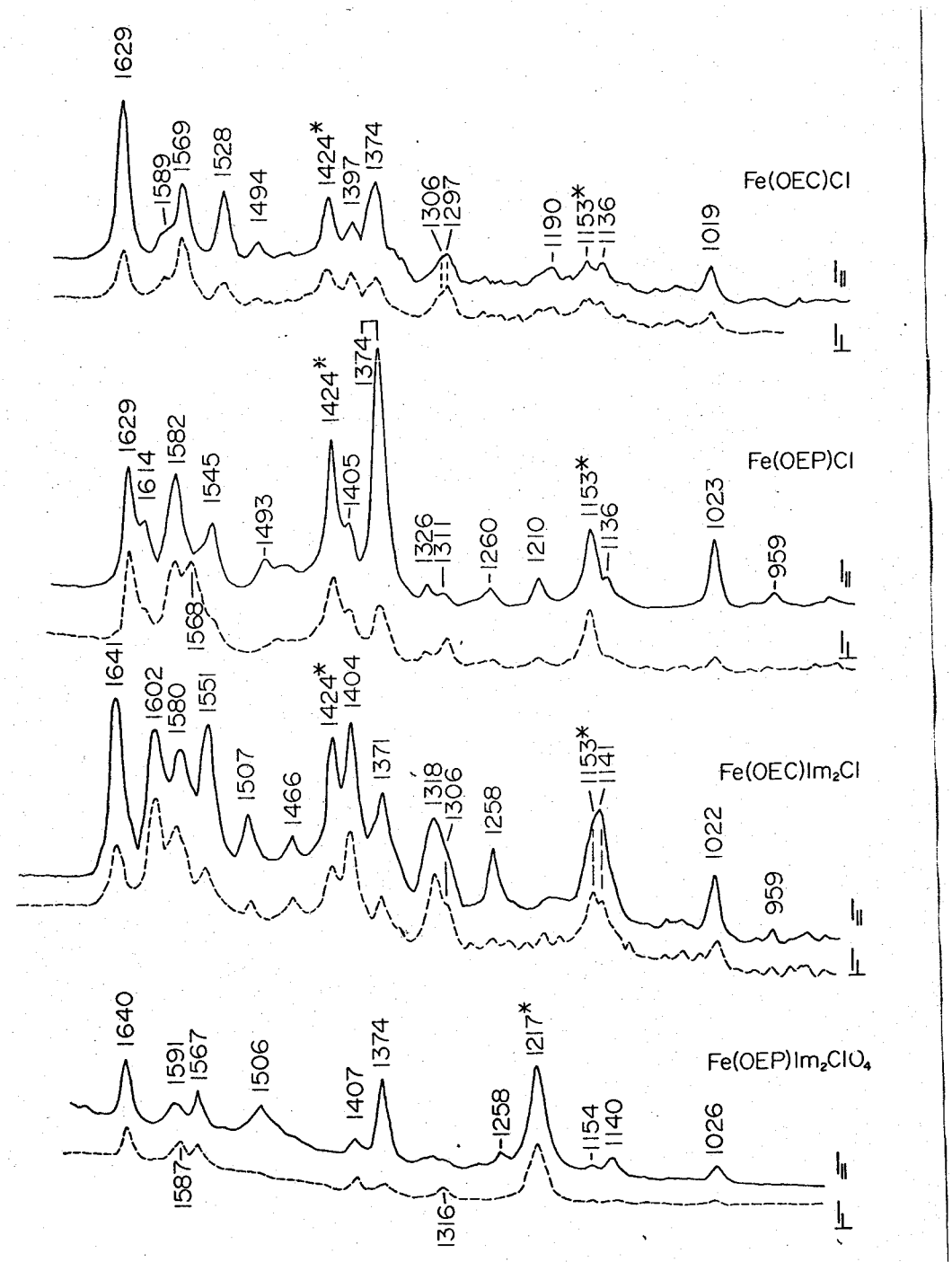

Fig. 1 Raman spectra of Fe(OEC)Cl, Fe(OEP)Cl, Fe(OEC)$(Im)_2$Cl (CH_2Cl_2) and Fe(OEP)$(Im)_2ClO_4$ ($CHCl_3$) excited by the 488.0 nm line. The solid lines and broken lines denote the electric vector of the scattered radiation to be parallel and perpendicular to that of the incident light, respectively. The Raman lines marked by an asterisk are due to solvent. Instrumental conditions: power 400 mW; slit width 7 cm^{-1}; sens 1000counts/sec; scan speed 9 cm^{-1}/min; time constant 2.0 sec; rate 0.5 sec.

(32). Cu(OEC)-$^{15}N_4$ was then derived from Fe^{3+}(OEP)Cl (33). The infrared and mass spectra confirmed that ^{15}N substitution of pyrrole nitrogen was completed (~97%). Upon the measurement of their Raman spectra, 200 μl of ca. 0.3 mM M(OEC) solution (CH_2Cl_2, or THF) was put in a cylindrical cell. For Cu(OEC)-d_2 deuterated solvent (CD_2Cl_2) was used.

Raman spectra were excited by Ar^+-Kr^+ mixed gas laser (Spectra Physics Model 164) and were reported on a JEOL-400 D or JEOL-02AS Raman spectrometer. Frequency calibration of the spectrometer was performed with indene (600-1700 cm^{-1})(34) and D_2 gas (100-650 cm^{-1}) (35) for each of excitation lines. The estimated errors of frequencies and depolarization ratios are within ± 1 cm^{-1} and 0.1, respectively.

RESULTS

The Raman spectra of Fe(OEC)Cl and Fe(OEC)Im_2Cl are compared with those of Fe(OEP)Cl and Fe(OEP)Im_2ClO_4, respectively, in Fig. 1. Two polarized Raman lines at 1629 (p) and 1528 (p) cm^{-1} and a depolarized line at 1397 (dp) cm^{-1} Fe(OEC)Cl correspond to three depolarized Raman lines of Fe(OEP)Cl at 1629 (dp), 1545 (dp), and 1405 (dp) cm^{-1}. Two anomalously-polarized lines at 1569 (ap) and 1297 (ap) cm^{-1} correspond to the anomalously-polarized Raman lines of Fe(OEP)Cl at 1568 (ap) and 1311 (ap) cm^{-1}, respectively. The polarized Raman lines of Fe(OEC)Cl at 1494 (p), 1374 (p), 1136 (p), and 1019 (p) cm^{-1} are reasonably correlated with the polarized lines of Fe(OEP)Cl at 1493 (p), 1374 (p), 1136 (p), and 1023 (p) cm^{-1}. Similar correlations can be valid between the Raman lines of Fe(OEC)Im_2Cl and those of Fe(OEP)Im_2ClO_4 as shown in Table 1. These good correspondence of prominent Raman lines between Fe(OEC) and Fe(OEP) implies that the vibrational assignment established for M(OEP) by normal coordinate calculations can be approximately applied to M(OEC).

Fig. 2. illustrates the Raman spectra of Fe(OEC)Im_2Cl upon the excitation at 488.0, 514.5 and 568.2 nm. The apparent intensities of the Raman lines look weaker for 568.2 nm excitation. However, the actual intensity enhancement is largest for 568.2 nm excitation. It is seen from the fact that peak intensities of most Raman lines relative

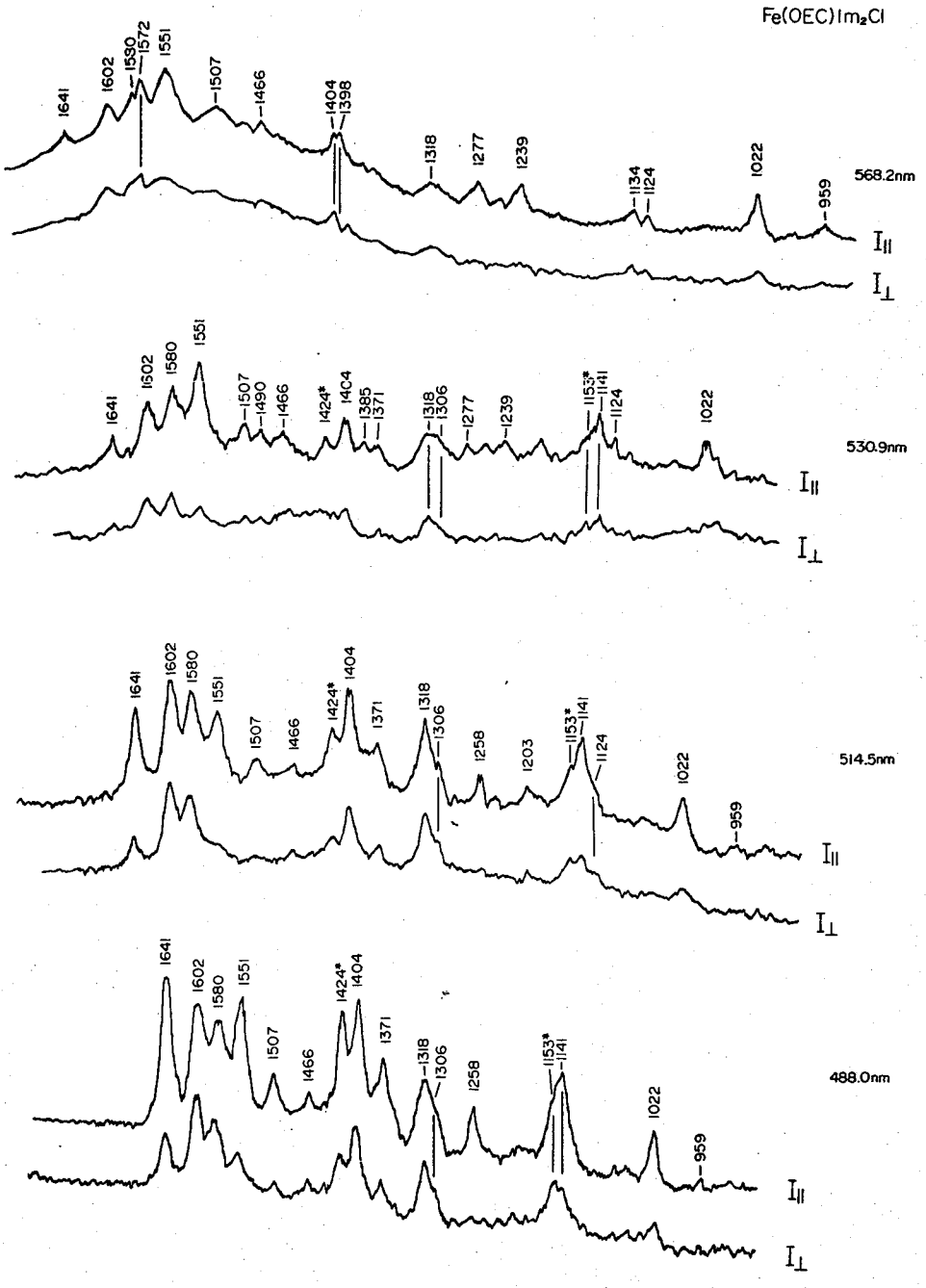

Fig. 2 Raman spectra of $Fe(OEC)(Im)_2Cl$ in CH_2Cl_2 excited by the 488.0, 514.5, 530.9, and 568.2 nm lines. Instrumental conditions; power 100-400 mW; other conditions are same as those in Fig. 1.

Table 1. Observed wavenumbers of Raman bands for Fe(OEC) and Fe(OEP) (cm^{-1})

Fe(OEC)		Fe(OEP)	
high spin	low spin	high spin	low spin
1629 (p)	1641 (p)	1629 (dp)	1640 (dp)
1589 (ap)	1602 (ap)	1582 (dp)	1591 (dp)
1569 (ap)	1580 (ap)	1568 (ap)	1587 (ap)
1528 (p)	1551 (p)	1545 (dp)	1567 (dp)
1494 (p)	1507 (p)	1493 (p)	1506 (p)
1397 (dp)	1404 (dp)	1405 (dp)	1407 (dp)
1374 (p)	1371 (p)	1374 (p)	1374 (p)
1306 (ap) 1297 (ap)	1318 (ap) 1306 (ap)	1311 (ap)	1316 (ap)
	1258 (p)	1260 (p)	1258 (p)
1153 (dp)	1153 (dp)	1153 (dp)	1154 (dp)
1136 (p)	1141 (p)	1136 (p)	1140 (p)
1019 (p)	1022 (p)	1023 (p)	1026 (p)

to that at 1424 cm^{-1} of CH_2Cl_2 which is not resonanced with visible excitation light, are extremely larger for 568.2 nm excitation. This intensity enhancement for 568.2 nm is particularly notable for Raman lines below 1300 cm^{-1} of all M(OEC) measured. To the contrary, double bond stretching vibrations in higher frequency region are more enhanced by excitation lines with shorter wavelength. The four Raman lines at 1641, 1602, 1580, and 1551 cm^{-1} are more intense for excitation at 488.0 nm but their relative intensities vary with excitation wavelength. A new Raman line appered at 1572 cm^{-1} upon an excitation at 568.2 nm.

Fig. 3. illustrates the Raman spectra of Fe(OEC)Cl for three wavelengths of excitation (488.0, 514.5, and 568.2 nm). The Raman lines of Fe(OEC)Cl below 1400 cm^{-1} are much intensified for the excitation at 568.2 nm as in the case of $Fe(OEC)Im_2Cl$. Especially the Raman lines at 1130, 1210, 1233, and 1271 cm^{-1} which are not or very weakly recognized upon 568.2 nm excitation. This inclination was also observed for Ni(OEC).

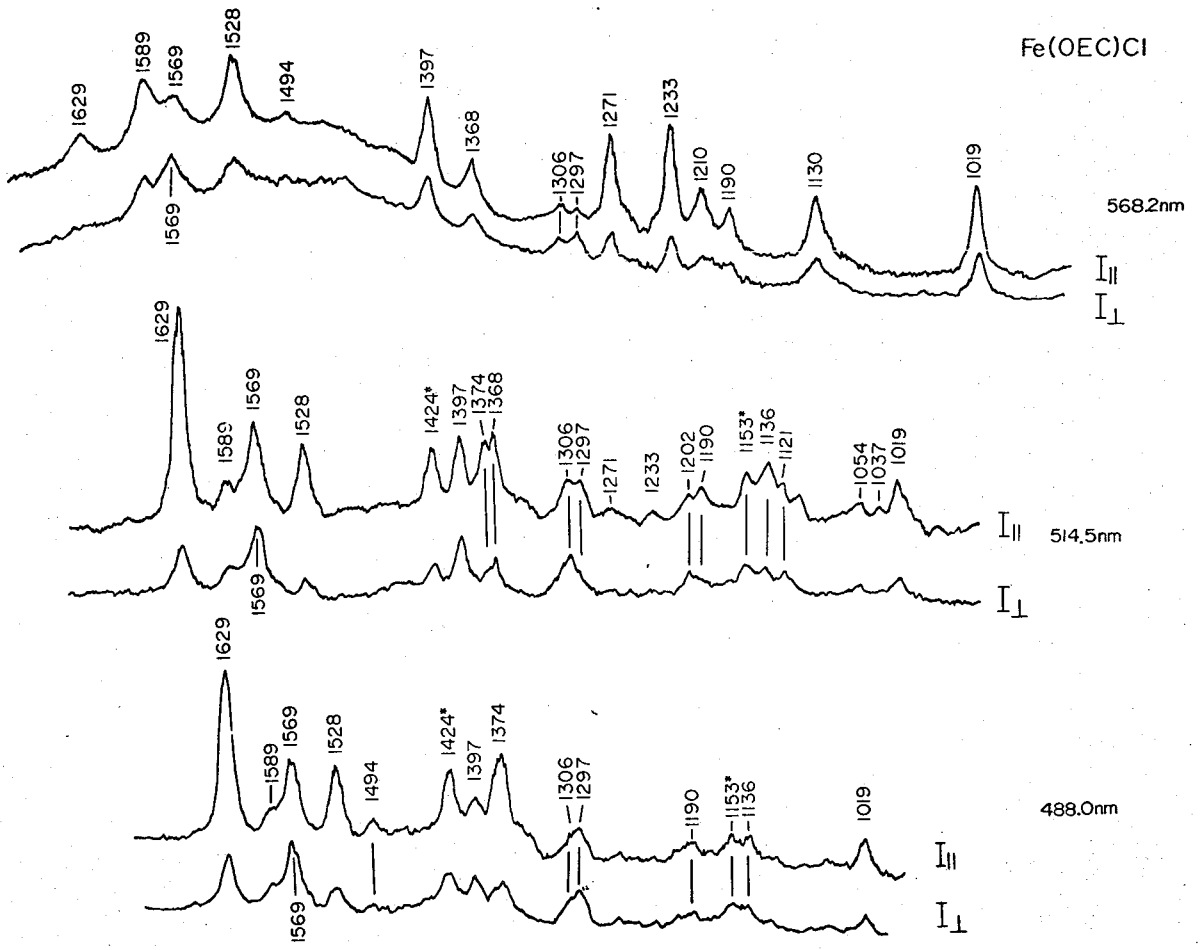

Fig. 3 Raman spectra of Fe(OEC)Cl in CH_2Cl_2 excited by 488.0, 514.5, 568.2 nm lines. The instrumental conditions are same as those in Fig. 2.

Therefore it seems peculiar to M(OEC) that the resonance enhancement of Raman intensity occurs to the modes around 1100-1300 cm^{-1} upon excitation at 568.2 nm.

Fig. 4 shows the resonance Raman spectra of Ni(OEC), Cu(OEC), Cu(OEC)-d_2, and Cu(OEC)-$^{15}N_4$ in CH_2Cl_2 (CD_2Cl_2) solution. Both Ni(OEC) and Cu(OEC) are supposed to have a square planar structure for MN_4 core of chlorin skeleton, giving rise to a similar pattern of Raman spectra. However, the stretching frequencies of chlorin skeleton are somewhat higher in Ni(OEC) than in Cu(OEC) particularly for the modes above 1450 cm^{-1}. It indicates that π bond-strength in the conjugated double bonds of Ni(OEC) is stronger than that of Cu(OEC). Similar feature was observed between Cu(OEP) and Ni(OEP).

Upon the deuterium substitution of γ,δ-methine hydrogen, the Raman lines at 1643 (p), 1584 (ap), 1546 (ap), 1506 (p), and 1317 cm^{-1} (ap) of Cu(OEC) shifted to 1638 (p), 1580 (ap), 1527 (ap), 1502 (p), and 1294 cm^{-1} (ap), respectively. Since only two of the four methine hydrogen atoms are replaced by deuterium atoms, the isotopic frequency shifts observed both in the Raman spectra is not as large as the case of Ni(OEP). On the other hand upon the ^{15}N substitution of four pyrrole nitrogens, the Raman lines at 1372 (p), 1362 (p), 1317 (ap), 1157 (dp), 1129 (ap), 1023 (p), and 960 cm^{-1}(p) of Cu(OEC) shifted to 1366 (p), 1357 (p), 1312 (ap), 1148 (dp), 1110 (ap), 1020 (p) and 957 cm^{-1} (p), respectively. The Raman lines above 1500 cm^{-1} which shift clealy upon the γ,δ-meso-deuteration didn't show lower frequency shift, upon the nitrogen substitution.

The Raman spectrum of Fe(OEC)F is almost the same as that of Fe(OEC)Cl in the frequency region from 900 to 1700 cm^{-1}. However, in the lower frequency region Fe(OEC)F yields its characteristic Raman line at 608 cm^{-1}. The Raman spectra of Fe(OEC)F as well as other metallo-chlorins in the lower frequency region are shown in Fig. 5. Although there is a Raman line of solvent (THF) near 608 cm^{-1} the existence of the 608 cm^{-1} line for Fe(OEC)F is evident from their relative intensities. The Raman line at 361 cm^{-1} is characteristic of Fe(OEC)Cl. There is no such Raman line for Ni(OEC) and Cu(OEC) which have no axial ligand. When there are two axial ligands as in

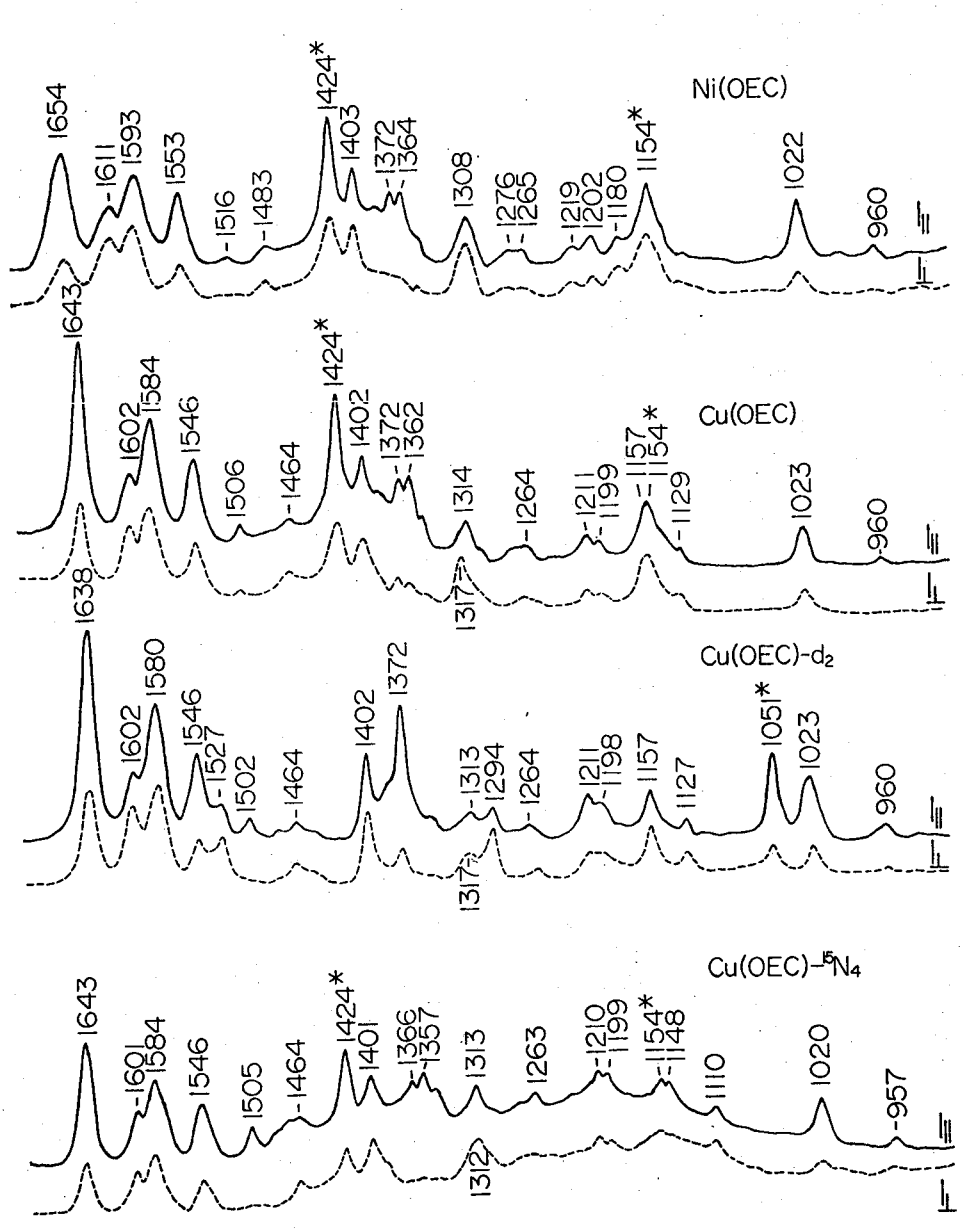

Fig. 4 Polarized Raman spectra of Ni-(OEC), Cu(OEC), Cu(OEC)-d_2, and Cu(OEC)-$^{15}N_4$ excited by the 488.0 nm line. The Raman lines at 1424 and 1154 cm^{-1} marked by an asterisk are due to solvent (CH_2Cl_2), while the line at 1051 cm^{-1} is due to solvent (CD_2Cl_2). The Raman line at 1157 cm^{-1} of Cu(OEC) was confirmed by the measurement of TFA solution. Only these spectra were measured with the use of JEOL-400 D Raman spectrometer equipped with a cooled HTV-R649 photomultiplier. Instrumental conditions: power 200 mW; slit width 3 cm^{-1}; sensitivity 1000 counts/sec; scan speed 25 cm^{-1}/min; time constant 3.2 sec.

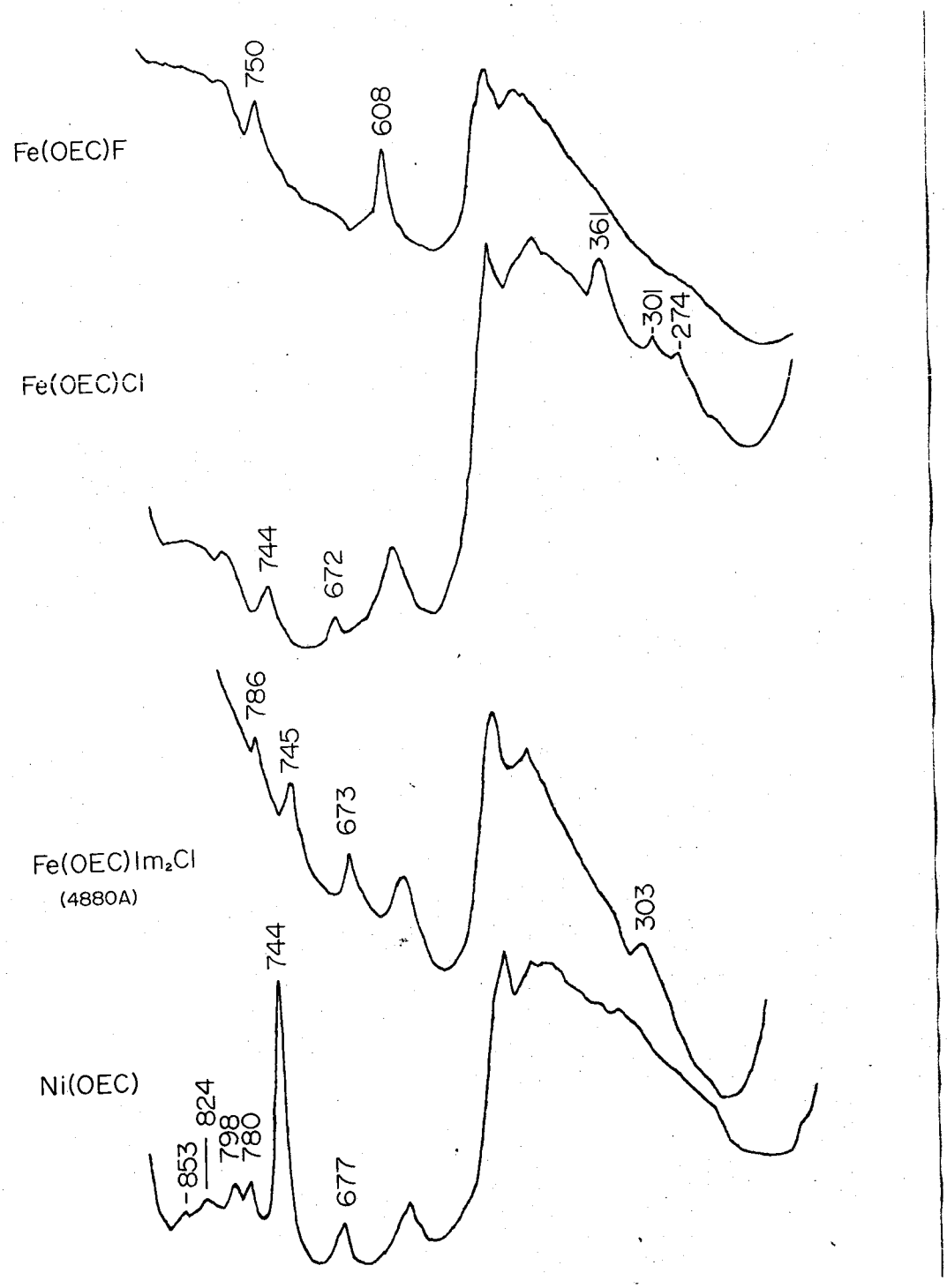

Fig. 5 Raman spectra in the frequency region of 100-850 cm^{-1} of Fe(OEC)F, Fe(OEC)Cl, Ni(OEC) (excited by the 514.5 nm line) and $Fe(OEC)(Im)_2Cl$ (excited by the 488.0 nm line) in THF. Raman lines marked by an asterisk are due to solvent or cell, however the 608 cm^{-1} line of Fe(OEC)F is overlapped with the line due to the Fe-F stretching.

$Fe(OEC)(Im)_2Cl$, two stretching vibrations of iron-axial ligands are expected. The Raman line at 303 cm^{-1} of $Fe(OEC)(Im)_2Cl$ is assignable to the symmetric stretching mode between iron and two axial ligands.

DISCUSSION

Similarities and differences between Raman spectra of M(OEC) and M(OEP)

The chemical structure of M(OEC) and M(OEP) are close except that the C_β-C_β bond of ring IV is saturated in M(OEC) but not in M(OEP)(see Fig. 6). Molecular symmetry of Ni(OEP) in solution is D_{4h} (10,36). If approximately the same molecular geometry is retained in Ni(OEP), the effective molecular symmetry of Ni(OEC) is regarded as C_{2v}. The symmetry correlation between in-plane vibrations of Ni(OEP) and Ni(OEC) are shown in Table 2. where the C_4 axis of Ni(OEP) and C_2 axis of

Table 2. Symmetry correlation diagram between resonance Raman active species of the D_{4h} group [Ni(OEP)] and those of C_{2v} [Ni(OEC)].

D_{4h} [Ni(OEP)]	C_{2v} [Ni(OEC)]
A_{1g} (p)	
B_{1g} (dp)	A_1 (p)
E_u*	
A_{2g} (ap)	
B_{2g} (dp)	B_2 (ap or dp)

*Raman inactive

Ni(OEP) are taken as z axis for the D_{4h} and C_{2v} groups, respectively (the C_4 axis of Ni(OEP) and the C_2 axis of Ni(OEC) are at right angles to each other). Thus the A_{1g} and B_{1g} species of the D_{4h} group are correlated with the A_1 species of the C_{2v} group while the A_{2g} and B_{2g} species of D_{4h} are correlated with B_2 species of C_{2v}.

Since the visible absorption bands (Q and Soret) of metallo -chlorin belong to the A_1 or B_2 species, the resonance enhancement of

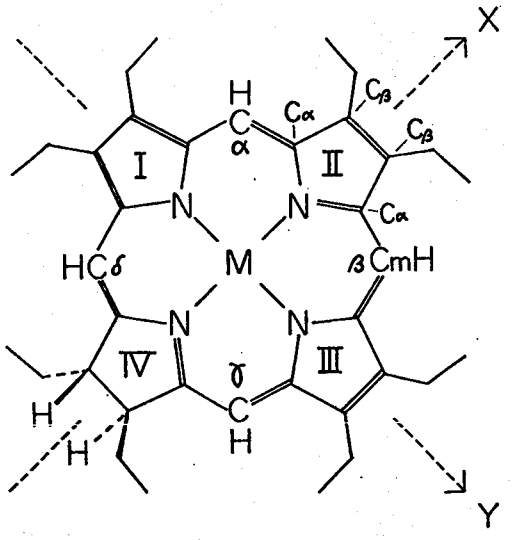

Fig. 6 Chemical structure of metallo-trans-octaethylchlorin. The z and y coordinates thus defined are used for the symmetry representation of Ni(OEC) (C_{2v}) in Table 1. $C_\beta C_\beta$ bond of ring IV is a double bond for M(OEP).

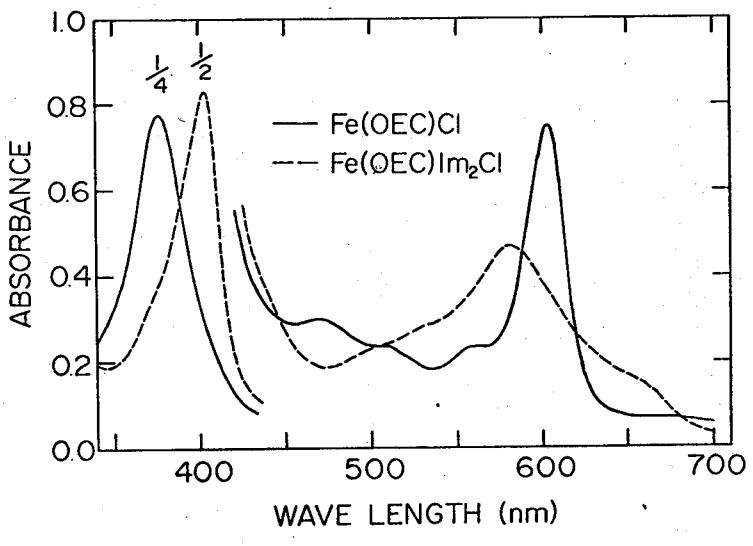

Fig. 7 Visible absorption spectra of Fe(OEC)Cl and Fe(OEC)$(Im)_2$Cl (in CH_2Cl_2 solution).

Raman intensity by visible excitation light is expected for the vibrations with the A_1 and B_2 symmetry. Raman inactive E_u species of the D_{4h} group is correlated with Raman active A_1 and B_2 species of C_{2v} and therefore we may have more Raman lines for M(OEC) than M(OEP). According to the tensor pattern for two-photon process (37) the Raman lines with A_1 symmetry are expected to be polarized whereas those with B_2 symmetry may possibly be depolarized or anomalously-polarized.

As to the iron-chlorin derivatives, the situation is more complicated. The Fe^{3+} ion of $Fe(OEC)(Im)_2Cl$ may presumably be located in the porphyrin plane as in the case of $Fe(OEP)(Im)_2ClO_4$ (38). Then the effective symmetry of $Fe(OEC)(Im)_2Cl$ can be approximated as C_{2v} and the same consideration as for Ni(OEC) may be applied to $Fe(OEC)(Im)_2Cl$. However, Fe^{3+} ion of Fe(OEC)Cl is probably located out-of-plane as in the case of chlorohemin (39), resulting in C_s symmetry. Then all the vibrations are Raman active in principle.

Despite the different symmetry, however, there is a good correspondence betweem Raman lines M(OEC) and M(OEP). On the basis of the symmetry correlation of Table 1, the depolarized Raman lines of $Fe(OEP)(Im)_2ClO_4$ at 1640 and 1567 cm^{-1} are assigned to the B_{1g} species, while that at 1407 cm^{-1} should be assigned to the B_{2g} species of D_{4h} group. The good correspondence of distinctive Raman lines for $Fe(OEC)(Im)_2Cl$ and $Fe(OEP)(Im)_2ClO_4$ implies that the E_u like vibrational modes of D_{4h} group do not gain sufficient resonance Raman intensity even upon the lowering of molecular symmetry (C_{2v}). Furthermore the Raman lines at 1641 and 1507 cm^{-1} of $Fe(OEC)(Im)_2Cl$ (low spin) and those at 1629 and 1494 cm^{-1} of Fe(OEC)Cl (high spin) may be used as the spin state indicator of Fe^{3+} ion of heme d as was so for protoheme and Fe(OEP) derivatives (40).

Since M(OEC) complexes have an intense absorption band at around 600 nm (see Fig. 7), it is reasonable that the Raman scattering of M(OEC) is intensified upon the excitation at 568.2 nm, near the wavelengths of the 0-1 transitions. However, it is noted as distictive difference between M(OEP) and M(OEC) that the intensity enhancement occurs to the modes around 1100-1300 cm^{-1} for M(OEC) but not for M(OEP). The vibrational modes with such frequencies involve appreciable

contribution from the $C_\alpha C_\beta$ and $C_\alpha N$ stretching coordinate (22). Accordingly it is deduced that the 600 nm band characteristic of M(OEC) corresponds to the π electronic transition which involves the $C_\alpha C_\beta$ and $C_\alpha N$ bonds in the conjugation system more significantly than in the case of the Q band of M(OEP).

As a minor difference between Raman spectra of M(OEP) and M(OEC) the latter derivatives have a few extra Raman lines. The Raman line at 1466 cm^{-1} of $Fe(OEC)(Im)_2Cl$ and those at 1483 and 1202 cm^{-1} of Ni(OEC) do not have their counterpart in M(OEP). Moreover the totally -symmetric mode of the pyrrole ring breathing like vibrations, which was observed as a single intense polarized Raman line at 1380 cm^{-1} for Ni(OEP), are observed as doublet at 1364 and 1372 cm^{-1} for Ni(OEC). Since this type of modes are factorized into $3A_1 + B_2$, the extra Raman line might be caused by appearance of the E_u like modes, although detailed normal coordinate analysis is required to confirm it.

Assignments of the Raman lines of Cu(OEC) The Raman lines of Cu(OEC) at 1643 (p), 1584 (ap), 1546 (ap), and 1506 cm^{-1} (p) which show the definite isotopic frequency shift upon the γ,δ-meso-deuteration can be readily assignment to the methine-bridge stretching vibrations. The corresponding modes of Ni(OEC) were found at 1654 (p), 1593 (ap), 1553 (ap), and 1516 cm^{-1} (p). As for Ni(OEP) three Raman lines at 1655 (ap), 1603 (ap), and 1519 cm^{-1} (p) were assigned to the methine -bridge stretching vibrations (8,9). The Raman lines at 1546 cm^{-1} of Cu(OEC) and 1553 cm^{-1} of Ni(OEC) were overlapped with two Raman lines as clearly shown by γ,δ-meso-deuteration experiment of Cu(OEC), namely the ap band at 1546 cm^{-1} of Cu(OEC) which was due to methine-bridge stretching vibration shows the definete lower frequency shift and the dp band at 1546 cm^{-1} of Cu(OEC) never shows the isotopic frequency shift. This ap band may be characteristic to chlorins.

The Raman line at 1317 cm^{-1} (ap) of Cu(OEC) which shifted to 1294 cm^{-1} upon the deuterium substitution is assignable to in-plane CH deformation vibration as in the case of 1309 cm^{-1} line Ni(OEP) (8,9).

^{15}N substitution experiments was quite useful for elucidation of the nature of the Raman oxidation state marker band of hemoproteins

(17). This marker band could be deu to the ring vibration of pyrrole accompanied with in-phase displacement of the four pyrrole nitrogens toward the heme iron. Polarized Raman lines corresponding to the oxidation state marker band of hemoproteins were observed at 1377 [Ni(OEP)], 1369 [Fe(OEP)Cl], and 1372 cm^{-1} [$Fe(OEP)(Im)_2ClO_4$] which were shifted to lower frequency from those of the ^{14}N compounds by 6,5,and 6 cm^{-1}, respectively. The present experiment as for Cu(OEC)-$^{15}N_4$ indicate that two Raman lines at 1372 and 1362 cm^{-1} of Cu(OEC) could correspond to the oxidation state marker. The strong enhancement of the 1372 cm^{-1} line and the disappearance of the 1362 cm^{-1} line in Cu(OEC)-d_2 suggest that the latter line shifted to 1372 cm^{-1}. The oxidation state marker of $Fe(OEC)(Im)_2Cl$ and Fe(OEC)Cl were observed 1371 cm^{-1} and 1374 cm^{-1}, respectively (Fig. 1). These were located at similar position to those of Fe(OEP). It is noticeable that the vibrational frequencies of the $C_\beta C_\beta$ stretching mode are lower in M(OEC) than in M(OEP). The corresponding Raman line is observed at 1576 cm^{-1} for Ni(OEP) (22) and 1553 cm^{-1} for Ni(OEC) (Fig. 4). Such frequency difference is also found between $Fe(OEP)(Im)_2ClO_4$ (1567 cm^{-1}) and $Fe(OEC)(Im)_2Cl$(1551 cm^{-1}) (low spin derivatives) and between Fe(OEP)Cl (1545 cm^{-1}) and Fe(OEC)Cl (1528 cm^{-1})(high spin derivatives). It implies that the saturation of one of the four $C_\beta C_\beta$ bonds in metallo-porphyrin results in reduction of effective force constants for the coordinate involving the linear combination of the four $C_\beta C_\beta$ stretching coordinates.

As stated above the vibrational assignment established for M(OEP) by normal coordinate calculations can be approximately applied to M(OEC). The 1159 (dp) and 1121 cm^{-1} (ap) line of Ni(OEP) showed isotopic frequency shifts upon the ^{15}N substitution. They were also associated mainly with C_α-N stretching vibrations (25). Analogously the 1157 (dp) and 1129 cm^{-1} (ap) line of Cu(OEC) are assignable to C_α-N stretching vibrations.

Iron-axial ligand stretching mode Raman lines at 608 cm^{-1} of Fe(OEC)F and at 361 cm^{-1} of Fe(OEC)Cl (Fig. 5) are assigned to Fe-F and Fe-Cl stretching vibrations, respectively. These frequencies agree closely with those of Fe(OEP)F (606 cm^{-1}) and Fe(OEP)Cl (364 cm^{-1})

observed in their Raman spectra (13). This assignment is also supported by the infrared bands of the Fe-L stretching mode of Fe(OEC)L in the solid state, which was identified at 589 cm^{-1} for L=F and at 352 cm^{-1} for L=Cl (33).

In the case of the complexes of $Fe(OEC)L_2$ type, there are symmetric and antisymmetric L-Fe-L stretching modes. The former is considered to be more intense in Raman spectrum and to have lower vibrational frequency. The Raman line at 303 cm^{-1} was assigned to the symmetric (Im)N-Fe-N(Im) stretching mode of $Fe(OEC)Im_2Cl$. The frequency is close to the 290 cm^{-1} of $Fe(OEP)Im_2ClO_4$. Thus it can be said that the bond -strength of iron-axial ligand is not affected so much by the change of π electronic state such as the saturation of the conjugated bond.

Raman spectra of Mg(OEC) and chlorophyll Spaulding et al. (10) reported the frequencies of methine-bridge stretching vibrations of Mg(OEP) at 1610 (dp), 1558 (ap), and 1482 cm^{-1} (p), which are lower by 45, 45, 37 cm^{-1} than those of Ni(OEP)(9), respectively. The pyrrole ring vibration of Mg(OEP) (1379 cm^{-1}) (10) is almost the same as that of Ni(OEP) (1383 cm^{-1}) (9). On the basis of the frequency difference described above and the frequencies observed for Ni(OEC) (Fig. 4), the frequencies of the methine-bridge stretching modes of Mg(OEC) could be predicted approximately 1610, 1550, and 1480 cm^{-1} from the frequencies of 1654, 1593, and 1516 cm^{-1} of Ni(OEC) (9). The pyrrole ring vibration of Mg(OEC) may be expected at about 1360 cm^{-1}. Accordingly the Raman lines at 1612, 1555, and 1495 cm^{-1} of chlorophyll a (28) may possibly be due to the methine-bridge stretching modes and that 1348 cm^{-1} may be associated with the pyrrole ring mode. However in general the correspondence of Raman lines between chlorophyll and OEC is not so good, impling that the existence of cyclopentanone ring has strong effects on the Raman spectrum of chlorophyll. The present results on Fe(OEC) derivatives have rather constituted a basis for the analysis of the resonance Raman spectrum of heme d than that for chlorophyll.

ACKNOWLEDGMENT

The author wishes to express his thanks to Dr. Kenkichi Sonogashira for his kindness of measuring the mass spectrum of Cu(OEC)$_2$-d_2.

REFERENCES

1. Burger, H., Burczyk, K., Buchler, J. W., Fuhrhop, J. H., Hofler, F., and Schrader, B. (1970) Inorg. Nucl. Chem. Lett. 6, 171.
2. Verma, A. L., Mendelsohn, R., and Bernstein, H. J. (1974) J. Chem. Phys. 61, 383.
3. Verma, A. L. and Bernstein, H. J. (1974) J. Chem. Phys. 61, 2560.
4. Verma, A. L. and Bernstein, H. J. (1974) J. Raman Spectrosc. 2, 163.
5. Mendelsohn. R., Sunder, S., Verma, A. L., and Bernstein, H. J. (1975) J. Chem. Phys. 62, 37.
6. Sunder, S., Mendelsohn, R., and Bernstein, H. J., (1975) J. Chem. Phys. 63, 573; (1975) Biochem. Biophys. Res. Commun. 62, 12.
7. Mendelsohn, R., Sunder, S., and Bernstein, H. J. (1975) J. Raman Spectrosc. 3, 303.
8. Kitagawa, T., Ogoshi, H., Watanabe, E., and Yoshida, Z. (1975) Chem. Phys. Lett. 30, 451.
9. Kitagawa, T., Ogoshi, H., Watanabe, E., and Yoshida, Z. (1975) J. Phys. Chem. 79, 2629.
10. Spaulding, L. D., Chang, C. C., Yu, N. T., and Felton, R. H. (1975) J. Am. Chem. Soc. 97, 2517.
11. Shelnutt, J. A., O'Shea, D. C., Yu, N. T., Cheung, L. D., and Felton, R. H. (1976) J. Chem. Phys. 64, 1156.
12. Gaughan, R. R., Shriver, D. F., and Boucher, L. J. (1975) Proc. Nat. Acad. Sci. 72, 433.
13. Kitagawa, T., Abe, M., Kyogoku, Y., Ogoshi, H., Watanabe, E., and Yoshida, Z. (1976) J. Phys. Chem. 80, 1181.
14. Ksenofontova, N. M., Maslov, V. G., Sidorov, A. N., and Bobovitch, Ya. S., (1976) Opt. Spectrosk. 40, 809.
15. Verma, A. L., Asselin, M., Sunder, S., and Bernstein, H. J. (1976) J. Raman Spectrosc. 4, 295.
16. Warshel, A. (1976) Chem. Phys. Lett. 43, 273.
17. Warshel, A. and Dauber, P. (1977) J. Chem. Phys. 66, 5477.
18. Kitagawa, T., Abe, M., Kyogoku, Y., Ogoshi, H., Sugimoto, H., and Yoshida, Z. (1977) Chem. Phys. Lett. 48, 55.
19. Shelnutt, J. A., Cheung, L. D., Chang, R. C. C., Yu, N. T., and Felton, R. H. (1977) J. Chem. Phys. 66, 3387.

20. Nishimura, Y., Hirakawa, A., and Tsuboi, M. (1977) J. Mol. Spectrosc. 68, 335.
21. Stein, P., Burke, J. M., and Spiro, T. G. (1975) J. Am. Chem. Soc. 97, 2304.
22. Abe, M., Kitagawa, T., and Kyogoku, Y. (1976) Chem. Lett. 249.
23. Sunder, S. and Bernstein, H. (1976) J. Raman Spectrosc. 5, 351.
24. Susi, H. and Ard, J. S. (1977) Spectrochim. Acta 33A, 561.
25. Abe, M., Kitagawa, T., and Kyogoku, Y. submitted to J. Chem. Phys.
26. Lutz, N., (1972) Compt. Rend. Acad. Sci. Serie B 275, 497.
27. Lutz, N. and Breton, J. (1973) Biochem. Biophys. Res. Commun. 35, 413.
28. Lutz, M. (1974) J. Raman Spectrosc. 2, 497.
29. Lutz, M., Kleo, J., and Reiss-Husson, F. (1976) Biochem. Biophys. Res. Commun. 69, 711.
30. Yamanaka, T. and Okunuki, K. (1974) "Microbial Iron Metabolism" (Neilands, J. B. ed.) p 394 Academic Press, New York.
31. Kincaid, J. and Nakamoto, K. (1976) Spectrosc. Lett. 9, 19.
32. Ogoshi, H., Watanabe, E., Yoshida, Z., Kincaid, J., and Nakamoto, K. (1973) J. Am. Chem. Soc. 95, 2845.
33. Ogoshi, H., Watanabe, E., Yoshida, Z., Kincaid, J., and Nakamoto, K. (1975) Inorg. Chem. 14, 1344.
34. Hendra, P. J. and Loader, E. J. (1968) Chem Ind. 718.
35. Stoicheff, B. P. (1957) Can. J. Phys. 35, 730.
36. Cullen, D. A. and Meyer, Jr. E. F. (1974) J. Am. Chem. Soc. 96, 2095.
37. McClain, W. M. (1971) J. Chem. Phys. 55, 2789.
38. Takenaka, A., Sasada, Y., Watanabe, E., Ogoshi, H., and Yoshida, Z. (1972) Chem. Lett. 1235.
39. Hoard, J. L. (1971) Science, 174, 1295.
40. Kitagawa, T., Iizuka, T., Saito, M., and Kyogoku, Y. (1975) Chem. Lett. 849.
41. Spiro, T. G. and Strekas, T. C. (1974) J. Am. Chem. Soc. 96, 338.
42. Weiss, Jr. C. (1972) 44, 37.

PART II ^{15}N-Nuclear Magnetic Resonance Studies on the Nature of Metal-axial Ligand Bond in Metallo-octaethylporphyrins

Chapter 1.

Nitrogen-15 Nuclear Magnetic Resonance Spectra of ^{15}N-Enriched Metallo-octaethylporphyrins

ABSTRACT

97% ^{15}N-enriched octaethylporphyrin was synthesized by the use of $Na^{15}NO_2$ as a starting material. ^{15}N-NMR spectra at 10 MHz were obtained for the metal complexes of $^{15}N_4$-OEP with Mg(II), Fe(II), Co(III), Ni(II), Zn(II), and Cd(II). ^{13}C-NMR spectra at 25 MHz were also measured for Mg(II), Fe(II), Ni(II), Zn(II), and Cd(II) complexes. The ^{15}N resonance of Ni(II)-complex of $^{15}N_4$-OEP is distinct from the other diamagnetic metallo-octaethylporphyrins without axial ligands and is located in remarkably higher field. Similar distinct shift was observed for the ^{13}C resonance of the C_α carbon of the Ni(OEP). These fact can be explained by the effect of strong Ni-N bonding. The axial ligand effects were examined for $^{15}N_4$-Fe^{2+}(OEP) and $^{15}N_4$-Co^{3+}(OEP). In the case of Fe(II) complexes the ^{15}N chemical shifts depend upon the bonding nature of the iron-axial ligand. The π type bonding induces the delocalization of the electron charge density of the porphyrin ring which may result in the decrease of σ_p term. However the change in basicity of the axial ligands gave very small effects to the ^{15}N resonances of the porphyrin. Such substitution seems to give rise only secondary effect to the chemical shift of the ^{15}N nuclei at the cis position.

INTRODUCTION

Nuclear magnetic resonance spectroscopy of nitrogen-15 has become a powerful probe in structural and functional studies of coordination compounds and biological molecules, since nitrogen atom is generally located at the sites interacted with other groups or molecules. Even in the study of porphyrins ^{15}N-NMR seemed to play an important role because the nitrogen atom of pyrrole ring interacted directly with

central protons or coordinated to the metal of porphyrins. ^{15}N-NMR revealed its significance in the NH tautomerism study of porphyrins (1-6).

In the previous works ^{15}N-NMR of ^{15}N-enriched octaethylporphyrin ($^{15}N_4$-$OEPH_2$) demonstrated the direct evidence of NH tautomerism and supported the discussion based on ^{1}H-and ^{13}C-NMR data (3). Similar conclusions by the use of ^{15}N-NMR were recently obtained independently by other groups on ^{15}N-enriched protoporphyrin-IX (2) and tetraphenylporphin (TPP) (4,5). Further, the NH tautomerism study was extended to N-substituted-octaethylporphyrins (6) and octaethylchlorin (7).

When the metal ions are coordinated to the nitrogen atoms of porphyrins, the electron density of the nitrogen must be most sensitively affected by the nature of the metal-nitrogen bonding. It can be also expected that the ligand substitution at the fifth and sixth coordination positions would induce the chemical shift change of ^{15}N nuclei (8). The iron complexes of OEP with axial ligands and cobalt porphyrins are very useful model compounds of hemoproteins and vitamin B_{12}, respectively. The investigations of the nature of metal-axial ligand of those model compounds are quite desirable for understanding the structure-function relationship of hemoproteins and vitamin B_{12}.

In this Chapter the ^{15}N-NMR spectra of some diamagnetic metal complexes of ^{15}N-OEP are reported and this anomaly of ^{15}N-resonance positions of $^{15}N_4$-Ni(OEP) is discussed in detail. The axial ligand effect was examined for ferrous iron complexes of $^{15}N_4$-OEP including CO, octylisonitrile-complexes and so on. The axial ligand and solvent effects were studied for six-coordinated $^{15}N_4$-Co^{3+}(OEP).

EXPERIMENTAL

The ^{15}N label was incorporated into $OEPH_2$ during the Knorr syntheses of ethyl 3-acetyl-4-ethyl-2-methylpyrrole-5-carboxylated using $Na^{15}NO_2$ (97.3 atom %, MercK). The infrared spectra in CsI disk and the mass spectra confirmed that ^{15}N substitution of pyrrole nitrogen was completed. Details of the synthesis of $OEPH_2$, its Mg(II), Fe(III), Co(III), Ni(II), Zn(II), and Cd(II) chelates were descrived in literatures (9,10,11).

The reduction of Fe(III) complex was performed by an excess amount of $SnCl_2$ in pyridine ($Fe^{2+}(OEP)(Py)_2$, $Fe^{2+}(OEP)(C_8H_{17}NC)(Py)$, and $Fe^{2+}(OEP)(CO)(Py)$) or in γ-picoline($Fe^{2+}(OEP)(\gamma\text{-picoline})_2$) under a vaccum. After the reduction octylisonitrile or CO gas was added to $Fe^{2+}(OEP)(Py)_2$ inside the vaccum line. The Fe-complexes was kept in ferrous low spin state in a sealded tube.

The ^{15}N spectra were obtained at frequency of 10.09 MHz with a JEOL PFT-100 pulse fourier transform NMR spectrometer. The spectra were recorded with the mode of proton decoupled n.O.e. to reduce the effect of negative n.O.e. Spectra were spread over 5 KHz region with 8192 data points; the resolution due to digitalization was 1.22 Hz, i.e., 0.12 p.p.m. for ^{15}N. For the measurement of metal complexes 10 sec was taken as interval because of long relaxation times of ^{15}N nuclei (a pulse width of 20 μs; 50° flip angle). Sample tubes used were 10 mm in diameter with a 2mm coaxial tube containing $^{15}NH_4{}^{15}NO_3$ solution in C_2D_6SO, with provides reference standard and the external upfield in p.p.m. relative to external $^{15}NO_3^-$. The temperature of the probe at the room temperature condition was about 30°C. ^{13}C-NMR spectra were obtained in FT mode on a JEOL FX-100 spectrometer operating at 25,01 MHz. Chemical shift were read relative to the resonance of tetramethylsilane. ^1H-^{15}N heteronuclear INDOR was perfomed on a JEOL PFT-100 spectrometer equipped with a PA-1 amplifying unit and fitted with a matching network tuned for 10 MHz. The rf field was changed manually and spectra were monitored on the display unit of a EC-100 computer.

RESULTS

The ^{15}N-NMR spectra of $^{15}N_4$-Mg(OEP), $^{15}N_4$-Ni(OEP), $^{15}N_4$-Zn(OEP), and $^{15}N_4$-Cd(OEP) gave non-inverted signals (Fig. 1) and the shift values are collected in Table 1. Pyrrole nitrogen-central metal nuclear spin coupling was clearly observed for $^{15}N_4$-Cd(OEP) ($^1J(^{15}N$-^{111}Cd, or $^{113}Cd)$ =151.4 Hz)(Fig. 1). This is the first observation of direct ^{15}N-Cd coupling. More striking is the higher field shift of the ^{15}N resonance of $^{15}N_4$-Ni(OEP). Although it was difficult to obtain spectra with

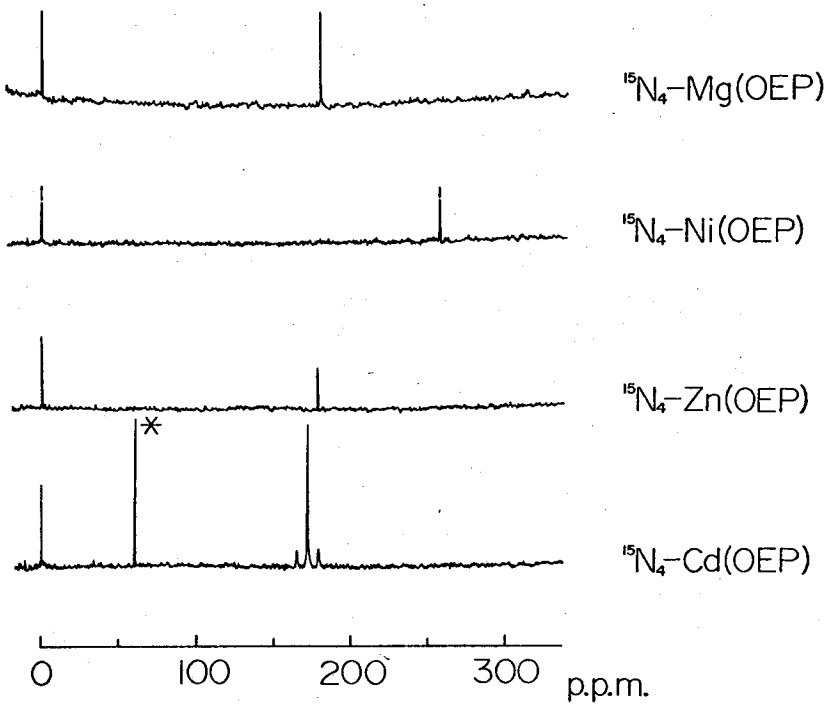

Fig. 1 ^{15}N-NMR spectra of metal complexes of ^{15}N-OEP. Solvents are given in Table 1. The concentrations of the solution are ranged in 0.02-0.06 M and spectra were accumulated 7000-10000 times with 10 sec intervals. Asterisk indicates the signal from pyridine.

Table 1. ^{15}N-Chemical Shifts of Metal Complexes of $^{15}N_4$-OEP

Compounds	Solvent	Chemical Shifts*
Mg(OEP)	$CDCl_3$ + Py**	179.9
Ni(OEP)	$CDCl_3$	257.0
Zn(OEP)	$CDCl_3$ + Py	179.2
Cd(OEP)	Py-d_5	173.1
Fe^{2+}(OEP)(Py)$_2$	Py-d_5	187.9
Fe^{2+}(OEP)(γ-picoline)$_2$	γ-picoline	185.5
Fe^{2+}(OEP)($C_8H_{17}NC$)(Py)	Py-d_5	210.6
Fe^{2+}(OEP)(CO)(Py)	Py-d_5	231.3
Co^{3+}(OEP)(Br)(Py)	CD_2Cl_2	259.4
Co^{3+}(OEP)(Br)(Py)	Py-d_5	260.0
Co^{3+}(OEP)(Br)(4-acetyl-Py)	4-acetyl-Py	262.5
Co^{3+}(OEP)(Br)(γ-picoline)	γ-picoline	260.3

*Shifts are relative to external $NH_4{}^{15}NO_3$ in DMSO-d_6 (p.p.m.).
**Py denotes pyridine.

high signal to noise ratio because of the long relaxation times of the non-protonated ^{15}N nuclei, the resonance positions were confirmed with INDOR by monitoring the methine proton resonances which were splitted by coupling to ^{15}N nuclei. The observed nitrogen chemical shifts of the metal complexes are 33-41 p.p.m. upfield from those of non-protonated nitrogens of $^{15}N_4$-OEPH_2 except $^{15}N_4$-Ni(OEP). The resonance position of $^{15}N_4$-Zn(OEP), 179.2 p.p.m. well corresponds to 175.2 p.p.m. of $^{15}N_4$-Zn(TPP) reported previously (4). It is also interesting to compare the nitrogen chemical shift of $^{15}N_4$-Mg(OEP) with those $^{15}N_4$-chlorophyll a (1), since the three nitrogens except the nitrogen of reduced ring in chlorophyll a are expected to resonate at the near frequency of $^{15}N_4$-Mg(OEP).

The ^{15}N resonance position of $^{15}N_4$-Mg(OEP) in $CDCl_3$ was the same as that of $^{15}N_4$-Mg(OEP) in $CDCl_3$ with pyridine (Py) within the experimental

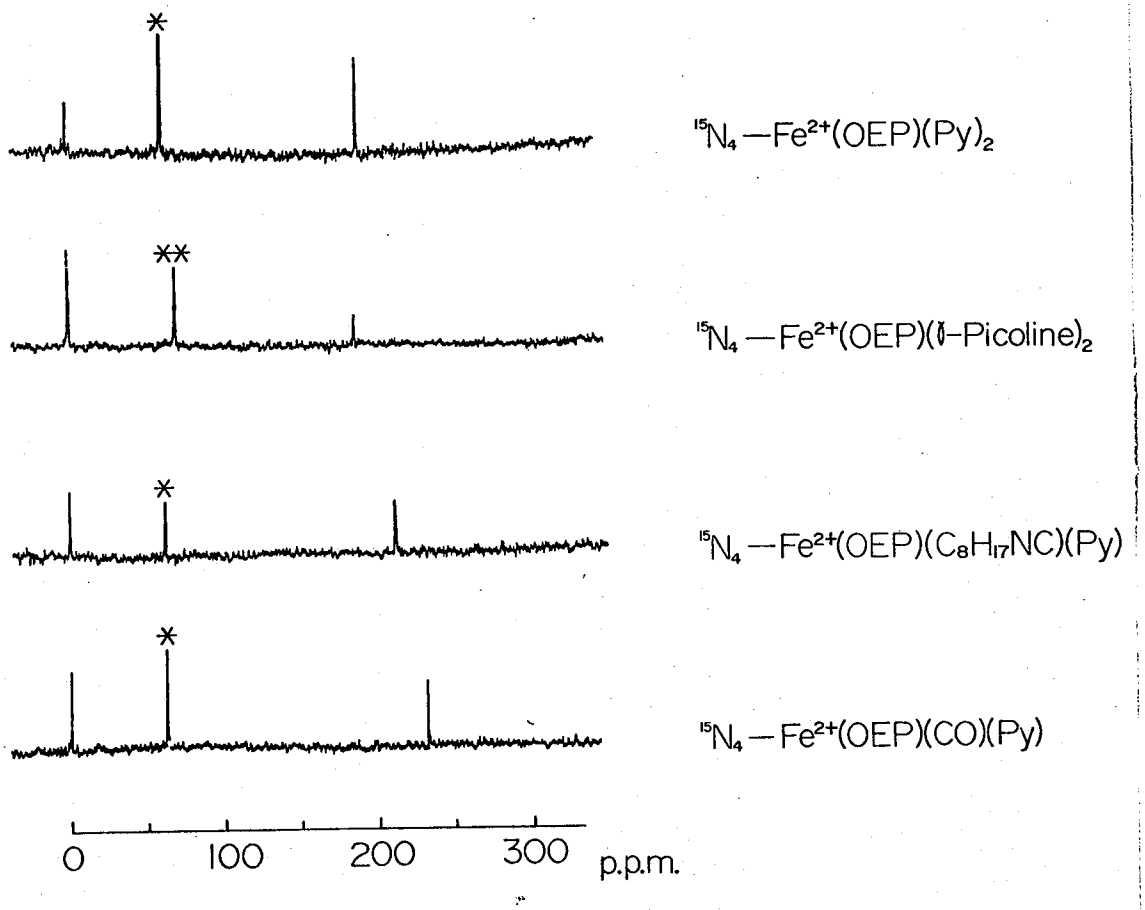

Fig. 2 ^{15}N-NMR spectra of ferrous iron complexes of $^{15}N_4$-OEP. Solvents are given in Table 1. The concentrations of the solution are ranged in 0.02-0.04 M and spectra were accumulated 3000-10000 times with 10 sec intervals. Asterisk and double asterisks indicate the signals from pyridine and γ-picoline, respectively.

error. The effect of ligation was not detected for Mg(OEP), however, when pyridine was added to $^{15}N_4$-Ni(OEP) in $CDCl_3$, the pronounced lower shift of ^{15}N signal with broading was observed (12). This phenomenon is due to the appearance of paramagnetic species which will be discussed in detail in the next Chapter. The ^{15}N-NMR spectra of $^{15}N_4$-Zn(OEP) and $^{15}N_4$-Cd(OEP) in $CDCl_3$ could not be obtained due to the highly dilute condition.

The ^{13}C chemical shifts of the above metallo-octaethylporphyrins are shown in Table 2. The anomaly of chemical shifts of $^{15}N_4$-Ni(OEP) was also observed for ^{13}C-NMR as in the case of ^{15}N-NMR i.e. the resonance positions of C_α- and C_β-carbons is inverted in Ni(OEP) compared with the other M(OEP).

Table 2. ^{13}C-Chemical Shifts of Metal Complexes of ^{15}N-OEP.

Compounds	Solvent	Chemical Shifts* C_α	C_β	methine	$-CH_2-$	$-CH_3$
Mg(OEP)	$CDCl_3$ + Py	147.6	142.4	98.0	20.1	19.0
$Fe^{2+}(OEP)(Py)_2$	Py	145.5[b]	145.0	97.5	20.2	19.0
Ni(OEP)	$CDCl_3$	140.3[b]	142.4	96.8	19.7	18.3
Zn(OEP)	$CDCl_3$ + Py	147.3	141.7	96.7	19.9	18.8
Cd(OEP)	$CDCl_3$ + Py	148.7	142.2	97.8	20.0	18.9

*Chemical shifts are relarive to TMS (p.p.m.). b; broad.

The ^{15}N-NMR spectra of the ferrous low spin derivatives of $^{15}N_4$-OEP are shown in Fig. 2. The ^{15}N resonance position were explicitly effected by the axial ligands. The ^{15}N chemical shifts of the CO and octhylisonitrile complexes of ferrous OEP in d_5-Py solution are 43 and 23 p.p.m. upfield from that of $Fe^{2+}(OEP)(Py)_2$ (Table 1). On the other hand, small down field shift was observed for $Fe^{2+}(OEP)(\gamma\text{-picoline})_2$.

Fig. 3 shows the ^{15}N-NMR spectra of $^{15}N_4$-$Co^{3+}(OEP)(Br)X$ (X=Py, γ-picoline, 4-acetyl-pyridine). The ^{15}N resonance signals of $Co^{3+}(OEP)(Br)(Py)$ appeared slightly broadened. The effect of substitution at the sixth ligand to the ^{15}N chemical shifts was very small.

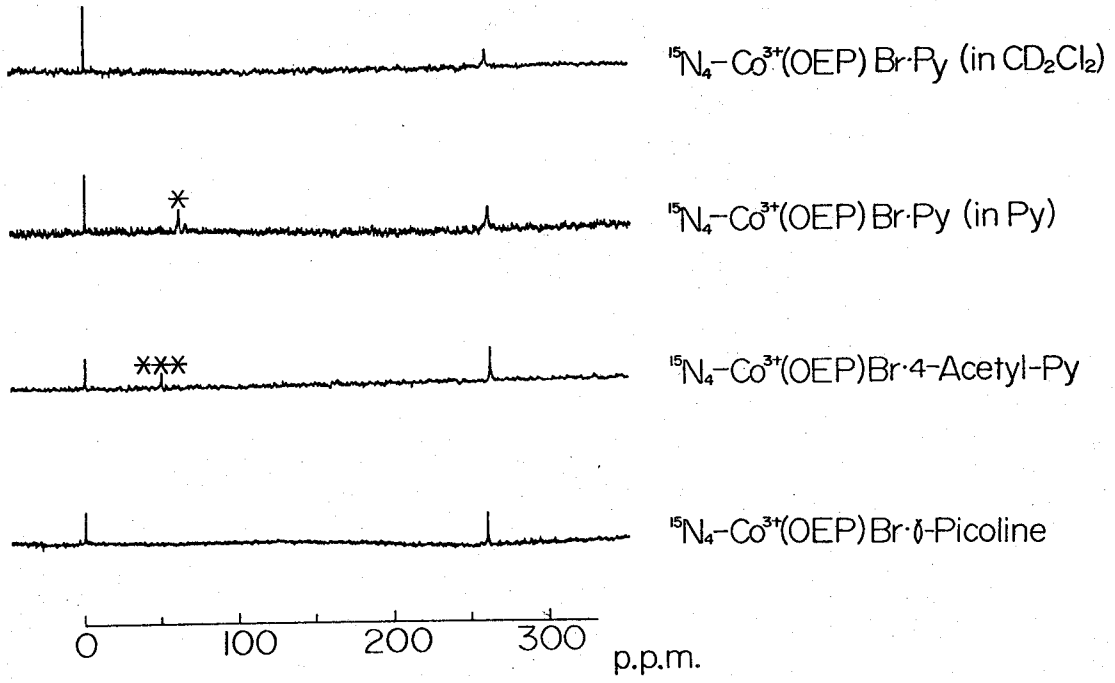

Fig. 3 ^{15}N-NMR spectra of cobalt complexes of $^{15}N_4$-OEP. Solvents are given in Table 1. The concentrations of the solution are ranged in 0.02-0.04 M and spectra were accumulated 3000-10000 times with 10 sec intervals. Asterisk and triple asterisks indicate the signals from pyridine and 4-acetyl -pyridine, respectively.

DISCUSSION

It is known that the resonance position of ^{14}N shifts to higher field by about 50 p.p.m. when free ammonia are complexed with a diamagnetic cobalt ion in $[Co(NH_3)_6]^{3+}$ (13). The reason is mainly attributed to the paramagnetic term σ_p in the shielding constant arised from magnetic mixing of excited states with the ground state (8,14). As is shown in Ramsey's formula (15), σ_p depends upon the values of excitation energy ΔEi, which are sometimes substituted by the longer-wavelength optical absorption maxima (8,14). The narrow distribution range of the ^{15}N chemical shifts of these metal complexes of OEP may be attributed to the similarities their positions of absorption maxima (16). Ni(OEP), however, gives a resonance at fairly higher field than the others. As the metal-^{15}N bond is stabilized, the value of ΔE seems to increase, absolute value of σ_p decreases and the ^{15}N resonance shifts to higher field. The large ΔE of Ni(OEP) is revealed as a little shorter wavelength absorptions manifested of Soret, α and β bands (Table 3)(17).

Table 3. Electronic Absorption Spectra of Metal Complexes of OEP (nm).

Compounds	Solvent	Soret	β-band	α-band
Mg(OEP)*	Benzene	411	546	582
Ni(OEP)*	Dioxan	391	516	551
Zn(OEP)*	Dioxan	407	536	572
Cd(OEP)*	Py	421	551	586
$Fe^{2+}(OEP)(Py)_2$	Py	408	517	547
$Fe^{2+}(OEP)(C_8H_{17}NC)(Py)$	Py	417	521	549
$Fe^{2+}(OEP)(CO)(Py)$	Py	408	528	558
$Co^{3+}(OEP)(Br)(Py)$*	Benzene	427	537	568

*Ref. 16.

The evidence of strong Ni-N bond is also manifested in the fairly higher

Ni-N stretching vibration frequency than those of other metal complexes. These facts well correspond to the high field shift of ^{15}N resonance of Ni(OEP).

To confirm the effect of strong Ni-N bonding, ^{13}C resonances were observed for the above metal complexes. As shown in Table 2 the resonance of the C_α carbon of Ni(OEP) is remarkably high compared with those of the other complexes. It has become clear that the effect of Ni-N bonding is still seen in the chemical shift of the second nearest nuclei.

Although the absorption maxima of ferrous iron complexes are close to those of Ni(OEP)(Table 3), their ^{15}N chemical shifts are 26-70 p.p.m. downfield from that of $^{15}N_4$-Ni(OEP). In the case of iron complexes the ^{15}N chemical shifts strongly depend on the nature of the bonding between iron and axial ligands. The iron complexes studied here are all ferrous low spin state. Kitagawa et al. suggested from the measurement of Raman spectra there are two kinds of ferrous low spin states in hemoproteins and they are specified by the binding nature of the sixth ligand to heme iron. The iron-axial ligand bond in HbNO and HbC_2H_5NC as well as in HbCO and HbO_2 is of π type while that in ferrous cytochromes b_5 and c is of σ type (19). The present result clearly shows that the nature of iron-axial ligand bond of $Fe^{2+}(OEP)(C_8H_{17}NC)(Py)$ and $Fe^{2+}(OEP)(CO)(Py)$ is in π type and different from the σ type of $Fe^{2+}(OEP)(Py)_2$ and $Fe^{2+}(OEP)(\gamma\text{-picoline})_2$ as in the case of hemoproteins. Probably a numalator part of σ_p is responsible for the difference of ^{15}N chemical shifts among $^{15}N_4$-$Fe^{2+}(OEP)(CO)(Py)$, $^{15}N_4$-$Fe^{2+}(OEP)(C_8H_{17}NC)(Py)$, and $^{15}N_4$-$Fe^{2+}(OEP)(Py)_2$. In $^{15}N_4$-$Fe^{2+}(OEP)(CO)(Py)$, it can be expected that π type interaction among the lowest empty π orbital of CO, the d_π orbital of Fe and the $\pi^*(e_g)$ orbital of porphyrin ring from the symmetry consideration (19). Therefore the electrons in the d_π(Fe) -π^*(porphyrin) orbital are delocalized from the Fe-OEP system to the axial ligand bond, when CO binds to Fe as an axial ligand. As is shown in the Ramsey's formula, σ_p depends on the ΔE_{ij} and c_i^2. If ΔE_{ij} do not differ from each compound, σ_p is affected by the magnitude of c_i^2. This condition may be applicable to the cases of CO, $C_8H_{17}NC$, Py and γ-picoline complex where the positions of absorption maxima are not so

different from each other. The decrease of C_i^2 means the decrease of the absolute value of σ_p and causes the upfield shift as the sign of σ_p is positive. The prediction is consistent with the observed result that the ^{15}N resonance of $Fe^{2+}(OEP)(CO)(Py)$ is in upperfield than that of $Fe^{2+}(OEP)(Py)_2$.

There are no or quite small differences among the ^{15}N resonance positions of $^{15}N_4$-$Co^{3+}(OEP)(Br)X$ complexes(Table 1). Also the resonance frequency of $^{15}N_4$-$Fe^{2+}(OEP)(Py)_2$ is almost the same to that of $^{15}N_4$-$Fe^{2+}(OEP)(\gamma\text{-picoline})_2$. The basicity of these axial ligands differ from each other. However such difference seems to give rise no influence to the chemical shift of the $^{15}NH_3$ nuclei in the porphyrin ring. The change of the basicity in the axial ligands may give only second order perturbation to the ^{15}N chemical shift of the porphyrin ring compared with the change in the nature of the metal-ligand bond. In the $Co(^{15}NH_3)_5Y$ complexes, the effect of ligand substitution is remarkable at the resonance of the $^{15}N_3$ group at the trans position, but not at cis position (8). The axial ligand locates at the cis position of the porphyrin nitrogen atoms.

The resonance positions of $Co^{3+}(OEP)(Br)X$ are in higher field than those of other metal complexes of $^{15}N_4$-OEP. However, at the present stage, it is hard to determine whether the origin of the upfield shift is due to the nature of the ^{15}N-Co^{3+} bonding or to the Co^{3+}-Br bonding, since there are no data of $^{15}N_4$-$Co^{3+}(OEP)$ itself or other $^{15}N_4$-$Co^{3+}(OEP)XY$ complexes. More detailed study is currently in progress for $Co^{3+}(OEP)CH_3$ or $Co^{3+}(OEP)C_6H_6$. The Co-axial ligand bond of these complexes has covalent character. It will be expected that serious modification of the bond character have strongly influence on the ^{15}N chemical shift.

REFERENCE

1. Boxer, S. G., Closs, G. L., and Katz, J. J. (1974) J. Am. Chem. Soc. 96, 7058.
2. Irving, C. S. and Lapidot, A. (1977) J. Chem. Soc. Chem. Comm. 184.
3. Kawano, K., Ozaki, Y., Kyogoku, Y., Ogoshi, H., Sugimoto, H., and Yoshida, Z. (1977) J. Chem. Soc. Chem. Comm. 226.
4. Gust, D. and Roberts, J. D. (1977) J. Am. Chem. Soc. 99, 3637.
5. Yeh, H. J. C., Sato, M., and Morishima, I. (1977) J. Magnetic Resonance, 26, 365.
6. Kawano, K., Ozaki, Y., Kyogoku, Y., Ogoshi, H., Sugimoto, H., and Yoshida, Z. (1978) J. Chem. Soc. Perkin II, in press.
7. Ozaki, Y., Kyogoku, Y., Ogoshi, H., Sugimoto, H., and Yoshida, Z. to be published.
8. Nakashima, Y., Muto, M., Takagi, I., and Kawano, K. (1975) Chem. Letters 1075.
9. Inhoffen, H. H., Fuhrhop, J. H., Voigt, H., and Brockmann, Jr. H. (1966) Justus Liebigs Ann. Chem. 695, 133.
10. Ogoshi, H., Watanabe, E., Yoshida, Z., Kincaid, J., and Nakamoto, K. (1973) J. Am. Chem. Soc. 95, 2845.
11. Ogoshi, H., Watanabe, E., and Yoshida, Z. (1976) Bull. Chem. Soc. Japan 49, 2529.
12. Ozaki, Y., Kyogoku, Y., Yoshikawa, K., Ogoshi, H., Sugimoto, H., and Yoshida, Z. to be published.
13. Badger, G., Harris, R., Jones, R., and Sasse, J., (1962) J. Chem. Soc. 4329.
14. Hervison-Evans, D. and Richards, R. E. (1964) Mol. Phys. 8, 19.
15. Ramsey, N. F. (1950) Phys. Rev. 78, 699.
16. Smith, K. M. ed. (1975) "Porphyrins and metalloporphyrins" p 884, Elsevier, Amsterdam.
17. Ogoshi, H., Masai, N., Yoshida, Z., Takemoto, J., and Nakamoto, K. (1971) Bull. Chem. Soc. Japan 44, 49.
18. Ogoshi, H., Saito, Y., and Nakamoto, K. (1972) J. Chem. Phys. 57, 4194.
19. Kitagawa, T., Iizuka, T., Saito, M., and Kyogoku, Y., (1975) Chem. Lett. 849.

Chapter 2.

Nitrogen-15 Nuclear Magnetic Resonance Study of Paramagnetic Species of Nickel-octaethylporphyrin.

ABSTRACT

^{1}H-NMR, ^{13}C-NMR, and ^{15}N-NMR were measured for ^{15}N-enriched nickel-octaethylporphyrin ($^{15}N_4$-Ni(OEP)) in nitrogenous base-chloroform mixed solution. The NMR studies succeeded in detecting a trace amount of molecular species of Ni(OEP) which was not found by electronic absorption and resonance Raman spectra. In $CDCl_3$ solution $^{15}N_4$-Ni(OEP) exhibited sharp nitrogen-15 resonance, however, in pyridine-$CDCl_3$ mixed solution the resonance signal of the pyrrole nitrogens showed marked shifts to lower field as well as greater broadening of resonance. These shift and broadening can be explained by assuming the presence of paramagnetic species which was formed as a consequence of the addition of two axial ligands. N-butyl amine was found to be more effective than pyridine for causing the paramagnetic shift and broadening. Although the similar paramagnetic effects were also observed in ^{1}H-NMR and ^{13}C -NMR, it was shown in the present study that ^{15}N-NMR was more sensitive and useful tool than the others for the detection of the paramagnetic species.

INTRODUCTION

The effects of peripheral substituents, axial ligands and solvents upon properties and reactivities of metallo-porphyrins have been extensively studied in the recent years. These studies provide further evidences for the evaluation of structure-function relationships of hemoproteins. McLees and Caughey reported the striking effects by substituent and ligand binding to the structure of nickel-deuteroporphyrins (1). On the basis of absorption spectra and magnetic susceptibility they showed that nickel-porphyrins consisted of two species in the presence of nitrogenous base. One species was considered to be a diamagnetic square-planar complex which has no axial ligand and the other species a tetragonally distorted octahedral complex which was

paramagnetic one. The relative concentrations of the two species varied markedly with changes in the porphyrin structure. Kitagawa and Inano investigated the absorption and resonance Raman spectra of nickel-octaethylporphyrin [Ni(OEP)], however, no clear difference was observed between the spectrum of Ni(OEP) in chloroform solution and that in pyridine solution (2). Therefore it was suggested that if there were another molecular species in the Ni(OEP) solutions containing nitrogenous bases, their concentrations would be very small. In the present study it was attempted to detect the paramagnetic species and to elucidate their structure and properties by the use of NMR spectroscopy.

NMR is widely used to investigated paramagnetic molecules, especially it has become a powerful and promising new research tool in the study of hemoproteins which has natural paramagnetic center (3). Since the observed paramagnetic shifts were ascribed to a combination of the contact term and the dipolar term, the origin of these effects was examined by the use of model iron-porphyrins. It was interesting to compare the present results on Ni(OEP) with those on iron-porphyrins.

EXPERIMENTAL

The ^{15}N atoms were incorporated into $OEPH_2$ during the Knorr synthesis of ethyl 3-acetyl-4-methylpyrrole-5-carboxylate using $Na^{15}NO_2$ (97.3 atom %) purchased from Merck. $^{15}N_4$-Ni(OEP) was obtained by the method employed for the synthesis of $^{14}N_4$-Ni(OEP) (4). The ^{15}N substitution of pyrrole nitrogen was confirmed by the measurement of infrared and mass spectra. The ^{15}N spectra were recorded on a JEOL PFT-100 pulse Fourier transform NMR spectrometer operating at 10.09 MHz. The spectra were obtained with the mode of proton decoupled without n.O.e. to reduce the diminishing of intensity by negative n.O.e. Spectra ranged over 5 KHz with 8192 data poins. The resolution due to digitalization was 1.22 Hz, i.e., 0.12 p.p.m. for ^{15}N. Pulse -free induction decay curves repeated 1-2 sec (50° flip angle, 20μs) were Fourier transformed after 100 times accumulations in the time domain. For the measurement of Ni(OEP) in the absence of nitrogenous base 10 sec was taken as interval because of long relaxation time of

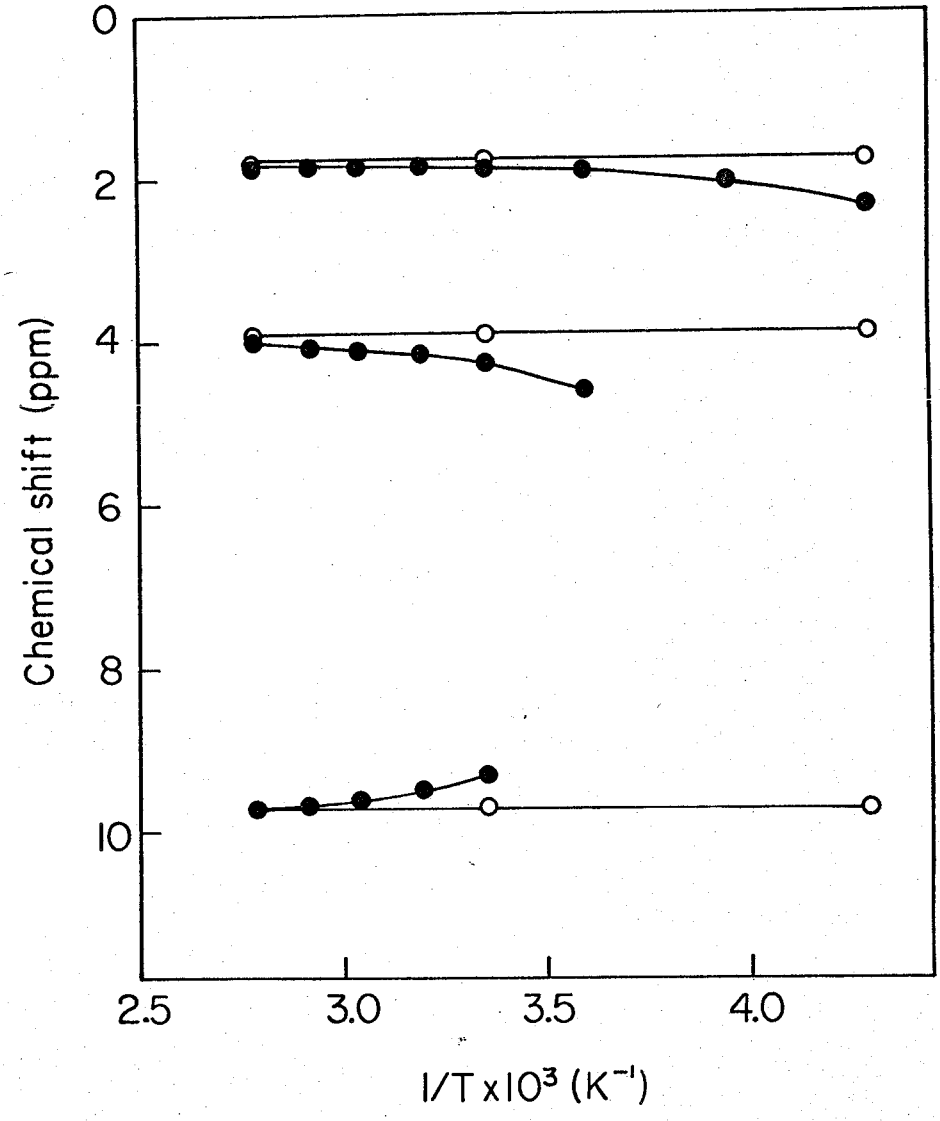

Fig. 1 Temperature dependence of the ^1H chemical shifts of Ni(OEP). (o ; in $CDCl_3$ solution, ● ; in C_5D_5N solution)

proton free ^{15}N nuclei. Sample tubes used were 10 mm in diameter with a 2 mm coaxial tube containing $^{15}NH_4{}^{15}NO_3$ solution in C_2D_6SO, which provides reference standard. Chemical shifs were measured in p.p.m. relative to external $^{15}NO_3^-$. The temperature of the probe at the room temperature condition was about 30°C. ^1H-NMR and ^{13}C-NMR spectra were obtained in FT mode on a JEOL FX-100 spectrometer operating at 99.6 and 25.01 MHz, respectively. Chemical shift were read relative to the resonance of tetramethylsilane (TMS) in both cases.

RESULTS

Fig. 1 shows the temperature dependences of the ^1H chemical shifts of Ni(OEP) in chloroform ($CDCl_3$) and pyridine-d_5 (C_5D_5N) solution. The signals observed near 2 and 4 p.p.m. were easily assignable to the methyl and methylene protons of ethyl groups, respectively, since the former was triplet and the latter quintet. The signal of the methine -bridge protons was located near 10 p.p.m. The ^1H-NMR spectrum of Ni(OEP) in C_5D_5N solution was similar to that in $CDCl_3$ solution at 80°C, however, as the temperature was lowered all the signals showed the definate shifts with broadening. The signal of methine-bridge protons could not be observed due to broadening below room temperatures.

The effect of pyridine concentration on the ^{13}C chemical shifts of Ni(OEP) are shown in Fig. 2. The assignments of ^{13}C signals were described in Chapter 1. The signals due to C_α and C_β carbons of pyrrole rings were located near those of C_5D_5N, therefore as the pyridine concentration was increased the observation of the signals became difficult.

Fig. 3 shows the temperature dependences of ^{13}C chemical shifts of Ni(OEP) in $CDCl_3$-C_5D_5N mixed solution ($CDCl_3$; 1.00 ml, C_5D_5N; 0.67 ml). As the temperature was lowered all the signals shifted markedly to the lower field.

The ^{15}N-NMR spectrum of $^{15}N_4$-Ni(OEP) in $CDCl_3$ solution gave a single sharp signal at 257.0 p.p.m. as shown in Fig. 4(1) As the pyridine concentration was increased the signal shifted to the lower

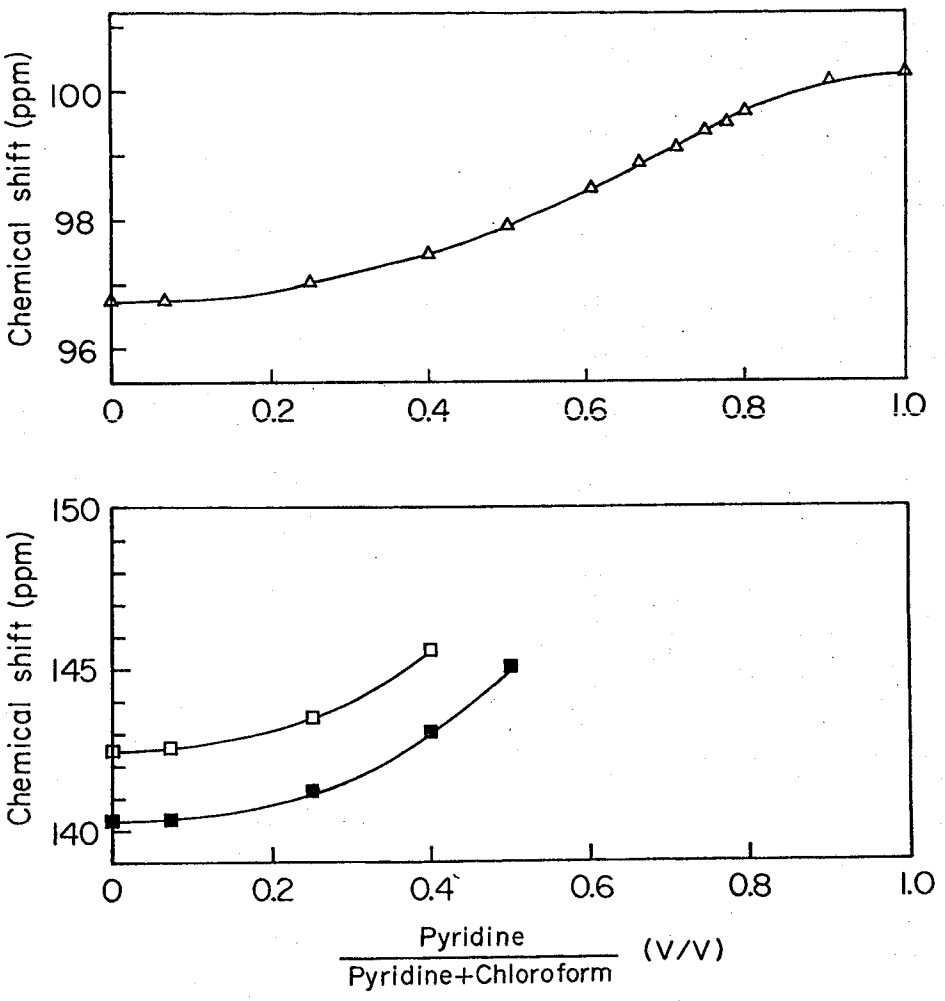

Fig. 2 Effect of pyridine concentration on the ^{13}C chemical shifts of Ni(OEP) (Δ ; methine-bridge carbon, ■; C_α-carbon, □; C_β-carbon)

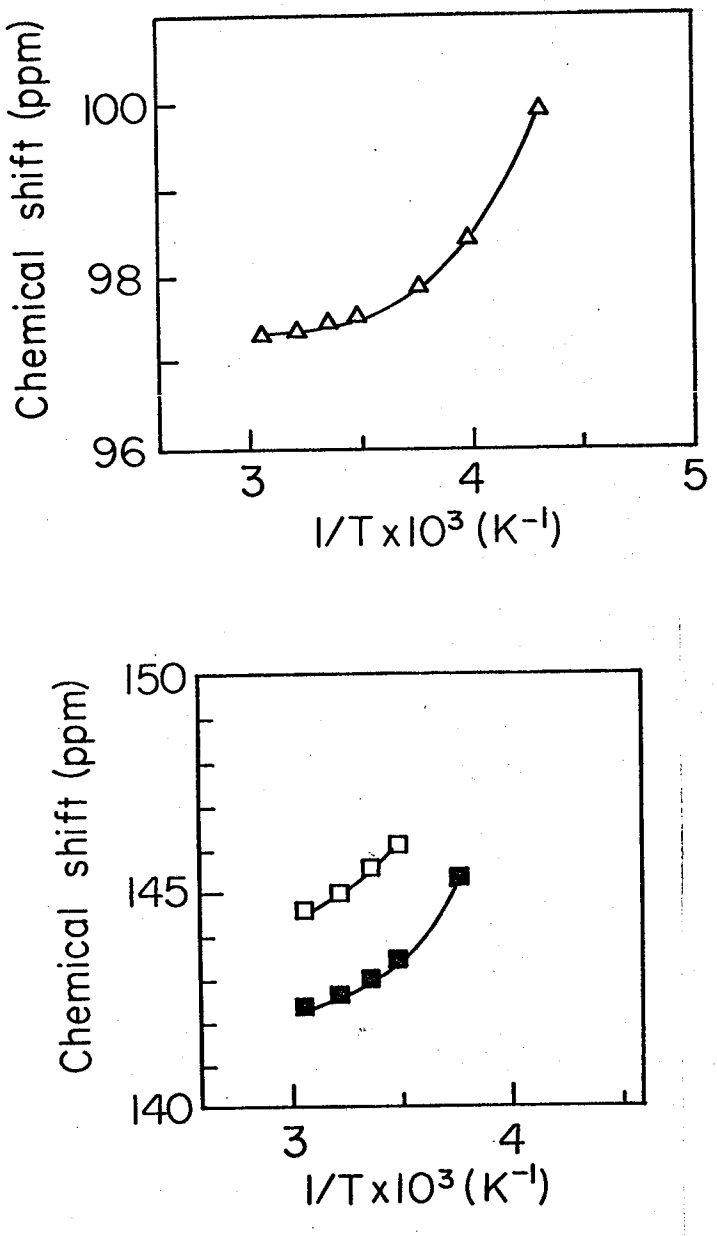

Fig. 3 Temperature dependence of ^{13}C chemical shifts of Ni(OEP) in $CDCl_3$-C_5D_5N mixed-solution. ($CDCl_3$ 1.00 ml, C_5D_5N 0.67 ml) (Δ ; methine-bridge carbon, ■ ; C_α-carbon, □ ; C_β-carbon)

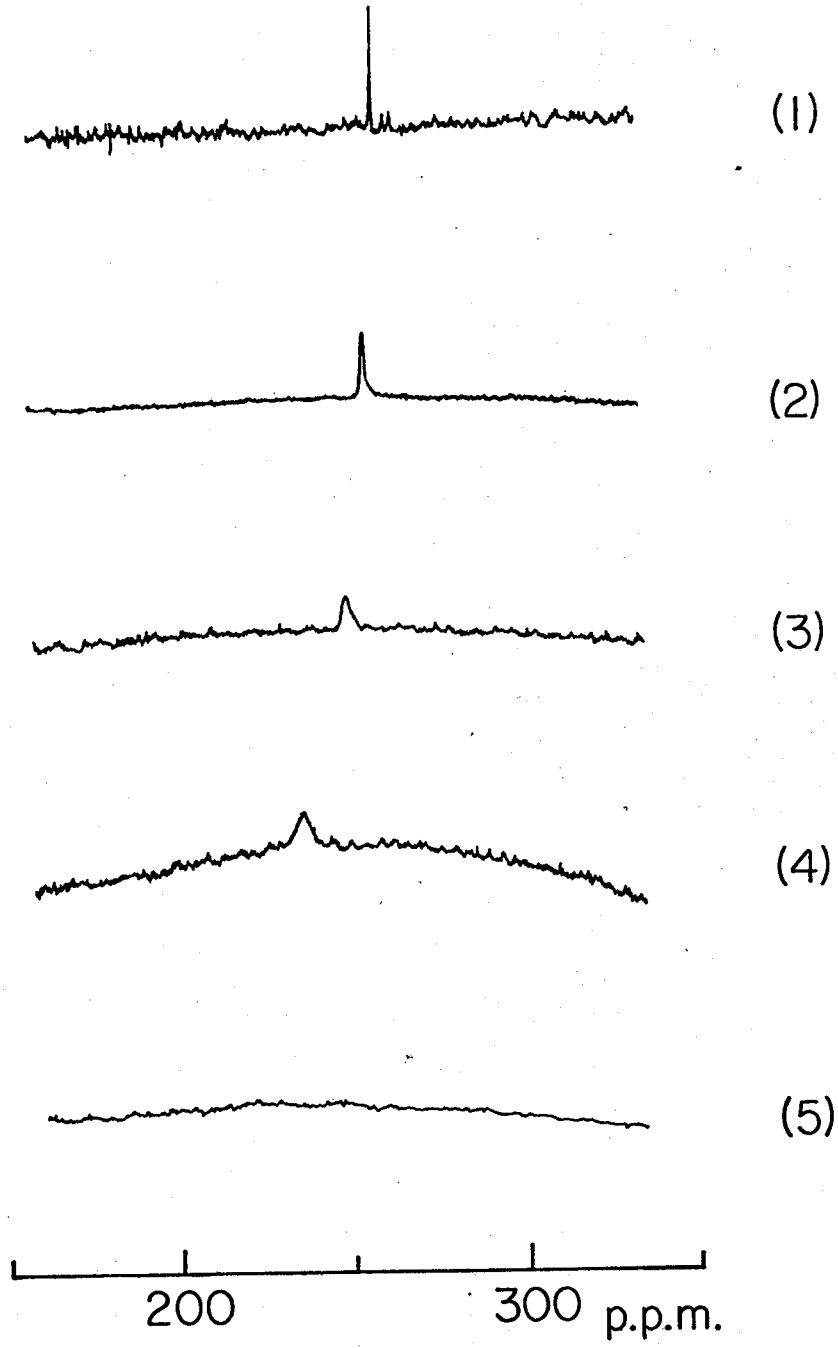

Fig. 4 Effect of concentration of nitrogenous bases to the ^{15}N-chemical shift of $^{15}N_4$-Ni(OEP)
(1) in $CDCl_3$ solution.
(2) in $CDCl_3$-C_5D_5N mixed solution($CDCl_3$ 1.5ml, C_5D_5N 0.07ml)
(3) in $CDCl_3$-C_5D_5N mixed solution($CDCl_3$ 1.5ml, C_5D_5N 0.16ml)
(4) in $CDCl_3$-C_5D_5N mixed solution($CDCl_3$ 1.5ml, C_5D_5N 0.3 ml)
(5) in $CDCl_3$-C_5D_5N mixed solution($CDCl_3$ 1.5ml, C_5D_5N 0.4 ml)

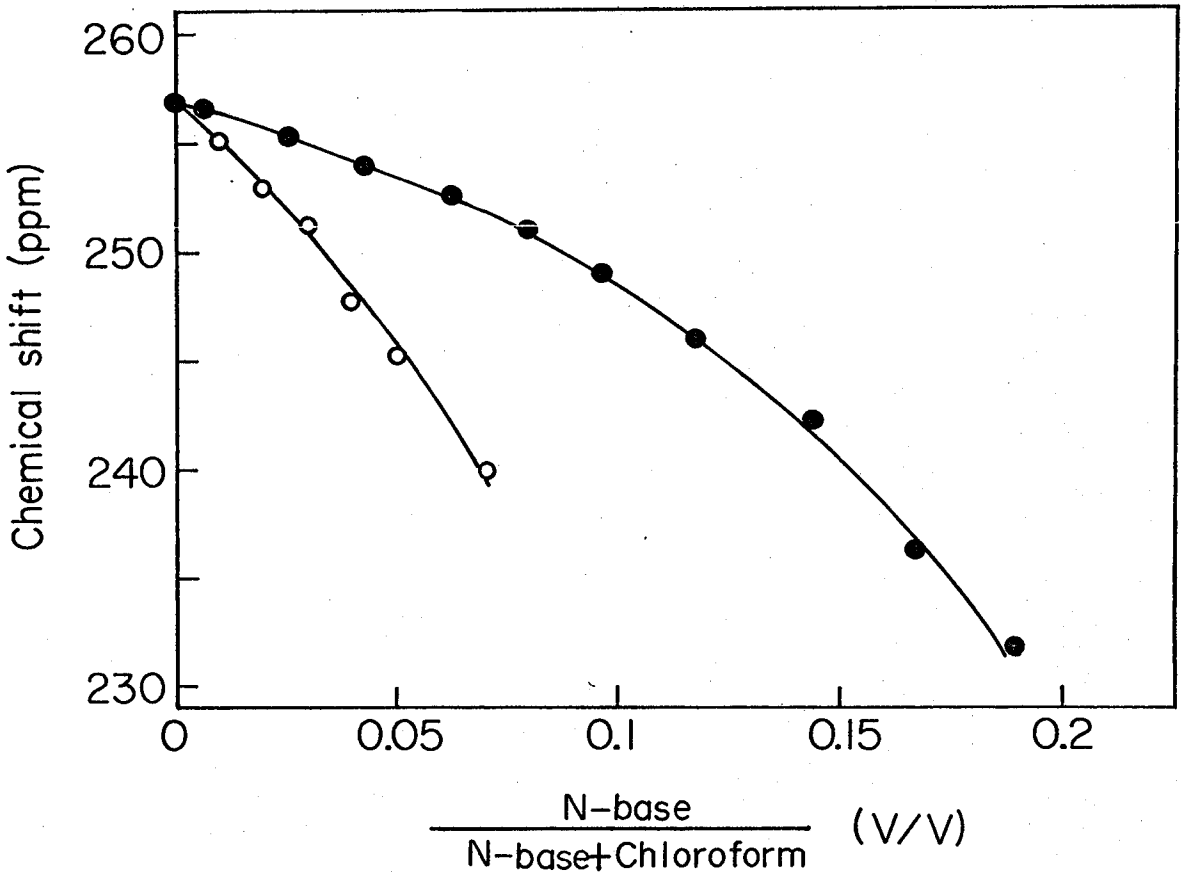

Fig. 5 Effect of concentration of nitrogenous bases to the ^{15}N -chemical shift of $^{15}N_4$-Ni(OEP).

(● ; in $CDCl_3$-C_5D_5N mixed solution, o ; in $CDCl_3$-n-$C_4H_9NH_2$ mixed solution)

field with greater broadening. The solutions in Fig. 4(2)-(5) contained 1.5 ml $CDCl_3$ plus 0.07, 0.16, 0.3, and 0.4 ml C_5D_5N, respectively. The ^{15}N signal exhibited ca. 20 p.p.m. lower field shift in Fig. 4(4) and the remarkable broadening prevented the observation of ^{15}N signal in Fig. 4(5).

Fig. 5 shows the effect of concentration of nitrogenous bases on the ^{15}N chemical shift. It was demonstrated that n-butyl amine ($n\text{-}C_4H_9NH_2$) was more effective than pyridine for causing the shift and broadening.

The temperature dependence of ^{15}N-NMR spectrum of $^{15}N_4$-Ni(OEP) in $CDCl_3$-C_5D_5N mixed solution ($CDCl_3$; 1.5 ml, C_5D_5N; 0.1 ml) are showed in Figs. 6 and 7. Between around 50°C and -40°C the spectra exhibited no large shift though the signal became broader at low temperatures. A steep shift was found below -40°C. However, it was noted that the resonance position of ^{15}N signal at -56°C was quite close to that in pure $CDCl_3$ solution.

DISCUSSION

The effect of substituents at the porphyrin side chains to the equilibrium of molecular species was indicated by McLees and Caughey; the equilibrium favored paramagnetic species when the 2,4-substituents were the more electron withdrawing (i.e. the less basic the porphyrins) (1). Therefore it is readily presumed that the formation of large amount of paramagnetic species is not favored for Ni(OEP). Actually it was difficult to detect the difference between the electronic absorption and resonance Raman spectra of Ni(OEP) in $CDCl_3$ solution and those in C_5D_5N solution, and only a small difference was detected between the spectra of $CDCl_3$ and $n\text{-}C_4H_9NH_2$ solutions (2).

However, the ^1H-NMR spectrum of Ni(OEP) in C_5D_5N solution was distinct from that in $CDCl_3$ at the room temperature as shown in Fig. 1, the signals showed the definite shifts as well as broadening. The similar results were obtained in ^{13}C- and ^{15}N-NMR as stated above. The temperature dependence of the absorption spectra of Ni(OEP) in $n\text{-}C_4H_9NH_2$ solution implied that Ni(OEP) formed the paramagnetic species resulted from the addition of two axial $n\text{-}C_4H_9NH_2$ ligands to a planar

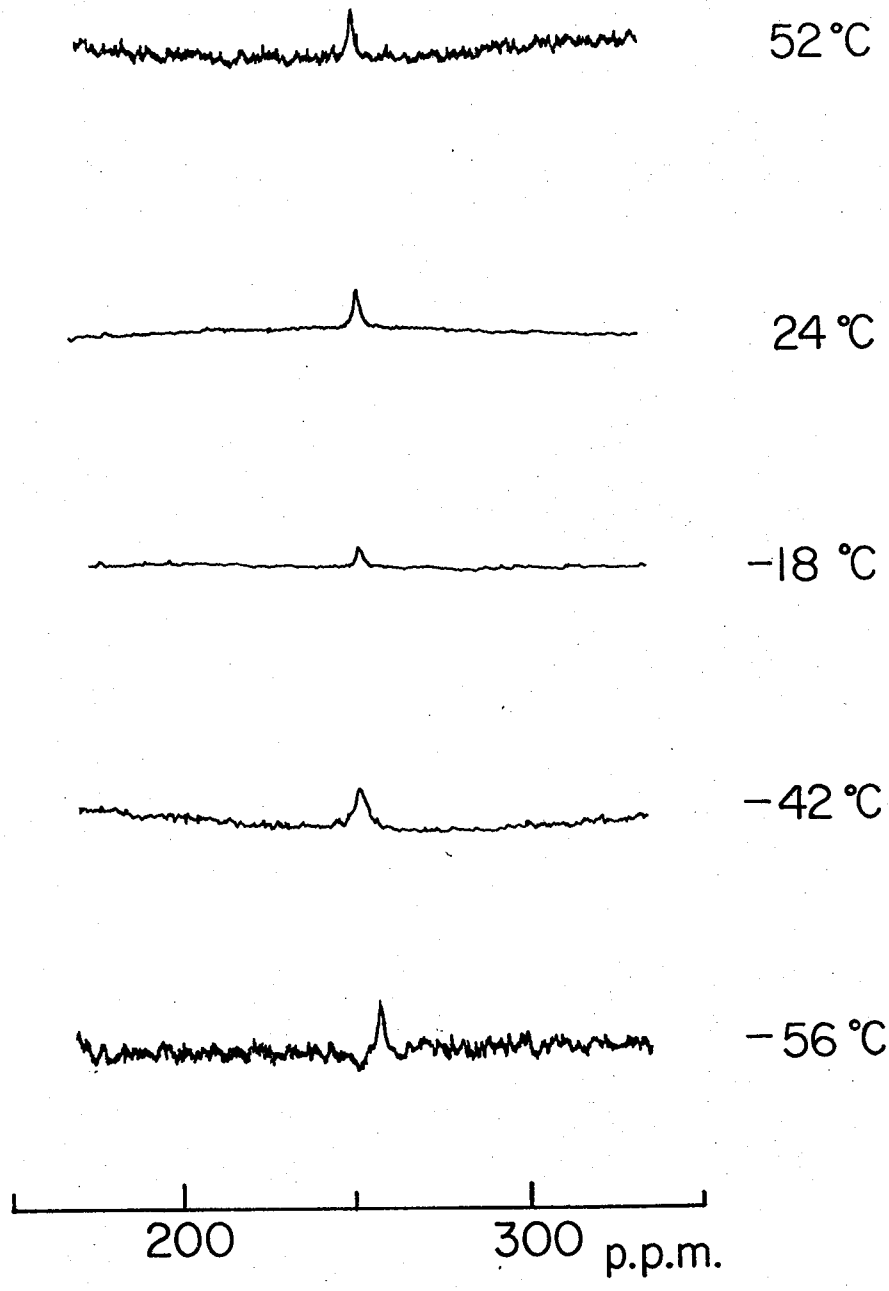

Fig. 6 ^{15}N-NMR spectra of $^{15}N_4$-Ni(OEP) at various temperatures in $CDCl_3$-C_5D_5N mixed solution. ($CDCl_3$ 1.5ml, C_5D_5N 0.1ml)

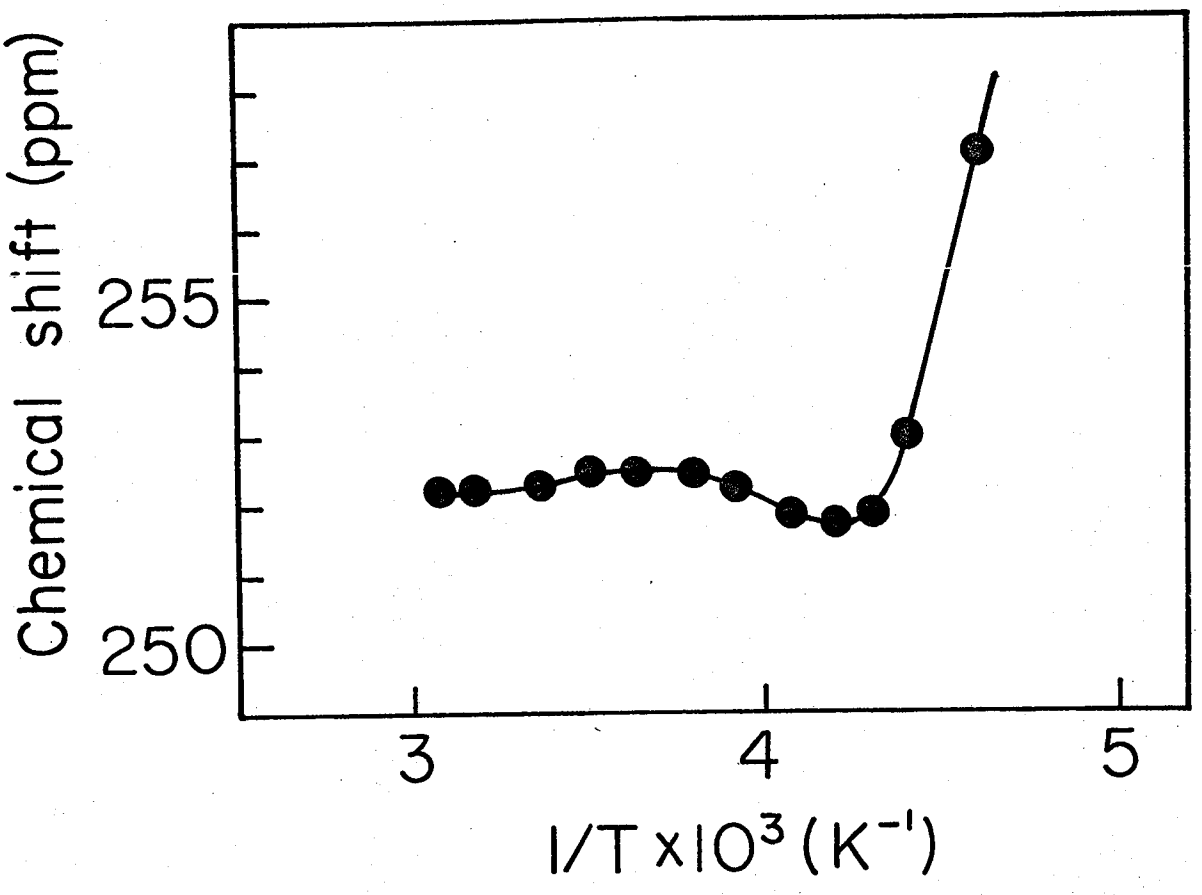

Fig. 7 Temperature dependence of ^{15}N resonances of $^{15}N_4$-Ni(OEP) in $CDCl_3$-C_5D_5N mixed solution. ($CDCl_3$ 1.5 ml, C_5D_5N 0.1 ml)

diamagnetic species (2). Therefore the results of Fig. 5 could be interpreted by assuming that Ni(OEP) even in $CDCl_3$-C_5D_5N solution also formed the paramagnetic species although the equilibrium favored extremely the diamagnetic species. It could be readily concluded that the shifts and broadening observed in ^1H-, ^{13}C-, and ^{15}N-NMR were due to the paramagnetic effects.

It was known that the paramagnetic shifts in resonance frequencies of Ni complexes were caused mainly by the contact interaction which was related to the electron spin density on the nuclei (4,5). The results of ^1H-NMR of Ni(OEP) could be compared with those of iron-porphyrins, where large pseudocontact shifts were expected. The contact shifts were estimated for ^1H-NMR of a few iron-porphyrins after subtracting the contribution from pseudocontact shifts (3). The ^1H signals of methyl group protons of iron-protoporphyrin, -deuteroporphyrin, and -mesoporphyrin showed large downfield contact shift, and the results were consistent with those of Ni(OEP). However, the ^1H signal of methine-bridge protons of Ni(OEP) exhibited the upfield contact shift, while those of iron-porphyrins were small downfield shifts. This discrepancy may be due to the difference in the nature of the molecular orbitals of Fe(OEP) and Ni(OEP).

The steep shift of ^{15}N resonances shown in Fig. 7 was rather puzzling. It had been expected from the results of Fig. 5 that as the temperature was lowered the signal shifted to the lower field monotonously. Probably the ^{15}N-signal at -56°C with slightly sharpening came from the diamagnetic species of Ni(OEP), since the resonance position was quite close to that in pure $CDCl_3$ solution. At such low temperature as -56°C the ligand exchange between the paramagnetic and diamagnetic species became slow enough to the appearance of separate signals, but the ^{15}N-signal due to the paramagnetic one was concealed owing to the extreme broadening. Small upfield bias of the ^{15}N shift at -50°C was presumably caused by the exchange broadening.

The present study demonstrated the sensitivity of ^{15}N-NMR in the investigation of paramagnetic species of porphyrins. The electronic absorption and resonance Raman spectra couldn't detect the paramagnetic species even in pure C_5H_5N solution nevertheless the species could be found easily by the use of ^{15}N-NMR in $CDCl_3$-C_5D_5N mixed solution

which included only 0.07 ml C_5D_5N for 1.5 ml $CDCl_3$. Compared with ^{13}C-NMR, ^{15}N-NMR was found to be more sensitive and useful. The fact that ^{13}C signals exhibited at most ca. 1 p.p.m. downfield shifts in the same process of Fig. 4(1)-(4) manifested the advantage of ^{15}N-NMR in detecting the paramagnetic effects.

REFERENCES

1. McLees, B. D. and Caughey, W. S. (1968) Biochemistry 7, 642.
2. Kitagawa, T. and Inano, M. to be published.
3. LaMar, G. N., Horrocks, Jr. W. D., and Holm, R. H. (1973) "NMR of Paramagnetic Molecules" p 435 Academic Press, New York.
4. Fitzgerald, R. J. and Drago, R. S. (1967) J. Am. Chem. Soc. 89, 2879.
5. Yonezawa, T., Morishima, I., and Ohmori, Y. (1970) J. Am. Chem. Soc. 92, 1267; Morishima, I., Okada, K., and Yonezawa, T. (1971) J. Chem. Soc. Chem. Comm. 33; Morishima, I., Okada, K., Yonezawa, T., and Goto, K (1971) J. Am. Chem. Soc. 93, 3922.

CONCLUSION

In this thesis, the author aimed to elucidate the nature of metal -ligand binding of hemoproteins and their model compounds by using resonance Raman spectroscopy and ^{15}N-NMR spectroscopy.

The following conclusions were drawn in this thesis.

The resonance Raman spectra were observed for the cytochrome P-450, their catalitically inactive form (P-420) and their heme-CO complex (P-450·CO and P-420·CO) in Chapter 1. The Raman spectra of reduced P-450 were unusual in a sense that the "oxidation-state marker" appeared at an unexpectedly lower frequency in comparison with those of other reduced hemoproteins. This anomaly in the Raman spectra of reduced P-450 demonstrated large delocalization of electrons to the porphyrin $\pi^*(e_g)$ orbital and accordingly the strong π basicity of the fifth ligand. The frequency of Band IV of P-450·CO was also markedly lower than those of HbCO and MbCO, indicating that the strong basicity of the fifth ligand was still causing the larger delocalization of electrons to the porphyrin $\pi^*(e_g)$ orbital of the heme-CO complexes of PB P-450 and PB P-448. The characteristic features observed for reduced P-450 and P-450·CO disappeared upon the conversion to P-420 and P-420·CO, respectively. This facts suggested that a status change or a replacement of the fifth ligand occurred and the $d_\pi(Fe^{2+})$-$p_y(S^-)$ -$\pi^*(e_g$, porphyrin) interactions would disappear upon the conversion. The two types of P-450 were also distinguished definitly in the reduced state, that is, the Band IV of reduced P-450 appears at 1341-1342 cm^{-1} or 1346-1348 cm^{-1} in accordance with whether its oxidized form takes low spin or high spin state. This indicated a significant difference in that π basicity of the fifth ligand between the two types of reduced P-450. It was notable that the Raman spectra of reduced $P\text{-}450_{cam}$·Mp and $P\text{-}450_{cam}$·Py complexes were closely similar to that of ferrous cytochrome b_5, in which two axial ligands are bound to the heme iron through the σ type interaction. The reduced PB P-420 converted from reduced PB P-450 by the laser illumination gave the two sets of Raman lines. This fact strongly suggested coexistence of two molecular species in the reduced PB P-420. Oxidized PB P-450 exhibited the Raman spectrum of typical

ferric low spin type while those of oxidized P-450$_{cam}$, PB P-450, and MC P-448 were of ferric high spin type. The frequencies of Band IV of oxidized P-450 exhibited no more such an anomaly as was pointed out for its reduced state, however, the similarity in the Raman spectra of PB P-450 and $MbSCH_3$ supported the coordination of RS^- to the heme iron in oxidized PB P-450, being a less conclusive evidence though. The Fe^{3+}-S^- interaction is not so strong in the oxidized state. The structure of ferric high spin hemes in the oxidized P-450$_{cam}$, PB P-448, and MC P-448 was deduced to suffer the protein control little.

In Chapter 2 the acid-base transition of ferric myoglobin (Mb) was studied by the resonance Raman spectroscopy. It was elucidated directly that two distinct molecular species of ferric Mb exist in the alkaline form whereas one molecular species exist in the acidic form. The predominant species of alkaline form was in the high spin state. The low spin content in the acidic (MbH_2O) and alkaline (MbOH) forms of Mb was estimated and compared with values deduced from their magnetic susceptibilities. It was emphasized that the high spin species at alkaline pH (MbOH h.s.) is evidently structural different from the high spin species at neutral pH (MbH_2O). It was also demonstrated that the relative intensity of the two Raman lines [R=I(675 cm^{-1})/I(755 cm^{-1})] might be dependent upon the planarity of the heme group.

Resonance Raman spectra were measured for various C-type cytochromes in reduced and oxidized states. The assignment of several Raman lines which are used as structural monitors were established. The frequencies of the oxidation state marker showed that the sixth ligand binds to the heme iron mainly through the σ type interaction in the reduced C-type cytochromes. The relative intensity of Raman lines in the reduced state might suggest that the cytochromes were apparently classified into two groups, however it could be concluded by the excitation profiles of the representatives of the two groups that vibrational-spectroscopically there was no large difference between two groups. The relative intensity of two Raman lines around 1585 and 1563 cm^{-1} of oxidized cytochromes suggested that the hemes of f-type have slightly more hydrophobic environment than those of C-type cytochromes.

The pH induced changes of the resonance Raman spectra observed for the C-type cytochromes were interpreted in terms of the replacement of the axial ligands and the change of hydrophobicity around the heme moieties in Chapter 4. An empirical rule to relate the Raman spectral characteristics with the identity of the axial ligands were fairly established. It could be considered that the Raman spectral transition with pK 9.3 of cyt c(Fe^{3+}) was associated with the replacement of the methionine-80 to arbitrary N-base such as lysine or histidyl imidazole. It could be also deduced from the Raman spectra the replacement of the axial ligand occurred at about pH 11.5 for cyt c-551 (Fe^{3+}). Ferrous and ferric protoporphyrin with various axial ligands were subjected to Raman spectroscopy in the presence and absence of detergents to examine the effect to the hydrophobicity in the heme pocket upon the resonance Raman spectra. From the model compound studies it was suggested that the heme pocket of ferric cytochrome b_5 is more hydrophobic than that of ferric cytochrome c.

In Chapter 5 cytochrome c' were characterized for its five states by the Raman spectra and the pH-dependent and detergent-induced structural alterations in the heme moiety of cytochrome c' were discussed. The author is attempted to conclude that Type I and Type II possess a similar domed structure of heme with histidine as the fifth ligand but the interaction between the heme iron and the fifth ligand is slightly different between the two states presumably due to the strain caused by the apoprotein. The change of electron distribution among the heme iron, porphyrin ring and the fifth ligand can possibly change the frequencies of the methine-bridge stretching vibrations. Type III takes normal low spin state with lysine as a likely sixth ligand of the heme iron. Type a gave the Raman spectra of rather normal high spin type. The frequency of the ligand sensitive Raman line suggested the coordination of lysine (N_ε) at the sixth position of the heme iron of Type n. The oxidation state marker of Type n indicates that the sixth ligand binds to the heme iron mainly through the σ type interaction.

Resonance Raman spectroscopy were applied to the structural studies of metallo-octaethylchlorins [M(OEC)] in Chapter 6. The vibrational frequencies of Ni(OEC) were close to those of the corresponding

derivatives of metallo-octaethylporphyrins [M(OEP)]. The methine -bridge stretching vibrations and ring vibrations of pyrrole were assigned on the basis of frequency shift upon the isotopic substitutions. The Raman lines due to iron-ligand (L) stretching vibrations of Fe(OEC)L were observed definetely at 608 cm^{-1} for L=F and at 361 cm^{-1} for L=Cl while L-Fe-L symmetric stretching mode of $Fe(OEC)L_2$ was found at 303 cm^{-1} when L=imidazole. It was suggested that the bond-strength of iron-axial ligand was not affected so much by the change such as the saturation of the conjugated bond at the C_β-C_β bond. In accord with the difference in their absorption spectra the dependence of Raman intensities upon the excitation wavelength clealy differ between M(OEC) and M(OEP).

In Chapter 1 of PART II nitrogen-15 nuclear magnetic resonance (^{15}N-NMR) spectra were measured for various metal complexes of $^{15}N_4$-OEP. The ^{15}N signal of $^{15}N_4$-Ni(OEP) was distinct from the other diamagnetic metallo-octaethylporphyrins without axial ligands and was located in remarkably higher field. Similar distinct shift was observed for the ^{13}C signal of C_α carbon of the Ni(OEP). These results could be explained by the strong Ni-N bonding. The axial ligand effects were examined for $^{15}N_4$-Fe^{2+}(OEP) and $^{15}N_4$-Co^{3+}(OEP). The ^{15}N chemical shifts of Fe(II) complexes strongly depended upon the bonding nature of the iron-axial ligand. The π type bonding induced the delocalization of the electron charge density of the porphyrin ring which may result in the decrease of σ_p term. The change of basicity in the axial ligands may give only second order perturbation to the ^{15}N chemical shift of the porphyrin ring compared with the change in the nature of the metal-ligand bond.

The paramagnetic species of Ni(OEP) were studied by the use of ^{15}N-NMR in Chapter 2. The NMR studies succeeded in detecting the trace amounts of molecular species of Ni(OEP) which were considered to be paramagnetic one having two axial ligands. The marked shift of pyrrole nitrogens of $^{15}N_4$-Ni(OEP) to lower field as well as greater broadening of resonance in $CDCl_3$-C_5D_5N mixed solution could be ascribed to paramagnetic effects. Although the similar paramagnetic effects were also observed in ^{1}H-NMR and ^{13}C-NMR, it was shown in the present study that ^{15}N-NMR was more sensitive and useful method than the others.

In closing, the author wishes to mention about the future of the investigation of hemoproteins. Now several kinds of hemoproteins are being studied by x-ray crystallography. Among them the studies of cytochromes c_3, c', and P-450$_{cam}$ are paticularly interesting. Cytochrome c_3 is a small protein as large as cytochrome c, however it has four heme groups. The arrangement of four hemes in the small capacity is a very interesting problem which may enable us to understand its activity. In addition Teraoka et al.(1) have found the pH dependence of the resonance Raman spectra of cytochrome c_3 and suggested that the stepwise replacement of the sixth ligand of its four hemes. It will make possible to compare the resonance Raman spectral data with x-ray data. The ligation properties of cytochrome c' and P-450$_{cam}$ are quite important for understanding their physiological role as stated in this thesis. The x-ray crystallographic studies on them will give significant progress in the investigation of ligation properties.

Novel spectroscopic methods are still introduced, for example, the extended x-ray absorption fine-structure spectrum (EXAFS) has been applied to the study of allosteric effect of hemoglobin by the Bell Laboratory group(2).They have concluded by EXAFS study that there are no substantial movement ($<$0.02 Å)of the iron to heme plane between the high-(R-form) and low-affinity (T-form) quaternary forms. Recently Asher et al. (3) have succeeded in observing the selective enhancements of axial ligand vibrations of hemoglobin. This study renewed the idea of the usefulness of resonance Raman spectra.

It is also quite desirable to investigate the structure of hemoproteins in more physiological environment. The interaction of hemoproteins with phodspholipids or their structure in membrance are being actively studied in recent years. Accordingly even in the near future the accumulation of the knowledges about hemoproteins will be enormous. If we should be able to straighten out and utilize them validly, we shall enjoy remakable progresses in the problems such as drug metabolism, cancer or hereditary diseases.

REFERENCES

1. Kitagawa, T., Ozaki, Y., Teraoka, J., Kyogoku, Y., and Yamanaka, T. (1977) Biochim. Biophys. Acta 494, 100.
2. Eisenberger, P., Shulman, R. G., Brown, G. S., and Ogawa, S. (1976) Proc. Natl. Acad. Sci. U. S. 73, 491.
3. Asher, S. A., Vickery, L. E., Schuster, T. M., and Sauer, K. (1977) Biochemistry 16, 5849.

ACKNOWLEDGMENTS

The present work has been performed under the direction of Professor Yoshimasa Kyogoku, Institute for Protein Research, Osaka University. The author would like to express his sincere gratitude to Professor Yoshimasa Kyogoku for his cordial guidances discussions, and intimate encouragements throughout his course of study. He also wishes to express his sincere thanks to Dr. Teizo Kitagawa for his continuing discussions and encouragements.

During the courseof study the author has received a number of fruiteful discussions, helpful comments and hearty encouragements from several persons.

As for PART I, the author is deeply indebted to Professor Ryo Sato, Dr. Yoshio Imai, and Mrs. Chikako Hashimoto-Yutsudo of Institute for Protein Research, Osaka University for their generous gift of microsomal cytochrome P-450, kind advices and valuable discussions. He is also greatly oblized to Professor Yuzuru Ishimura, Assistant Professor Tetsutaro Iizuka and Dr. Hideo Shimada of Keio University for their generous gift of cytochrome $P\text{-}450_{cam}$, valuable discussions, and continuous encouragements. The author's thanks are also due to Professor Takekazu Horio of Institute for Protein Research and Assistant Professor Tateo Yamanaka of the Faculty of Science, Osaka University for their generous gifts of various C-type cytochromes, and useful discussions. It is also his pleasure to thank Mr. Junji Teraoka for his active collaborations.

As for Chapter 6 of PART I and PART II the author is deeply grateful to Assistant Professor Hisanobu Ogoshi, Dr. Ei-ichi Watanabe, and Mr. Hiroshi Sugimoto of Kyoto University for their generous gift of octaethylporphyrins and octaethylchlorins, stimulating discussions, and warm encouragement. As for PART II he is also grateful to Dr. Keiichi Kawano of Nagoya University and Dr. Kenichi Yoshikawa of Tokushima University for their helpful discussions and kind advices.

The author wishes to express his cordial appreciation to Professor Tatsuo Miyazawa of the University of Tokyo who gives to the author intimate support and encouragement during the course of the study.

The instructive advices and suggestions received from Dr. Hiromu Sugeta, Dr. Hideo Akutsu, and Dr. Motoko Abe are greatfully acknowledged. The author wishes to express his sincere gratitude to Professor G. J. Thomas, Jr. of Southeastern Massachusetts University and Professor Byung Sul Yu of Seoul University for their academic stimulations given to the author.

The author's thanks are also due to all the members of Division of Molecular Biophysics of Institute for Protein Research. Furthermore, it is a great pleasure to acknowledge his intimate friends and classmates for their friendly goodwills and warm-hearted stimulations. Finally the author thanks sincerely to his parents for their unfailing understanding and affectionate encouragements.

Yukihiro Ozaki

LIST OF PAPERS

1. The contents of this thesis have been published or will be published in the following papers.

PART I

Resonance Raman Studies on the Ligand-iron Interactions in Hemoproteins and metalloporphyrins.

KITAGAWA, T., OZAKI, Y., and KYOGOKU, Y., "Advances in Biophysics" Vol. 11, p 153, The University of Toyko press (1978).

Chapter 1.	J. Biochem. (1976) 80, 1447. J. Am. Chem. Soc. submitted for publication.
Chapter 2.	FEBS Lett. (1976) 62, 369.
Chapter 3.	Biochim. Biophys. Acta (1977) 494, 100.
Chapter 4.	J. Raman Spectrosc. to be submitted.
Chapter 5.	Biochim. Biophys. Acta (1977) 495, 1.
Chapter 6.	J. Phys. Chem. submitted for publication.

PART II

Chapter 1.	J. Chem. Soc. to be submitted.
Chapter 2.	J. Chem. Soc. to be submitted.

2. List of the related papers.

1). Molecular Conformations and C-Cl Stretching Vibrations of 1-chloro-2-methylpropane and C-S Stretching Vibrations of 2-methyl-1-propanethiol and L-cysteine.

OZAKI, Y., SUGETA, H., and MIYAZAWA, T. (1975) Chem. Lett. 713.

2). ^{15}N Nuclear Magnetic Resonance Spectra of Octaethylporphyrin

KAWANO, K., OZAKI, Y., KYOGOKU, Y., OGOSHI, H., SUGIMOTO, H., and YOSHIDA, Z. (1977) J. Chem. Soc. Chem. Commun. 226.

3). ^{15}N and ^{1}H Nuclear Magnetic Resonance Spectra of Octaethylporphyrin and its Derivatives.

KAWANO, K., OZAKI, Y., KYOGOKU, Y., OGOSHI, H., SUGIMOTO, H., and YOSHIDA, Z. (1978) J. Chem. Soc. Perkin II in press.

4). The Molecular Conformations of γ-Aminobutyric Acid and γ-Amino-β-hydroxybutyric Acid in Aqueous Solution.

TANAKA, K., AKUTSU, H., OZAKI, Y., KYOGOKU, Y., and TOMITA, K. Bull. Chem. Soc. Japan submitted for publication.

5). The Excitation Profile of the Raman Spectrum of Ni-octaethylchlorin.

OZAKI, Y., KITAGAWA, T., KYOGOKU, Y., OGOSHI, H., WATANABE, E., and YOSHIDA, Z. J. Phys. Chem. to be submitted.